UCSF
UC San Francisco Electronic Theses and Dissertations

Title
Polyunsaturated fatty acids modulate TRPV-dependent sensory signaling in the nematode Caenorhabditis elegans

Permalink
https://escholarship.org/uc/item/39z4x46d

Author
Kahn-Kirby, Amanda H

Publication Date
2005

Peer reviewed|Thesis/dissertation

eScholarship.org Powered by the California Digital Library
University of California

Copyright © 2004

By

Amanda H. Kahn-Kirby

This labor of love

is dedicated to three sources of strength and inspiration in my life:

my grandmother

Ruth E.P. Kahn, Ph. D.

(1905-1996)

my loving husband

Mason Robert Kirby

and our daughter

Julia Rae Kirby

born 12/8/2004

Acknowledgements:

I entered and ended the UCSF Neuroscience program captivated by the idea of studying the molecules underlying sensation. In the years between, I matured considerably as a scientist and a person through the guidance and companionship of my colleagues, for which I am immensely grateful.

The Neuroscience program is fortunate to have two dedicated and kind women, Pat Veitch and Deborah Rosenberg, as the day-to-day supervisors for its students. Lou Reichardt sets the pace for a remarkable community of faculty, post-docs, and students; I am lucky to have learned from such a talented, dynamic group of scientists. Special thanks to the UCSF members of my thesis committee: Lily Jan, Ulrike Heberlein, and Herwig Baier. Approaching Lily for a conversation about ion channel function is a little intimidating and very inspirational; her knowledge of the field is encyclopedic. Ulrike has been a generous teaching mentor and guide through the more frustrating experiments of my project. Herwig has offered sound criticism and encouragement through the course of this project, and was also a generous rotation advisor many summers ago in Tübingen. The fifth member of my thesis committee, Miriam Goodman at Stanford, has been a critical and thoughtful editor. Thanks, too, to my classmates and friends in the Neuroscience program and other graduate programs at UCSF, who have made my years here a lot more entertaining. You have made me laugh, think, reconsider, innovate, and relax; thank you for your companionship through the years.

Most of my time at UCSF has been spent in the awesome company of the Bargmann Lab. Erin Peckol Dolan and Steve McCarroll convinced me to come to UCSF. Erin continues to be a source of encouragement as I grow as a teacher, while Steve has been a sharp, funny, critical colleague and friend. Many people helped me when I was starting out in lab, including Emily Troemel, Gage Crump, Jen Zallen, Mario deBono, and Noelle L'Etoile. Noelle continues to be a good friend and confidante, and is one of the most creative and generous scientists I know. Rob Rutherford, Tim Yu, David Tobin, Maria Gallegos, and Yun Zhang have been fun and tolerant bay mates – and Maria has been a great neighbor, biking companion, keeper of secrets, source of gossip, editor, critic, teacher, and friend. This dissertation bears a strong imprint of David's scientific guidance as my rotation supervisor and collaborator studying TRPV signaling in *C. elegans*; none of this would have happened without his ideas, patient teaching, and encouragement. Thanks to Jesse Gray for adding some juicy intrigue to life in lab (and political conversations), to Carrie Adler for her impeccable taste in music, and to Jami Dantzker for being a fantastic collaborator. To the lab past and present, thank you for stimulating group meetings, heated post-seminar discussions in the hallway, entertaining lunches at Minh Tri, exhausting ski trips at Lake Tahoe, and just generally making every day in lab a pleasure, even when my experiments flat-out sucked.

My experiments in Chapter 2 were the fruits of an amazing collaboration with Jenny Watts at Washington State University. Jenny is a smart, creative scientist and good friend, and it has been a privilege to work together over the last few years, and perhaps in years to come.

Credit for any success of my graduate work is, in large part, due to Cori Bargmann's brilliance as a scientist and skill as a mentor. Tales of her scientific prowess and creativity are legion, and they are all true. She has an expansive knowledge of biology (not just of the sensory signaling field), a knack for figuring out provocative experiments that actually work, and remarkable skill at putting results together into a compelling and important story. Time and again, she nudged me in directions I could not see, but which would eventually prove fruitful. She did this not by micro-managing, but by stimulating real excitement at possible experimental outcomes. Cori is a gifted writer and editor: clear, precise, measured, direct. This dissertation was immeasurably improved by her careful reading and comments. Beyond her scientific mentorship, Cori has been a generous advisor and friend; I appreciate the conversations we've had about everything from families to traveling to politics to literature. Thank you for helping me get this far.

I would also like to thank my family, who have resigned themselves to flying all the way from New York to visit me in San Francisco. My father Alan Kahn and grandfather Irving Kahn continue to offer and elicit scientific advice; your interest in my field is remarkable, and I feel bad that I just can't muster up the same enthusiasm for undervalued securities and shareholder rights litigation. My mother Blanche Kahn, stepmother Linda Kahn, and sister Kimberly Kahn have eased the pressures of graduate school with many visits and conversations. Special thanks to my mother for helping out with Julia during my final days of editing this dissertation. Thanks, too, to my extended family by marriage, including my cousin Rose Norberg, for her genuine interest in me and my work.

Last of all, let me thank my immediate family, human and otherwise. Chess and Bumblebee have been (mostly) patient and unquestioningly loving companions, even when I've been a self-absorbed, mildly neglectful dog parent. Mason, thank you for joining me in San Francisco, for listening to me vent when experiments go badly, for amplifying my enthusiasm when they succeed, for making me laugh, for keeping me balanced, for putting up with my relentless stare at the screen as I've written and written and written over the last year. Final thanks go to Julia (formerly known as HeShe), who kicked and poked me through the duration of my last experiments in grad school and the writing of my thesis, and who provided an incredible biological deadline for the submission of this work (and then had the nerve to be born late). I can't wait to buy you your first microscope in a couple of years.

Polyunsaturated fatty acids modulate TRPV-dependent sensory signaling in the nematode *Caenorhabditis elegans*

Amanda H. Kahn-Kirby

Abstract

Sensory neurons allow an organism to acquire information about its surroundings, leading to altered neural circuit activity and, ultimately, behavioral responses. At the molecular level, sensory information is conveyed through conserved signal transduction pathways. Members of the TRP ion channel family have a prominent role in sensory signaling from fungi to man. TRP channels are implicated in thermosensation, osmosensation, auditory sensation, pheromone detection, mechanotransduction, and nociceptive chemosensation. They also have less-explored roles in diverse non-sensory physiological functions, including vasodilation. A variety of exogenous lipids and synthesized ligands can stimulate the activity of heterologously-expressed TRP channels. A major unsolved question is the identity of molecules and pathways that regulate TRP channel function *in vivo*.

Here we show that polyunsaturated fatty acids (PUFAs) modulate TRP sensory signaling pathways *in vivo*. The soil nematode *C. elegans* relies on the *osm-9* and *ocr-2* TRP channels to sense attractive odors and avoid noxious stimuli in its environment. Animals mutant in specific PUFA synthesis genes exhibit behavioral defects consistent with reduced *osm-9/ocr-2* channel activity in the AWA and ASH sensory neurons. Cell-specific sensory defects can be reversed

rapidly by dietary supplementation of adult animals with certain PUFAs. Acute exposure to PUFAs induces calcium transients and ASH-mediated, *osm-9*-dependent avoidance behavior, independent of PUFA synthesis pathways. Our behavioral, genetic, and imaging data strongly suggest that PUFAs or a PUFA product are endogenous modulators of *osm-9* / *ocr-2* signaling pathways.

TRP channels are also essential for activity-dependent regulation of gene expression in the AWA sensory neuron. We employed a visual reporter of AWA gene expression to characterize genes and pathways that regulate TRP-dependent transcription. A variety of known signaling molecules impinge upon *osm-9*-dependent transcriptional pathways, including G-proteins, calcium-calmodulin dependent kinase II, insulin signaling pathways, and PUFAs. A forward genetic screen identified additional, novel modulators of *osm-9*/*ocr-2*-dependent transcriptional regulation.

Given the conservation of TRP channel sensory functions across species, we speculate that PUFAs and other modulators of *osm-9* sensory signaling may also regulate vertebrate and mammalian TRP channels *in vivo*.

Graduate Advisor

Table of Contents

Chapter One: An introduction to TRP channels 1

Chapter Two: Specific polyunsaturated fatty acids drive TRPV-dependent sensory signaling *in vivo* 54

Chapter Three: Activity-dependent regulation of gene expression in sensory neurons 104

Chapter Four: Future directions 173

Appendix A: Mammalian TRPV ion channels respond to applied PUFAs 180

List of Figures

Chapter One

Figure 1-1. Chemosensory transduction pathways in *C. elegans* 45

Figure 1-2. Analogous sensory transduction pathways 47

Figure 1-3. Natural and synthetic ligands for mammalian TRPV channels 49

Figure 1-4. TRP structure and select *C. elegans* TRP channels 51

Figure 1-5. Expression patterns of C. elegans TRPV subunits 53

Chapter Two

Figure 2-1. Lipid synthesis pathways in *C. elegans* 87

Figure 2-2. *fat-3* mutants show cell-specific chemotaxis defects 89

Figure 2-3. Defective nociception in *fat-3* mutants 91

Figure 2-4. Sensory stimuli elicit calcium transients in ASH neurons 93

Figure 2-5. ASH synaptic transmission is spared in *fat-3; sra-6::TRPV1* animals 95

Figure 2-6. Rescue of *fat-3* behavioral defects by restoring PUFAs 97

Figure 2-7. Exogenous PUFAs elicit avoidance responses 99

Figure 2-Supplementary 1. Cell-specific sensory defects in *elo-1(wa7)* mutants 101

Figure 2-Supplementary 2. Absence of sensory defects in the synaptic neurotransmission mutant *rab-3(y250)* 103

Chapter Three

Figure 3-1. Model for AWA signal transduction 148

Figure 3-2. Activity-dependent regulation of *odr-10*::GFP expression 150

Figure 3-3. G-proteins and Ca^{2+} signaling regulate *odr-10*::GFP expression 152

Figure 3-4. odr-3(XS) is an osm-9 suppressor in AWA and ASH 154

Figure 3-5. PUFA synthesis mutants have diet-dependent *odr-10*::GFP expression defects 156

Figure 3-6. Model for integrated regulation of dauer development 158

Figure 3-7. Insulin signaling can regulate odr-10::GFP expression 160

Figure 3-8. Candidate genes for a neuronal RNAi screen 162

Figure 3-9. OSM-9(*n2743*) channels are mislocalized 164

Figure 3-10. Identification of *osm-9(n2743)* suppressors 166

Figure 3-11. AWA, AWC, and ASH phenotypes of *ky456* and *ky440* 168

Figure 3-12. *ky440* suppression of *osm-9(n2743)* is TRPV-dependent 170

Figure 3-13. *ky440* maps between *osm-9* and *dpy-13* 172

Appendix A

Figure A-1. TRPV channels specify ASH-mediated lipid avoidance 185

Chapter One:

An introduction to TRP channels

I envision my childhood home frosted by an early snowstorm, and recall the velvet softness and surprising lightness of a pet bird on my shoulder. I remember the oniony smell of my grandmother's Passover brisket, the bittersweet taste of that pink medicine for earaches, the rasping sound of ice skates landing after a jump. A lifetime of experiences and memories is assembled from sensory impressions: how are those perceptions generated? How do we construct our understanding of the world?

Our ability to detect sensory cues resides in the nervous system, the network of peripheral and central neurons that absorbs, transmits, processes, selects, and stores salient information about our environment. Sensory neurons have specialized structures that endow them with the capacity to detect a particular quality of information, such as an individual odor or a certain wavelength of light. When a stimulus is detected by a sensory neuron, a change in the cell's electrical activity induces a chemical signal to the next neuron within a circuit. The process repeats and ramifies, so that a variety of areas within the brain can be stimulated in parallel by a given sensory input. Discrete brain regions participate in selecting information to extract from a perceptual stream, encoding memories, and storing them in such a way that they are accessible and potent decades later.

My graduate work addresses a central question of sensory perception, but skirts the complexity of studying this issue in the human brain. Instead of delving into the awesome tangle of neurons in the human body, I chose to study the relatively compact neural network of the soil nematode *C. elegans*. First appreciated as a genetic model organism by Sydney Brenner (Brenner, 1974), worms have gained a substantial following for several reasons. The 302-cell

neural network of *C. elegans* has been reconstructed by serial electron microscopy (White et al., 1986). This unique resource allows researchers to identify the primary sensory neurons, interneurons, and motoneurons involved in detecting, processing, and responding to a stimulus. A collection of genetic resources and molecular biology tools makes it possible to manipulate individual cells, thereby dissecting the role of a given cell or circuit in controlling a neural response. At the time I began these studies, *C. elegans* was the only multicellular organism with a sequenced genome, which greatly facilitates the identification and interpretation of mutant alleles. Collectively, these tools facilitate the use of *C. elegans* as an *in vivo* resource for the detailed study of sensory function at the molecular level.

A central challenge in understanding how organisms perceive their world is determining what, exactly, an individual can detect. Humans can verbally recount their subjective sensory experiences, and their motor reactions serve as an index of perception. Mammals such as rodents or primates can be trained to convey sensory perception through motor responses. Alternatively, electrical recording or Ca^{2+} imaging can assay the activity of specific populations of sensory neurons. For model organisms such as zebrafish, *Drosophila*, and *C. elegans*, researchers rely on the animal's behavior to reveal which sensory circuits are activated by a given stimulus. Worms are unable to see, but navigate their soil environment by detecting odors, water-soluble chemicals, mechanical stimuli, gases, and thermal cues. Behavioral assays allow *C. elegans* researchers to understand how a given gene mutation or molecular manipulation affects a specific sensory modality.

In Cori Bargmann's lab, a major focus has been the identification of cells and molecular pathways underlying chemosensation. By systematically ablating a given morphological class of neuron and challenging animals with a chemotaxis assay, she determined the sensory neurons responsible for detecting water-soluble (Bargmann and Horvitz, 1991) or volatile (Bargmann et al., 1993) compounds. Further studies revealed the molecular signal transduction components required for basic chemosensation in the AWA and AWC sensory neurons, which detect volatile odors (Figure 1-1) (Coburn and Bargmann, 1996; Colbert et al., 1997; L'Etoile and Bargmann, 2000; Roayaie et al., 1998; Sengupta et al., 1996; Sengupta et al., 1994). The genes required for *C. elegans* olfaction are strikingly similar to their counterparts in other organisms: AWC chemotaxis proceeds by a pathway like that used in mammalian olfaction (Firestein, 2001) and vision (Baylor, 1996), while AWA chemotaxis requires molecules like those used in mammalian pheromone sensation (Dulac and Torello, 2003) and *Drosophila* phototransduction (Hardie, 2001) (Figure 1-2). Given these similarities across evolutionary time and complexity, lessons learned from *C. elegans* chemosensation are germane to the study of related molecules in other organisms' cells, tissues, and physiological processes.

At the time I began studying the molecular mechanisms underlying chemosensation, the TRP ion channel and its relatives were attracting widespread attention. First appreciated as the transduction channels in *Drosophila* photoreceptors (Hardie and Minke, 1992; Montell and Rubin, 1989; Phillips et al., 1992), mammalian TRP channels were cast into a sensory spotlight when David Julius and colleagues cloned the heat, pH, and capsaicin-sensitive TRP channel VR1(Caterina et al., 1997). A passel of TRP channels with intriguing

sensory roles have been identified in the years since, including channels involved in mammalian heat sensation (Caterina et al., 1999; Peier et al., 2002b; Smith et al., 2002; Xu et al., 2002), cold sensation (McKemy et al., 2002; Peier et al., 2002a), osmosensation (Liedtke et al., 2000; Strotmann et al., 2000), pheromone sensation (Liman et al., 1999), and audition (Corey et al., 2004). In other species, related channels occupy similar sensory roles (Colbert et al., 1997; Kim et al., 2003; Tracey et al., 2003; Walker et al., 2000), and in some cases a mammalian relative can functionally substitute for the invertebrate orthologue (Liedtke et al., 2003). Non-sensory roles for TRP channels are increasingly under investigation, including cardiovascular functions (Hassock et al., 2002; Zygmunt et al., 1999), renal functions (Mochizuki et al., 1996), and lysosomal functions (Sun et al., 2000). The remarkable expansion and increasing importance of TRP channels in sensory and non-sensory signaling made them an attractive subject for my graduate studies.

Despite great progress in identifying new TRP family members and analyzing their myriad cellular functions, there remains a good deal of controversy about the molecules and pathways that regulate TRP channel function *in vivo*. Pharmacological approaches and heterologous cell experiments have identified a slew of candidate TRP channel regulators, but such studies often fail to reveal which pathways are relevant for a channel in its native cellular context. In the experiments detailed in chapters 2 and 3 of my dissertation, I describe an alternative approach to exploring TRP channel function *in vivo*. By using genetics and behavior to identify genes and molecular pathways important for TRP channel function in intact *C. elegans*, we may reveal core shared components of TRP channel regulatory pathways across species. Such molecules

will demystify how the initial events of sensation work, and may also lead to the discovery of therapeutic interventions for diseases caused by defects in TRP family channels.

Here, I will review the sensory functions of TRP channels in mammalian and invertebrate systems. The biophysical properties and diverse functions of mammalian TRP channels have been reviewed recently and extensively by Clapham (Clapham, 2003), so I will focus more detail on physical sensation and signal transduction by *C. elegans* and *Drosophila* TRPs. I have endeavored to highlight significant commonalities and controversies in the understanding of how an individual channel class functions. With respect to the function of TRP family proteins in *C. elegans*, I have underscored how a whole-animal physiology approach to studying channel function complements and extends vertebrate studies.

What makes a TRP channel, and how are they distinguished?

TRP channels are defined by their sequence similarity to the *Drosophila* phototransduction channel *trp* (Hardie and Minke, 1992; Montell and Rubin, 1989). Major structural motifs include 6 transmembrane domains and a variable number of ankyrin motifs (which may participate in protein-protein interactions) (Figure 1-3). Homology outside these core regions can be quite low among TRP family channels, although members of individual TRP subfamilies may share other motifs, such as TRP boxes or PDZ binding sites. TRP channels assemble into homo-and hetero-tetramers, and are cation-selective (Clapham, 2003).

TRP subfamily members can be quite divergent in their protein structures, tissue distribution, cellular functions, and modes of regulation. There are six

human TRP structural subfamilies, representing twenty-eight channel subunits: TRPV (vanilloid; six members), TRPC (classical/short, seven members including a pseudogene), TRPM (melastatin/long, eight members), TRPML (mucolipin, three members), TRPP (polycystin, three members), and TRPA (one member) (Montell et al., 2002). Non-mammalian vertebrates also have a TRPN subfamily (one member), which can participate in nociceptive and auditory functions (Sidi et al., 2003; Walker et al., 2000). While TRP family functions have been studied extensively in sensory neurons, TRP channels are found elsewhere including non-sensory brain regions (Mezey et al., 2000), bladder (Avelino et al., 2002), the gastrointestinal tract (Ward et al., 2003), heart (Zahner et al., 2003), and sperm (Castellano et al., 2003). TRP family members have been proposed as the sought-after Ca^{2+} store-operated channels; other possible modes of regulation are by thermal stimuli, mechanical stimuli, lipid signaling molecules and their derivatives, voltage, and pH (Clapham, 2003). There is no consensus on a single, unifying mode of regulation; instead, it seems that some TRPs serve as integrators of multiple regulatory pathways, and others are activated by one predominant pathway. A comparison of the functions and regulatory modes of sensory and non-sensory TRP family members demonstrates the impressive range of cellular activities subserved by these channels.

TRP channels as osmosensors and mechanoreceptors

A cell's ability to regulate its internal osmolarity in the context of changing external osmolarity is critically important. Without the ability to sense hypo- or hyper-osmolar conditions and regulate fluid transport accordingly, cells are in danger of swelling or shriveling. Depending on their environmental contexts,

multicellular organisms can monitor external or internal osmolarity, and use behavioral or homeostatic mechanisms to find an optimal osmotic condition for discrete tissues. A related physical (as opposed to chemical) sensory process is mechanosensation, the detection of forces. Mechanical stimuli may include the ubiquitous sensation of gravity, the pleasurable sensation of gently scratching the skin, the painful sound of a subway train screeching to a halt, or the abrupt acceleration of a passenger when the train resumes motion. Mechanoreceptor cells, like auditory hair cells, have specialized sensory stereocilia that facilitate or amplify the detection of a force stimulus. Osmosensation and mechanosensation are hypothesized to proceed through physical deformation of a cell's membrane or surface, and concomitant stretching of channels. Channel deformation could occur directly, or indirectly through attachment to other molecules, either external or internal.

While an extensive literature implicates members of the degenerin channel family as mechanosensors (Goodman and Schwarz, 2003), vertebrate and invertebrate TRP family members have been implicated as osmosensitive or mechanosensitive channels in a variety of cellular contexts. TRPV4, also known as OTRPC4 or VR-OAC, was the first candidate vertebrate osmosensor (Liedtke et al., 2000; Strotmann et al., 2000). In transfected cells, exposure to hypotonic solutions induces a TRPV4-dependent Ca^{2+} current. Consistent with its role as an osmosensor, the channel is found in osmosensitive or mechanosensitive cells such as the circumventricular organ, the Organ of Corti, kidney epithelium, and mechanosensory neurons. Several groups have derived TRPV4 -/- mice, which show mild nociceptive defects, as well as osmoregulatory defects consistent with altered circumventricular organ function (Liedtke and Friedman, 2003; Mizuno et

al., 2003; Suzuki et al., 2003). In addition to osmotic or mechanical stimuli, TRPV4 can also respond to lipid signaling molecules and mild temperature changes, as discussed below. A *Drosophila* relative of TRPV4, *nanchung*, has defects in hypo-osmolarity sensing, and localizes to the cilia of the mechanosensory chordotonal organ (Kim et al., 2003).

Our most visible and substantial sensory organ, the skin, is a mechanosensitive surface, yet the identity of the ion channels underlying human touch sensation -- and the related process of auditory sensation -- is not yet certain. Recently, the TRPA1 channel was identified as a candidate mechanosensor in mammalian auditory hair cells and zebrafish mechanosensory lateral line organs (Corey et al., 2004). The channel is expressed at a time consistent with the onset of mechanosensory function, and is localized to the distal sensory cilia of hair cells along with known auditory transduction components. Down-regulation of TRPA1 using zebrafish morpholinos or siRNA in mice results in reduced auditory cell function, providing functional evidence that TRPA1 may be a component of the long sought-after auditory transduction channel. TRPA1 has an unusually large number of ankyrin repeats in its N-terminal region (17), and it has been hypothesized that a coil of ankyrin repeats may constitute the mechanosensor (Howard and Bechstedt, 2004). Intriguingly, TRPN channels contain a large number of ankyrin repeats (29), and have roles in *Drosophila* mechanotransduction (Walker et al., 2000) and zebrafish hair cell mechanotransduction (Sidi et al., 2003).

Outside the nervous system, TRP family members serve tissue-specific sensory roles. Within the kidney, the polycystin channel TRPP2 was identified as a disease gene in families with autosomal dominant polycystic kidney disease

(Mochizuki et al., 1996). TRPP2/PKD2 is a nonselective cation channel that localizes to the plasma membrane of ciliated kidney epithelial cells (Gonzalez-Perrett et al., 2001), where it is hypothesized to participate in the sensation of fluid forces. A *Drosophila* TRPP2 homologue, *almost there (amo)*, localizes to the ciliated posterior tip of sperm cells (Watnick et al., 2003). Male flies mutant for *amo* have novel fertility defects: their sperm are motile, but are not stored in female flies. *amo* sperm may lack subtle aspects of movement; alternately, they may fail to detect a sensory cue essential for migration to sperm storage organs.

The identification and characterization of mechanosensitive and osmosensitive TRP channels suggests certain shared principles. All of these channels reside in cilia or microvillar stereocilia, underscoring the importance of these cellular specializations in detecting (or, in the case of *amo*, potentially generating) physical forces. The candidate auditory TRPA1 and TRPN channels have an extensive ankyrin repeat bundle, raising the elegant possibility that the channel architecture contains an intrinsic force detection apparatus (Corey et al., 2004; Howard and Bechstedt, 2004). Osmolarity-detecting TRP channels have a smaller number of ankyrin repeats, perhaps suggesting that local membrane deformation or other cues are more likely to modulate these channels in concert with thermal stimuli or second messengers.

Thermal detection by TRP channels

Perhaps the most spectacular and novel aspect of the TRP family story is the identification of TRP channels as thermosensors, detectors of high and low temperature. Cold-blooded organisms need to avoid fire, frost, and other extrinsic tissue-damaging extremes of temperature; warm-blooded animals also

must regulate their body temperature to ensure adequate metabolism. Mammalian thermosensory TRP channels can detect and respond to plant-derived chemical compounds that produce the psychophysical impression of warmth or coolness, demonstrating an unexpected molecular unity between thermal and chemical sensations of "hot" and "cold." The temperature range of thermosensitive TRPs spans the physiological range of temperatures compatible with terrestrial life.

The TRPV1 channel was cleverly identified as a receptor for the chili pepper vanilloid compound capsaicin, but also responds to acid pH and mildly noxious heat (Caterina et al., 1997; Tominaga et al., 1998). Its characterization established the principle that the culinary percept of "heat" is, on a cellular level, mechanistically related to elevated temperature detection. A recent study demonstrates that TRPV1 has an intrinsic voltage sensitivity, and that capsaicin shifts the voltage sensitivity towards resting membrane potentials (Voets et al., 2004). Polymodal channel responses may thus be a molecular integration of ligand- and thermal-induced structural deformations at particular sites on the channel. Other TRPV channels can function as molecular integrators: studies in heterologous cells and cultured keratinocytes suggest that TRPV4 can respond to warm temperatures, and that this response can be enhanced by exposure to hypo-osmotic solutions (Chung et al., 2003; Guler et al., 2002). The related TRPV2 (Caterina et al., 1999) and TRPV3 (Peier et al., 2002b; Smith et al., 2002; Xu et al., 2002) channels are not vanilloid-sensitive, but may serve as high- and moderate-threshold thermoreceptors, respectively. In addition to its expression in nociceptive sensory neurons, TRPV1 is found in non-sensory CNS regions (Mezey et al., 2000), the gastrointestinal tract (Anavi-Goffer and Coutts, 2003;

Ward et al., 2003), heart (Zahner et al., 2003), and bladder (Avelino et al., 2002). In these internal tissues, TRPV1 channels are unlikely to respond to substantial temperature shifts, underscoring the importance of identifying intrinsic chemical channel modulators.

Cold detection is achieved by members of other TRP subfamilies. Originally identified as a prostate tumor cell marker (Tsavaler et al., 2001), the TRPM8/CMR1 channel was shown to respond to cool temperatures, the plant compound menthol, and the synthetic cooling compound icilin (McKemy et al., 2002; Peier et al., 2002a). TRPM8 responses to cold and icilin are sensitive to pH modulation within physiological ranges (Andersson et al., 2004), and icilin responses require coincident Ca^{2+} increases (Chuang et al., 2004). Like TRPV1, TRPM8 thermal responses are exquisitely sensitive to membrane voltage (Voets et al., 2004), suggesting that TRPM8 is also a molecular integrator of voltage, temperature, pH, and chemical stimuli. In addition to its role as a putative mechanoreceptor, TRPA1 has been characterized as a noxious cold-sensing channel (Story et al., 2003) which is also capable of responding to pungent mustard oils, the psychoactive compound tetrahydrocannabinol (Jordt et al., 2004), and the cinnamon oil component cinnemaldehyde (Bandell et al., 2004). While there are some discrepancies among the various papers with respect to TRPA1 cold sensitivity, a possible interpretation is that coactivation of TRPM8 and TRPA1-expressing neurons conveys the paradoxical sensation of burning cold (Bandell et al., 2004). Both thermal and mechanical sensitivity of TRPA1 channels are shared across species: the *Drosophila* TRPA/TRPN channel *painless* is required for avoidance of a heated probe (Tracey et al., 2003), and oocyte-

expressed *Drosophila* dANKTM1 responds to warm temperatures (Viswanath et al., 2003).

With the identification of temperature-sensing TRP channels spanning the range of physiological temperatures, the next step is to characterize cellular and circuit mechanisms of thermal sensation *in vivo*. Antibody staining of nociceptive sensory neurons suggests that distinct TRP subunits can be coexpressed (and that certain subunits are never coexpressed), raising the possibility that a combinatorial range of heteromeric channels in different neurons endows an organism with broad, precise thermosensory capacity. Alternately, there may be a limited set of subunit compositions, with temperature or chemical stimuli activating a small set of sensory "labeled lines." It will be particularly interesting to understand how fluctuations in voltage, Ca^{2+}, osmolarity, and pH gate the activity of thermosensitive TRP channels, altering the organism's thresholds for determining if a stimulus is noxious or not. As discussed below, the identification of inflammatory and lipid-signaling modulators of temperature-sensitive TRP channels will reveal functions for these channels beyond their roles in primary sensation.

TRP channels mediate pheromone sensation and taste

In non-nociceptive neurons, TRP channels can function as transduction channels in G-protein coupled receptor cascades, rather than direct sensors of force, temperature, or chemicals. *Drosophila* TRP, TRPL, and TRPγ comprise the phototransduction channel, and have been the subject of extensive analysis as components of a model G-protein coupled cascade (Montell, 2003). Vertebrate

TRP channels have not been implicated as mediators of vision, but participate in the chemical detection of pheromones and tastants.

TRPC2 is expressed on the sensory microvilli of rodent vomeronasal (VNO) neurons that mediate pheromone detection (Liman et al., 1999). Consistent with our species' rational and considered approach to sexual behavior, human TRPC2 is a pseudogene. Mice with targeted deletions of TRPC2 lack VNO responses to urine pheromone compounds, although they can still mate (Leypold et al., 2002; Stowers et al., 2002). TRPC2-/- males do not initiate male-male aggressive or territorial behaviors. Furthermore, they vocalize towards and mount other male mice, behaviors more appropriate for male-female interactions. Female TRPC2 -/- mice also exhibit diminished maternal aggression. These data are consistent with a role for TRPC2 as an essential transduction component in pheromone-sensing, aggression circuit-related rodent VNO neurons, although the molecular details of TRPC2 activation are not completely understood.

TRPM5/Mtr1 was originally identified as a conserved transcript in a human cancer-susceptibility region (Prawitt et al., 2000), but was later found to be preferentially expressed in a subset of taste receptor cells (Perez et al., 2002). Mice mutant for TRPM5 show specific defects in sweet, bitter, and umami taste, consistent with the expression pattern of TRPM5 (Zhang et al., 2003). There is some disagreement about whether Ca^{2+} stores activateTRPM5, but multiple studies of heterologously-expressed TRPM5 agree that elevated Ca^{2+} alone is sufficient to gate a monovalent cation current (Hofmann et al., 2003; Liu and Liman, 2003; Prawitt et al., 2003).

Progress in understanding the functions of receptor-coupled TRP channels will require identification of the intracellular pathways that modulate TRP channels, particularly in their native cellular milieu. A dizzying array of pharmacological agents and signaling pathways *can* activate TRP channels (particularly those overexpressed in heterologous cells). What are the salient modulators of channels in their usual location, with their appropriate signaling complex partners, and with a physiological stimulus? At present, answers to these questions remain elusive.

If not SOC, then what?

An elusive goal within the ion channel field is the channel responsible for conducting the mysterious I_{CRAC}, a Ca^{2+} release activated Ca^{2+} current. In many cell types pharmacological depletion of endoplasmic reticulum Ca^{2+} stores leads to an inward Ca^{2+} current termed I_{CRAC}, but its molecular substrate is unknown. Accompanying the cloning of seemingly every new TRP family member has been a paper investigating whether that particular channel represents I_{CRAC}, or is at least whether it is sensitive to emptying of internal Ca^{2+} stores (thus, a store-operated current, or SOC). Without delving into this convoluted and tedious corner of the TRP literature, let me summarize by saying that some TRP channels are probably gated by store depletion, but many others are not. What, then, are some relevant modes of regulation for TRP channels?

For TRP channels involved in osmosensory and mechanosensory force detection, the most elegant model would be that the channel itself acts as the force sensor. Shear force in a local fluid environment or apposed membrane could deform the gating regions of the channel, opening or closing the pore.

Alternately, the channel could be linked to the plasma membrane by a protein or lipid tether, which would transduce membrane deflection to the channel. In that way, the membrane would act as a force sensor, and stimuli would be passively transmitted to the channel. A third possibility is that a separate protein is the force sensor, and a rapid second messenger cascade conveys stimuli to a transduction channel. This model seems least likely, given that auditory mechanotransduction takes place on a submillisecond time scale (Corey and Hudspeth, 1979), while the *Drosophila* phototransduction cascade, the fastest G-protein pathway known, takes about 20 milliseconds (Montell, 2003).

TRP-dependent thermosensory responses can also occur on a millisecond time scale (Tracey et al., 2003), suggesting that a channel-proximate mechanism may underlie thermosensation. Support for this model comes from the recent study of the voltage dependence of TRPM8 and TRPV1 thermal responses, which concluded that thermal sensitivity is a consequence of voltage-dependent activation energies for channel opening and closing (Voets et al., 2004). Binding sites have been defined for capsaicin on TRPV1 (Jordt and Julius, 2002) and icilin on TRPM8 (Chuang et al., 2004); for both channels, sensitivity to these chemical agonists maps to the same TM2-TM3 loop region. Ligand binding shifts the voltage dependence of channel opening towards less-extreme thresholds, leading to a high open probability at room temperature. Future studies of thermosensitive TRP channel architecture and gating should clarify how the bound and unboundTM2-TM3 region influences voltage-dependent activity, and whether a similar principle might apply to other voltage-sensitive cation channels.

Lessons from *Drosophila*: lipids underlie phototransduction

Increasing evidence suggests that TRP channels can be modulated by lipids. This rapidly-progressing area of study draws strongly on lessons learned from *Drosophila* TRP. Fly phototransduction requires rhodopsin, Gαq, and phospholipase C (PLC) cleavage of the membrane lipid PIP_2 (Hardie, 2003). The identity of the second messenger(s) downstream of PLC was a controversial subject for many years: was inositol trisphosphate (IP_3) or diacylglycerol (DAG) the relevant second messenger, and did these molecules act directly or indirectly to activate TRP channels? Based on its function in other cells, IP_3 seemed likely to act by releasing Ca^{2+} from internal stores. However, analysis of fly eyes lacking the IP_3 receptor excludes IP_3 receptor-mediated Ca^{2+} release as a transduction mechanism (Acharya et al., 1997; Raghu et al., 2000).

This leaves the other product of PLC metabolism, DAG, as a strong candidate for a TRP modulator. Genetic evidence for the importance of DAG as a TRP modulator is provided by mutations in *rdgA* diacylglycerol kinase, which metabolizes DAG to phosphatidic acid. Mutations in *rdgA* increase DAG levels, and are capable of suppressing hypomorphic mutations in Gq or PLC (Hardie et al., 2002). In spite of this result, DAG itself need not be the second messenger; many lipids can be produced by DAG metabolism, including polyunsaturated fatty acids (PUFAs). Indeed, Hardie and colleagues demonstrated that application of the PUFAs arachidonic acid (AA, 20:4n6) and linolenic acid (LNA, 18:3n-3) to intact photoreceptors activates TRP and TRPL currents (Chyb et al., 1999). Exogenous LNA elicits currents even in photoreceptors lacking PLC (Hardie et al., 2003).

These genetic and electrophysiological data are consistent with LNA acting as a second messenger ligand for TRP, but are not conclusive. Direct interaction of LNA with TRP or TRPL was not demonstrated; the existence of a lipid binding site on the channel would provide strong support that lipids gate TRPs. In spite of intensive screening for *Drosophila* phototransduction mutants, alleles of DAG lipase (an enzyme which releases PUFAs from DAG) have not been identified. The *rolling blackout* membrane lipase acts in the PIP_2 hydrolysis pathway and has phototransduction defects, but its activity is more consistent with feedback regulation than with primary transduction (Huang et al., 2004). Enzymes that produce PUFA-derived second messengers such as endocannabinoids have not yet been implicated in *Drosophila* phototransduction. Specific genetic or biochemical depletion of DAG or PUFAs in fly photoreceptors would be predicted to eliminate light responses, but such data are lacking at present.

Loads of lipids modulate TRP channels *in vitro*

Studies with other TRP channels point to a consensus that lipids modulate TRPs, and in some cases address the gaps in the *Drosophila* phototransduction story. Most of these studies characterize the voltage or Ca^{2+} responses of heterologously-expressed channels, but do not address the activity of channels in a native context. Individual channels have been shown to respond to multiple lipids, raising the question of which lipids are relevant signaling molecules *in vivo*.

The membrane phospholipid PIP_2 binds to and activates cation channels, most notably the cytoplasmic C′ tail of inwardly-rectifying K^+ channels (Huang et al., 1998; Zhang et al., 1999). By analogy, PIP_2 binding represents a potential mechanism for TRP channel modulation by cell-intrinsic second messenger pathways. Indeed, depletion of plasma membrane PIP_2 by bradykinin or nerve growth factor PLC-coupled pathways potentiates TRPV1 pH, capsaicin, and temperature responses (Chuang et al., 2001). A PIP_2-responsive site was identified in the C′ region of TRPV1; replacement of the TRPV1 site with one from the IRK1 K^+ channel alters the chimeric channel's responses to capsaicin and temperature (Prescott and Julius, 2003). A non-sensory TRP channel, TRPM7, is regulated by PIP_2 in an opposite fashion: depletion of PIP_2 by activation of muscarinic acetylcholine receptor pathways or by a PIP_2 antibody inactivates TRPM7 single-channel activity, and PIP_2 addition promotes current recovery (Runnels et al., 2002). These two studies provide precedent for positive *or* negative regulation of TRP channels by membrane phospholipids, and directly demonstrate channel-phospholipid interactions. The TRPV1 study reveals a plausible molecular mechanism for the burning sensation associated with inflammation: bradykinin release depletes PIP_2, lowering the channel's thermal activation threshold to body temperature. TRPV1 in non-exposed tissues can thus transmit a burning percept – or, if the affected neurons map to brain areas that do not encode burning, topographic information about inflammation. The TRPV1 PIP_2 binding site is distinct from the capsaicin binding site; it will be interesting to see how the channel integrates voltage, PIP_2, and capsaicin binding, and to see if other lipids also interact with this channel region.

Numerous studies have also shown that DAG and its cell-permeable analogues can stimulate TRP family activity, particularly in heterologous expression systems. In patch-clamp studies, TRPC6 and TRPC3 currents are activated by certain DAG analogues in the 10-100 μM concentration range (Hofmann et al., 1999); TRPV1 is DAG-insensitive. Expression of TRPC7 in HEK 293 cells also results in enhanced DAG analogue currents (Okada et al., 1999). Heterologously-expressed TRPV4 is not sensitive to DAG analogues, although the phorbol ester compound 4α-phorbol 12,13-didecanoate (4α-PDD) activates Ca^{2+} responses independently of an effect on protein kinase C (Watanabe et al., 2002). Similarly, the cloned TRPA1 channel underlies an oleoyl-acetyl-glycerol-(OAG-) evoked Ca^{2+} influx, although the latency of this response seems inconsistent with rapid cellular signaling mechanisms (>200 sec) (Bandell et al., 2004). In one of the relatively few studies of mammalian TRP channels in their native context, DAG analogues activate a rapid (>1 sec) cation current in patches pulled from the dendritic tips of vomeronasal neurons (Lucas et al., 2003). Notably, this current is diminished in vomeronasal neurons from TRPC2-/- mice. The authors of that study used pharmacological approaches to suggest that DAG itself, and not a metabolite or IP_3 effect, is responsible for such responses. More studies using native channels, rather than expressed channels, will be helpful in establishing cellular contexts where DAG activates TRP channel currents.

DAG metabolism can produce numerous lipid signaling molecules, depending on the identity of specific acyl side chains. A promising and novel area of TRP signaling research has been the identification of candidate fatty acid

derivatives, including endocannabinoids, that may act as endogenous modulators of TRP channels. Endocannabinoids were initially appreciated as ligands for the cannabinoid receptors CB1 and CB2, but roles for these interesting molecules have been discovered in non-cannabinoid pathways. A role for endocannabinoids in modulating TRP channel activity was first noted in vasodilation studies: the arachidonic acid metabolite anandamide activates TRPV1 in sensory nerve preparations and in expression systems, causing release of the vasodilator neuropeptide CGRP (Zygmunt et al., 1999). Interestingly, a similar process of anandamide- andTRPV1-induced vasodilation has been proposed as a mechanism underlying migraine (Akerman et al., 2004).

Since the initial description of anandamide-TRPV1 interactions, a plethora of lipid signaling candidates have been tested on TRPV channels. The anandamide analogue and potential satiety factor oleoyl ethanolamide (which is also found in chocolate) can also activate expressed TRPV1 (Ahern, 2003), although a physiological role for this interaction has not been demonstrated. Various products of 12-lipoxygenase metabolism of AA induce TRPV1 currents in isolated DRG neurons (Hwang et al., 2000), but prostaglandins and certain PUFAs have no such effect. Yet another class of fatty acid derivatives, the endovanilloids N-arachidonoyldopamine and N-oleoyldopamine, can activate TRPV1 (Chu et al., 2003; Huang et al., 2002). TRPV4 is also responsive to anandamide and its precursor AA (Watanabe et al., 2003). This interaction is indirect, in that cytochrome P450 epoxygenase-mediated metabolism of AA yields the active epoxyeicosatrienoic acid ligand of native TRPV4 channels. Through these and related studies, it is clear that a broad structural class of molecules with polyunsaturated lipid side chains can modulate TRPV channels

(Figure 1-4). The structural similarity to capsaicin raises the possibility that all of these lipid ligands may interact with the same TM2-TM3 region of the channel. Although it is interesting to see candidate TRPV ligands that are found *in vivo* (as opposed to synthetic ligands like 4α-PDD or plant-derived compounds like capsaicin), most of these studies fall short of demonstrating cellular synthesis of these ligands in response to a physiological stimulus. It will be important to demonstrate which of these candidate lipid ligands actually modulate TRPV activity *in vivo*, and the structural basis of their interaction with the channel.

***C. elegans*: a model system for understanding TRP channel function**

The soil nematode *C. elegans* provides an opportunity to study TRP channel functions in their native, *in vivo* context. Worms have at least one member of each mammalian TRP subfamily (Figure 1-3), and mutants are available for many of these loci. Interestingly, many roles of *C. elegans* TRP channels have been studied in non-neural tissues, and may therefore provide insight into other cellular functions of mammalian relatives. The challenge of performing electrophysiological analysis in worms has necessitated alternate approaches; *C. elegans* studies of TRP channels have focused less on the molecular gating and biophysical properties of the channels, and more on their integration into cellular pathways and neural circuits. As such, they are a useful complement to biophysical and pharmacological studies of mammalian counterparts.

C. elegans TRPV channels in nociception

Worms have five members of the TRPV family: *osm-9*, *ocr-1*, *ocr-2*, *ocr-3*, and *ocr-4* (Colbert et al., 1997; Tobin et al., 2002). *osm-9* is 60% similar to *Drosophila inactive*, a candidate auditory channel (Gong et al., 2004). The transmembrane regions of *osm-9* and the *ocr* genes are 26% identical and 51% similar with rat TRPV1. *ocr-4* shares 37% identity and 55% similarity to the *Drosophila nanchung* mechanosensory channel, and 36% identity and 55% similarity to *ocr-3*. The other three full-length *ocr* genes are approximately 45% identical to one another, and ~28% identical to *osm-9*.

The founding member of this subfamily, *osm-9*, was identified in behavioral screens for mutants with defects in chemosensory and mechanosensory behaviors. Animals mutant for *osm-9* fail to detect repellents sensed by the ASH polymodal nociceptive neurons, including high osmolarity solutions, nose touch, benzaldehyde, and quinine (Colbert et al., 1997; Hilliard et al., 2002). *osm-9* is defective for AWA chemotaxis (Colbert et al., 1997), and for olfactory adaptation to a subset of odorants detected by the ciliated AWC neurons (Colbert and Bargmann, 1995). Finally, *osm-9* participates in transcriptional regulation of certain neuronal genes, including the *odr-10* diacetyl GPCR in AWA neurons and *tph-1* tryptophan hydroxylase, an enzyme essential for serotonin biosynthesis, in ADF (Chapter 3 of this dissertation; (Tobin et al., 2002; Zhang et al., 2004). *osm-9* is expressed in many *C. elegans* ciliated neurons, including most of the amphid sensory neurons, the phasmid neurons PHA and PHB, the OLQ, PVD, and FLP mechanosensory neurons, and the IL2 neurons. Expression is also seen in non-neural tissues, including rectal gland and uterine cells. GFP-tagged, functional OSM-9 proteins localize to neuronal sensory cilia,

consistent with a role in sensory transduction. Like their counterparts in *Drosophila* photoreceptors, *C. elegans* neurons appear to employ *osm-9* as a sensory transduction channel downstream of GPCRs and Gα proteins (Hilliard et al., 2004; Roayaie et al., 1998), although the molecular mechanism of *osm-9* gating is unclear. Its roles in detecting physical stimuli such as high osmolarity or nose touch suggest direct force sensation, while participation in AWA and ASH volatile repellent detection suggests activation by molecules downstream of GPCR activation.

Additional insight into the distinct cellular functions of TRPV channels came with the identification and characterization of the *ocr* subunits (Tobin et al., 2002). Each of the four *ocr* genes is more similar to one another than to *osm-9* or mammalian TRPV channels; the closest *Drosophila* relative is the mechanosensory channel *nanchung* (Kim et al., 2003). Animals mutant for *ocr-2* show AWA chemotaxis and ASH polymodal avoidance phenotypes similar to *osm-9*. *ocr-2* and *ocr-1* affect AWA transcriptional regulation of *odr-10*, and *ocr-2* participates in ADF regulation of *tph-1* expression (Zhang et al., 2004). The mutant phenotypes of *ocr-3* and *ocr-4* have not been described. Interestingly, *ocr* subunits are expressed in a subset of *osm-9* containing cells, as shown in Figure 1-5; all *ocr*-containing cells also have *osm-9* expression. In neurons such as AWA or ASH which express *osm-9* and at least one *ocr* subunit, TRPV channels are thought to function as the major sensory transduction conductance. By contrast, in cells with *osm-9* as the only TRPV subunit, other channels such as the TAX-2/TAX-4 cyclic nucleotide gated (CNG) channel appear to be responsible for primary sensory transduction (Coburn and Bargmann, 1996), and *osm-9* appears to have a modulatory role.

Like OSM-9, OCR-2 is localized to sensory cilia. OSM-9 and OCR-2 are mutually dependent for normal subcellular localization: in the absence of *ocr-2*, OSM-9 is found in the soma and *vice versa*. Ectopic expression of OCR-2 in AWC neurons is sufficient to drive OSM-9 to the cilia, where it is not normally detected. These findings are suggestive of a physical interaction between OSM-9 and OCR-2 subunits in certain sensory neurons, although there is no direct biochemical evidence for formation of a heteromeric *C. elegans* TRPV channel. The *Drosophila* TRP/TRPL and mammalian TRPC1/TRPC5 channels can form heteromers (Bahner et al., 2002; Strubing et al., 2001). If heteromer formation is a general property of TRP channels, distinct subunit combinations may have unique conductances, localization, modes of modulation, or sensory thresholds.

osm-9 and *ocr-2* also participate in the *npr-1*-dependent aggregation and bordering responses of *C. elegans* (de Bono et al., 2002). Some natural isolates of *C. elegans* forage on bacteria in a solitary manner, while others have a 'social' phenotype, and clump together on the borders of a bacterial lawn. Social feeders have a reduction-of-function allele of the neuropeptide Y receptor homologue *npr-1* (deBono and Bargmann, 1998). Mutations in *osm-9* or *ocr-2* suppress the bordering and clumping responses of *npr-1* mutants, and OCR-2 is specifically required in ASH or ADL neurons for this effect (de Bono et al., 2002). Clumping and bordering behaviors are an integrated response to volatile and gaseous aversive stimuli detected by multiple classes of sensory neurons. TRPV activity in ASH and ADL promotes social behavior in response to volatile cues associated with bacteria, while activity of a guanylyl cyclase/CNG channel pathway in the AQR, PQR, and URX neurons stimulates aggregation and bordering in hyperoxic environments (Gray et al., 2004). It will be interesting to see how TRPV-

dependent signaling pathways intersect with oxygen-sensing neural circuits to modulate social behavior in the presence of complex aversive stimuli.

Expression of mammalian TRPV channels in *C. elegans* can lead to behavioral responses, and has been used to characterize the specific sensory capacities of individual channel subunits. Rat TRPV1 fails to rescue the ASH nociception and AWA chemotaxis defects of *osm-9* or *ocr-2* mutants. Rather, it functions as a capsaicin-gated channel independent of native signal transduction pathways, generating ASH-appropriate avoidance behavior (Tobin et al., 2002). By contrast, expression of rat TRPV4 in ASH rescues the *osm-9* defect in sensing physical stimuli such as high osmolarity and nose touch, but not volatile odorants (Liedtke et al., 2003). TRPV4 function requires the endogenous ASH signaling molecules appropriate to each sensory modality, suggesting that it couples to ASH signal transduction pathways, rather than bypassing them. Certain differences between *osm-9* and TRPV4 are apparent, including TRPV4-dependent enhancement of nose touch avoidance responses at higher temperatures, and lower TRPV4 thresholds for detecting osmolarity. Thus, TRPV4 functions as an *osm-9* orthologue, while retaining a distinct sensory signature.

An important unsolved question in AWA and ASH TRPV signaling is how these channels are gated and modulated by cellular sensory transduction pathways. At present, OSM-9 and OCR-2 have not been amenable to electrophysiological analysis in a heterologous system. Genetic analysis has implicated G-proteins in activating worm TRPV channels, but there is no strong evidence for a phospholipase C role in activating *osm-9* or *ocr-2*. In chapter 2 of my dissertation, I demonstrate a role for PUFAs in modulating TRPV activity *in*

vivo. In chapter 3, I provide evidence for insulin and CaM kinase modulation of TRPV signaling, and identify a candidate gene that may be a component of TRPV pathways.

A candidate mechanosensory TRPN in *C. elegans*

nompC has been described as a sensory channel in mechanoreceptive cells of Drosophila and zebrafish (Sidi et al., 2003; Walker et al., 2000). The *C. elegans nompC* relative, Y71A12B.4/*trp-4*, has 45% identity/63% similarity to zebrafish *nompC*. A *trp-4*::GFP minigene is expressed in the CEP and ADE mechanosensory neurons, and in DVA and DVC interneurons (Walker et al., 2000). CEP and ADE are dopaminergic cells that detect the mechanosensory stimulus of a bacterial lawn, inducing the animal to move slowly in the presence of food (Sawin et al., 2000). DVA modulates mechanosensory circuits that mediate forwards and backwards movement (Driscoll and Kaplan, 1997); the function of DVC has not yet been described. Although the expression pattern and family history of *trp-4* is suggestive of a role in mechanotransduction, a *C. elegans* mutant is not yet available in this gene. Worms also have a TRPA family member, C29E6.2, with 88% identity to the candidate *Drosophila* thermosensory channel ANKTM1. No expression or phenotypic information is available for this intriguing gene.

TRPC, TRPM, and TRPP channels: a fertile field

A panoply of TRP channels are involved in multiple aspects of *C. elegans* fertility, including gonadogenesis, behavioral responses of males towards potential hermaphrodite mates, and sperm activation. Individual channels may

be detecting a specific type of physical force, conducting a specific ion flux, or transducing a fertility-associated odor cue in order to promote fertilization.

The TRPM subfamily member *gon-2* shares 40% identity / 58% similarity to human TRPM7, and is required during mid-larval stages for proper development of gonadal tissues (Sun and Lambie, 1997). By northern analysis, *gon-2* message is present even in animals lacking gonadal tissue, suggesting that this gene is expressed more broadly than the gonad precursor cells (West et al., 2001). There are two other TRPM subunits in *C. elegans*, *gtl-1* and *gtl-2*, whose functions and expression patterns have not been described. A genetic suppressor of *gon-2* reduction-of-function alleles, *gem-4*, was identified as a member of the copine family of Ca^{2+}-dependent phospholipid binding proteins (Church and Lambie, 2003). *gem-4* fails to suppress in a *gon-2* reduction-of-function, *gon-2*(RNAi) genetic background in which *gon-2* activity is minimized, suggesting that it acts by modulating GON-2 activity. *gem-4* contains C2 Ca^{2+} binding motifs and a Mg^{2+} binding domain, raising the possibility that *gon-2* promotes gonadogenesis by specifically promoting the flux of divalent cations. *gem-4* is expressed in non-gonad tissues, underscoring the possibility that the *gon-2* pathway functions in other, unknown developmental pathways.

The TRPP proteins and polycystin orthologues *pkd-2* and *lov-1* underlie the behavior that male worms exhibit when they encounter a hermaphrodite. Males use an elaborate sensory apparatus in their tail to execute a stereotyped search for the hermaphrodite vulva, followed by spicule insertion and sperm release (Liu and Sternberg, 1995). *lov-1* was identified in a screen for male mutants with defective responses to contact with a hermaphrodite, and is expressed in the cilia of the male-specific CEM, HOB, and ray neurons (Barr and

Sternberg, 1999). *pkd-2* was found to have the same expression pattern and behavioral defects as *lov-1*, whereas other TRP mutants such as *osm-9* or *gon-2* had no apparent role in male mating behavior (Barr et al., 2001). *pkd-2; lov-1* double mutants show the same behavioral defects as the single mutants, demonstrating that they function together in the same pathway. This is consistent with the function of mammalian polycystin-1 and polycystin-2 proteins, which physically interact in the sensory cilia of renal cells (Newby et al., 2002; Yoder et al., 2002). In spite of their sequence-level similarity, PKD-1 and PKD-2 proteins cannot functionally substitute for one another, suggesting that they serve distinct cellular functions, or are both required in a signaling complex.

TRPP channels have been hypothesized to serve as determinants of cilia structure, and as transducers of physical force. *C. elegans* studies appear to support a sensory signaling role, rather than a ciliogenesis function as worms mutant in either gene show normal ciliogenesis. Cilia localization is an obligate function of PKD-1 and PKD-2: in the *osm-5* ciliogenesis mutant, GFP-tagged channels are found in the stunted CEM cilia (Qin et al., 2001). PKD-1 and PKD-2 could comprise a physical sensor in the exposed ending of male tail neurons or contribute to detecting a chemical cue secreted by hermaphrodites. Analysis of additional mutants with similar male mating phenotypes, or identification of genetic suppressors of *pkd-1/pkd-2* mutations, should clarify if established signaling pathways couple to these channels.

A handful of studies have identified genes that may be involved in specification or function of *pkd-1/pkd-2* neurons. Expression of *pkd-1* and *pkd-2* is regulated by the transcription factor *egl-46*, which specifies the properties of several mechanosensory *C. elegans* neurons (Wu et al., 2001; Yu et al., 2003).

Recently, a microarray analysis identified four genes that are coexpressed with *pkd-1* and *pkd-2* in male-specific neurons (Portman and Emmons, 2004); the authors speculate that these novel, secreted proteins are components of an extracellular force-sensing matrix.

A third TRP family member, the TRPC protein *trp-3 / spe-41*, is found exclusively in sperm, and is required for a late step in fertilization (Xu and Sternberg, 2003). Male *trp-3* mutants are sterile, even though they execute mating behavioral programs, and have motile, morphologically normal sperm. Ca^{2+} imaging of normal sperm reveals *trp-3*-dependent Ca^{2+} influx after depletion of internal stores, suggesting that TRP-3 functions as a store-operated channel in *C. elegans* sperm. Heterologously-expressed TRP-3 responds to both store depletion and Gq pathway activation. Lipids such as AA or OAG do not stimulate *trp-3*-mediated Ca^{2+} entry in sperm, lending further support to store depletion as an important endogenous mechanism for channel activation. Studies of mammalian TRPC subunits have provided conflicting evidence about the role of Ca^{2+} stores in regulating this subfamily (Nilius, 2004), so it is gratifying to see a native TRPC protein functioning as a store-operated channel.

The subcellular localization of TRP-3 is developmentally-regulated, providing an additional layer of channel regulation (Xu and Sternberg, 2003). TRP-3 protein is found in vesicular compartments of immature spermatids, and translocates to the plasma membrane following sperm activation. Mammalian TRPC5 and *Drosophila* TRPL dynamically regulate their subcellular localization upon stimulation, providing temporal control over cellular excitability (Bahner et al., 2002; Bezzerides et al., 2004). Stage-specific surface expression may be an exciting common property of TRPC channels. It also is intriguing to note that

several TRPC subunits are expressed in human sperm, hinting that *C. elegans* and humans may share ancient cellular mechanisms of fertilization (Castellano et al., 2003).

C. elegans has two other TRPC proteins, *trp-1* and *trp-2*. *trp-1* is expressed in a variety of head motoneurons and interneurons, the BAG ciliated neurons, vulval muscle, and intestinal muscle (Colbert et al., 1997). The expression pattern of *trp-2* has not been defined, and mutant phenotypes have not been described for these two genes.

***cup-5*: a lysosomal TRP with links to apoptosis**

A final subfamily of TRP channels, the mucolipins, are implicated in the rare human familial lysosome disorder mucolipidosis type IV. Human patients exhibit early-onset mental retardation and ophthalmic defects, including retinal degeneration. Worms have one TRPML gene, *cup-5*, with 35% similarity and 57% identity to human TRPML3. *cup-5* missense mutants were characterized on the basis of an endocytosis defect in coelomocytes, scavenger cells that filter soluble proteins from the *C. elegans* body cavity (Fares and Greenwald, 2001). *cup-5* is found in neurons and coelomocytes; mutant animals have large coelomocyte vacuoles that correspond to aberrant late endosomes or lysosomes. Separately, a null *cup-5* allele was identified in a screen for the presence of cell corpses in an apoptosis-defective genetic background (Hersh et al., 2002). These animals arrest at an early step of development, and also show excess lysosomes and vacuoles as defined by dye uptake and electron microscopy. The CUP-5 protein exists in long and short forms, differing in a 57-amino acid C-terminal stretch. Both isoforms rescue the lethality of *cup-5* null mutants, as does

mammalian TRPML1 expressed from a heat-shock promoter. Similarly, coelomocyte expression of mammalian TRPML1 or TRPML3 rescues the endocytosis defect of *cup-5* missense mutants (Treusch et al., 2004). Thus, human and *C. elegans* mucolipins share a function in lysosome biogenesis, and worms may be a useful *in vivo* system for characterizing additional genes involved in mucolipin-dependent lysosomal disorders. Heterologously-expressed TRPML1 was recently shown to be a cation channel inhibited at low pH (Raychowdhury et al., 2004); perhaps a decrease in CUP-5/TRPML1 activity accompanies or defines the maturation of lysosomes.

As for the apoptosis defect in *cup-5* null mutants, the authors suggest that it is secondary to the *cup-5* defect in lysosome and vacuole formation. A worm TRPM subunit, *ced-11*, has been identified as an apoptosis mutant with abnormal cell corpses (Stanfield and Horvitz, personal communication), but the mechanism for this phenotype has not been described.

C. elegans TRPs and open questions

The diverse cellular functions of *C. elegans* TRP channels offer several avenues for illuminating outstanding questions in the TRP field.

Clarification of the *in vivo* mechanisms of TRP channel gating would complement the many electrophysiological and imaging studies performed in heterologous systems. Mammalian studies highlight a wide variety of natural and synthesized compounds that can activate TRP channels in expression systems, but there is relatively scant evidence of the nature of relevant gating molecules of channels in their native environment. It would be particularly interesting to learn which compounds and mechanisms regulate TRP channels in

non-exposed, non-sensory tissues, so as to better understand channel roles beyond sensation.

Further study of *trp-3* and sperm activation may resolve the controversy about whether TRPC channels are components of store-operated Ca^{2+} entry pathways in endogenous (and perhaps conserved?) cellular contexts. Worm sperm are amenable to genetic manipulation, imaging analysis, and motility studies. It would be interesting to know which events trigger store-operated Ca^{2+} entry in *C. elegans* sperm, and if other TRPC channels are also involved in this process.

osm-9 and *ocr-2* are well-suited for exploring receptor-mediated TRPV modulation *in vivo*, since they participate in sensory transduction pathways and behaviors downstream of known GPCRs. As described in chapter 2, behavioral and Ca^{2+} imaging analysis of PUFA synthesis mutants suggests that specific lipids modulate native TRPV channel. Electrophysiological analysis of TRPV-containing *C. elegans* neurons would strengthen my conclusions, and add support for additional mechanisms of modulation, including direct physical force sensing. Furthermore, *in vivo* analysis of chimeric worm-mammalian TRPV channels or worm subunits bearing mutations in key residues of the channel would clarify how regulatory pathways couple to channel architecture. Additional forward and reverse screens for mutants in TRPV pathways may reveal shared modulators of sensory signaling. It would also be interesting to know if the male-specific CEM neurons detect hermaphrodite-derived chemical mating cues, and if so, whether PKD-1 / PKD-2 channels are involved in a novel sensory transduction pathway.

C. elegans has been an outstanding system for studying degenerin channel-mediated mechanosensation *in vivo* (reviewed in Goodman and Schwarz, 2003); significant progress could be made towards understanding TRP-mediated force sensing as well. Worms detect mechanical stimuli through receptor neurons specialized for specific topographic regions of the body. TRPV-, TRPN-, and TRPP-expressing cells such as OLQ, FLP, CEP, ADE, and ray neurons participate in mechanosensory function, but the optimal sensory stimuli and cellular transduction mechanisms for these cells could be further clarified. It would be particularly interesting to learn if some of these cells and channels can mediate acute thermal responses, in addition to touch. An obstacle to studying some worm TRPV/TRPA/TRPN channels has been the lack of available mutants, but neuronally-sensitized genetic backgrounds for RNAi may alleviate that problem (Kennedy et al., 2004; Simmer et al., 2002).

An emerging question in the TRP field is the importance of channel trafficking for cellular function. When channels such as TRP-3, CUP-5, TRPC5, or TRPL are contained in intracellular compartments, are they merely sequestered, or actively passing cationic currents? TRP channels in intracellular compartments are in some cases capable of passing cation currents, as demonstrated by studies of the mechanosensitive yeast vacuolar/lysosomal channel Yvc1 (Zhou et al., 2003). Alternately, certain compartmentalized TRP subunits may be inactive, and unable to pass cation currents until deposited on the cell surface. It will be interesting to clarify the mechanisms of channel translocation to surface compartments, and whether TRP channels actively participate in the recognition and trafficking of channel-containing vesicles. Worm sperm and coelomocytes are amenable to genetic manipulation and

accessible for Ca^{2+} imaging studies, making them a potentially useful system for exploring these questions with multiple approaches.

Why worms?

In conclusion, *in vivo* study of *C. elegans* TRP channels creates a physiological context for the detailed pharmacological and biophysical studies of mammalian TRPs. A similar logic can be extended to members of other neuronal gene families, where the complexity and experimental inaccessibility of brain regions limits the questions that can be asked in mammals. Once an ion channel or other sensory component has been implicated in a specific worm sensory modality and behavior, testable analogies can be drawn to related functions in more complex tissues and pathways. As bioinformatics studies reveal an increasing number of novel, conserved genes in mammals, *C. elegans* studies will be increasingly useful for clarifying these molecules' signaling partners and cellular roles. Worms may seem small and simple, but their minimalist neural network is a powerful resource for understanding perception – the foundation of our awareness and remembrance -- in exquisite molecular detail.

References:

Acharya, J. K., Jalink, K., Hardy, R. W., Hartenstein, V., and Zuker, C. S. (1997). $InsP_3$ receptor is essential for growth and differentiation but not for vision in *Drosophila*. Neuron *18*, 881-887.

Ahern, G. P. (2003). Activation of TRPV1 by the satiety factor oleoylethanolamide. J Biol Chem *278*, 30429-30434.

Akerman, S., Kaube, H., and Goadsby, P. J. (2004). Anandamide acts as a vasodilator of dural blood vessels in vivo by activating TRPV1 receptors. Br J Pharmacol *142*, 1354-1360.

Anavi-Goffer, S., and Coutts, A. A. (2003). Cellular distribution of vanilloid VR1 receptor immunoreactivity in the guinea-pig myenteric plexus. Eur J Pharmacol *458*, 61-71.

Andersson, D. A., Chase, H. W., and Bevan, S. (2004). TRPM8 activation by menthol, icilin, and cold is differentially modulated by intracellular pH. J Neurosci *24*, 5364-5369.

Avelino, A., Cruz, C., Nagy, I., and Cruz, F. (2002). Vanilloid receptor 1 expression in the rat urinary tract. Neuroscience *109*, 787-798.

Bahner, M., Frechter, S., Da Silva, N., Minke, B., Paulsen, R., and Huber, A. (2002). Light-regulated subcellular translocation of *Drosophila* TRPL channels induces long-term adaptation and modifies the light-induced current. Neuron *34*, 83-93.

Bandell, M., Story, G. M., Hwang, S. W., Viswanath, V., Eid, S. R., Petrus, M. J., Earley, T. J., and Patapoutian, A. (2004). Noxious cold ion channel TRPA1 is activated by pungent compounds and bradykinin. Neuron *41*, 849-857.

Bargmann, C. I., Hartwieg, E., and Horvitz, H. R. (1993). Odorant-selective genes and neurons mediate olfaction in *C. elegans*. Cell *74*, 515-527.

Bargmann, C. I., and Horvitz, H. R. (1991). Chemosensory neurons with overlapping functions direct chemotaxis to multiple chemicals in *C. elegans*. Neuron *7*, 729-742.

Barr, M. M., DeModena, J., Braun, D., Nguyen, C. Q., Hall, D. H., and Sternberg, P. W. (2001). The *Caenorhabditis elegans* autosomal dominant polycystic kidney disease gene homologs *lov-1* and *pkd-2* act in the same pathway. Curr Biol *11*, 1341-1346.

Barr, M. M., and Sternberg, P. W. (1999). A polycystic kidney-disease gene homologue required for male mating behaviour in *C. elegans*. Nature *401*, 386-389.

Bezzerides, V. J., Ramsey, I. S., Kotecha, S., Greka, A., and Clapham, D. E. (2004). Rapid vesicular translocation and insertion of TRP channels. Nat Cell Biol *6*, 709-720.

Brenner, S. (1974). The genetics of *Caenorhabditis elegans*. Genetics *77*, 71-94.

Castellano, L. E., Trevino, C. L., Rodriguez, D., Serrano, C. J., Pacheco, J., Tsutsumi, V., Felix, R., and Darszon, A. (2003). Transient receptor potential (TRPC) channels in human sperm: expression, cellular localization and involvement in the regulation of flagellar motility. FEBS Lett *541*, 69-74.

Caterina, M. J., Rosen, T. A., Tominaga, M., Brake, A. J., and Julius, D. (1999). A capsaicin-receptor homologue with a high threshold for noxious heat. Nature *398*, 436-441.

Caterina, M. J., Schumacher, M. A., Tominaga, M., Rosen, T. A., Levine, J. D., and Julius, D. (1997). The capsaicin receptor: a heat-activated ion channel in the pain pathway. Nature *389*, 816-824.

Chu, C. J., Huang, S. M., De Petrocellis, L., Bisogno, T., Ewing, S. A., Miller, J. D., Zipkin, R. E., Daddario, N., Appendino, G., Di Marzo, V., and Walker, J. M. (2003). N-oleoyldopamine, a novel endogenous capsaicin-like lipid that produces hyperalgesia. J Biol Chem *278*, 13633-13639.

Chuang, H. H., Neuhausser, W. M., and Julius, D. (2004). The super-cooling agent icilin reveals a mechanism of coincidence detection by a temperature-sensitive TRP channel. Neuron *43*, 859-869.

Chuang, H. H., Prescott, E. D., Kong, H., Shields, S., Jordt, S. E., Basbaum, A. I., Chao, M. V., and Julius, D. (2001). Bradykinin and nerve growth factor release the capsaicin receptor from PtdIns(4,5)P2-mediated inhibition. Nature *411*, 957-962.

Chung, M. K., Lee, H., and Caterina, M. J. (2003). Warm temperatures activate TRPV4 in mouse 308 keratinocytes. J Biol Chem *278*, 32037-32046.

Church, D. L., and Lambie, E. J. (2003). The promotion of gonadal cell divisions by the *Caenorhabditis elegans* TRPM cation channel GON-2 is antagonized by GEM-4 copine. Genetics *165*, 563-574.

Chyb, S., Raghu, P., and Hardie, R. C. (1999). Polyunsaturated fatty acids activate the *Drosophila* light-sensitive channels TRP and TRPL. Nature *397*, 255-259.

Clapham, D. E. (2003). TRP channels as cellular sensors. Nature *426*, 517-524.

Coburn, C. M., and Bargmann, C. I. (1996). A putative cyclic nucleotide-gated channel is required for sensory development and function in *C. elegans*. Neuron *17*, 695-706.

Colbert, H. A., and Bargmann, C. I. (1995). Odorant-specific adaptation pathways generate olfactory plasticity in *C. elegans*. Neuron *14*, 803-812.

Colbert, H. A., Smith, T. L., and Bargmann, C. I. (1997). OSM-9, A novel protein with structural similarity to channels, is required for olfaction, mechanosensation, and olfactory adaptation in *Caenorhabditis elegans*. Journal of Neuroscience *17*, 8259-8269.

Corey, D. P., Garcia-Anoveros, J., Holt, J. R., Kwan, K. Y., Lin, S. Y., Vollrath, M. A., Amalfitano, A., Cheung, E. L., Derfler, B. H., Duggan, A., *et al.* (2004). TRPA1 is a candidate for the mechanosensitive transduction channel of vertebrate hair cells. Nature *432*, 723-730.

Corey, D. P., and Hudspeth, A. J. (1979). Response latency of vertebrate hair cells. Biophys J *26*, 499-506.

de Bono, M., Tobin, D. M., Davis, M. W., Avery, L., and Bargmann, C. I. (2002). Social feeding in *Caenorhabditis elegans* is induced by neurons that detect aversive stimuli. Nature *419*, 899-903.

deBono, M., and Bargmann, C. I. (1998). Natural variation in a neuropeptide Y receptor homolog modifies social behaviot and food response in *C. elegans*. Cell *94*, 679-689.

Dulac, C., and Torello, A. T. (2003). Molecular detection of pheromone signals in mammals: from genes to behaviour. Nat Rev Neurosci *4*, 551-562.

Fares, H., and Greenwald, I. (2001). Regulation of endocytosis by CUP-5, the *Caenorhabditis elegans* mucolipin-1 homolog. Nat Genet *28*, 64-68.

Firestein, S. (2001). How the olfactory system makes sense of scents. Nature *413*, 211-218.

Gonzalez-Perrett, S., Kim, K., Ibarra, C., Damiano, A. E., Zotta, E., Batelli, M., Harris, P. C., Reisin, I. L., Arnaout, M. A., and Cantiello, H. F. (2001). Polycystin-2, the protein mutated in autosomal dominant polycystic kidney disease (ADPKD), is a Ca2+-permeable nonselective cation channel. Proc Natl Acad Sci U S A *98*, 1182-1187.

Goodman, M. B., and Schwarz, E. M. (2003). Transducing touch in *Caenorhabditis elegans*. Annu Rev Physiol *65*, 429-452.

Gray, J. M., Karow, D. S., Lu, H., Chang, A. J., Chang, J. S., Ellis, R. E., Marletta, M. A., and Bargmann, C. I. (2004). Oxygen sensation and social feeding mediated by a *C. elegans* guanylate cyclase homologue. Nature *430*, 317-322.

Guler, A. D., Lee, H., Iida, T., Shimizu, I., Tominaga, M., and Caterina, M. (2002). Heat-evoked activation of the ion channel, TRPV4. J Neurosci *22*, 6408-6414.

Hardie, R. C. (2001). Phototransduction in *Drosophila melanogaster*. J Exp Biol *204*, 3403-3409.

Hardie, R. C. (2003). Regulation of TRP channels via lipid second messengers. Annu Rev Physiol *65*, 735-759.

Hardie, R. C., Martin, F., Chyb, S., and Raghu, P. (2003). Rescue of light responses in the *Drosophila* "null" phospholipase C mutant, *norpAP24*, by the diacylglycerol kinase mutant, *rdgA*, and by metabolic inhibition. J Biol Chem *278*, 18851-18858.

Hardie, R. C., Martin, F., Cochrane, G. W., Juusola, M., Georgiev, P., and Raghu, P. (2002). Molecular basis of amplification in *Drosophila* phototransduction: roles for G protein, phospholipase C, and diacylglycerol kinase. Neuron *36*, 689-701.

Hardie, R. C., and Minke, B. (1992). The *trp* gene is essential for a light-activated Ca^{2+} channel in *Drosophila* photoreceptors. Neuron *8*, 643-651.

Hassock, S. R., Zhu, M. X., Trost, C., Flockerzi, V., and Authi, K. S. (2002). Expression and role of TRPC proteins in human platelets: evidence that TRPC6 forms the store-independent calcium entry channel. Blood *100*, 2801-2811.

Hersh, B. M., Hartwieg, E., and Horvitz, H. R. (2002). The *Caenorhabditis elegans* mucolipin-like gene *cup-5* is essential for viability and regulates lysosomes in multiple cell types. Proc Natl Acad Sci U S A *99*, 4355-4360.

Hilliard, M. A., Bargmann, C. I., and Bazzicalupo, P. (2002). *C. elegans* Responds to Chemical Repellents by Integrating Sensory Inputs from the Head and the Tail. Curr Biol *12*, 730-734.

Hilliard, M. A., Bergamasco, C., Arbucci, S., Plasterk, R. H., and Bazzicalupo, P. (2004). Worms taste bitter: ASH neurons, QUI-1, GPA-3 and ODR-3 mediate quinine avoidance in *Caenorhabditis elegans*. Embo J *23*, 1101-1111.

Hofmann, T., Chubanov, V., Gudermann, T., and Montell, C. (2003). TRPM5 is a voltage-modulated and Ca(2+)-activated monovalent selective cation channel. Curr Biol *13*, 1153-1158.

Hofmann, T., Obukhov, A. G., Schaefer, M., Harteneck, C., Gudermann, T., and Schultz, G. (1999). Direct activation of human TRPC6 and TRPC3 channels by diacylglycerol. Nature *397*, 259-263.

Howard, J., and Bechstedt, S. (2004). Hypothesis: a helix of ankyrin repeats of the NOMPC-TRP ion channel is the gating spring of mechanoreceptors. Curr Biol *14*, R224-226.

Huang, C. L., Feng, S., and Hilgemann, D. W. (1998). Direct activation of inward rectifier potassium channels by PIP2 and its stabilization by Gbetagamma. Nature *391*, 803-806.

Huang, F. D., Matthies, H. J., Speese, S. D., Smith, M. A., and Broadie, K. (2004). *Rolling blackout*, a newly identified PIP2-DAG pathway lipase required for *Drosophila* phototransduction. Nat Neurosci *7*, 1070-1078.

Huang, S. M., Bisogno, T., Trevisani, M., Al-Hayani, A., De Petrocellis, L., Fezza, F., Tognetto, M., Petros, T. J., Krey, J. F., Chu, C. J., *et al.* (2002). An endogenous capsaicin-like substance with high potency at recombinant and native vanilloid VR1 receptors. Proc Natl Acad Sci U S A *99*, 8400-8405.

Hwang, S. W., Cho, H., Kwak, J., Lee, S. Y., Kang, C. J., Jung, J., Cho, S., Min, K. H., Suh, Y. G., Kim, D., and Oh, U. (2000). Direct activation of capsaicin receptors by products of lipoxygenases: endogenous capsaicin-like substances. Proc Natl Acad Sci U S A *97*, 6155-6160.

Jordt, S. E., Bautista, D. M., Chuang, H. H., McKemy, D. D., Zygmunt, P. M., Hogestatt, E. D., Meng, I. D., and Julius, D. (2004). Mustard oils and cannabinoids excite sensory nerve fibres through the TRP channel ANKTM1. Nature *427*, 260-265.

Jordt, S. E., and Julius, D. (2002). Molecular basis for species-specific sensitivity to "hot" chili peppers. Cell *108*, 421-430.

Kennedy, S., Wang, D., and Ruvkun, G. (2004). A conserved siRNA-degrading RNase negatively regulates RNA interference in *C. elegans*. Nature *427*, 645-649.

Kim, J., Chung, Y. D., Park, D. Y., Choi, S., Shin, D. W., Soh, H., Lee, H. W., Son, W., Yim, J., Park, C. S., *et al.* (2003). A TRPV family ion channel required for hearing in *Drosophila*. Nature *424*, 81-84.

L'Etoile, N. D., and Bargmann, C. I. (2000). Olfaction and odor discrimination are mediated by the *C. elegans* guanylyl cyclase ODR-1. Neuron *25*, 575-586.

Leypold, B. G., Yu, C. R., Leinders-Zufall, T., Kim, M. M., Zufall, F., and Axel, R. (2002). Altered sexual and social behaviors in trp2 mutant mice. Proc Natl Acad Sci U S A *99*, 6376-6381.

Liedtke, W., Choe, Y., Marti-Renom, M. A., Bell, A. M., Denis, C. S., Sali, A., Hudspeth, A. J., Friedman, J. M., and Heller, S. (2000). Vanilloid receptor-related osmotically activated channel (VR-OAC), a candidate vertebrate osmoreceptor. Cell *103*, 525-535.

Liedtke, W., and Friedman, J. M. (2003). Abnormal osmotic regulation in trpv4-/- mice. Proc Natl Acad Sci U S A *100*, 13698-13703.

Liedtke, W., Tobin, D. M., Bargmann, C. I., and Friedman, J. M. (2003). Mammalian TRPV4 (VR-OAC) directs behavioral responses to osmotic and mechanical stimuli in *Caenorhabditis elegans*. Proc Natl Acad Sci U S A *100 Suppl 2*, 14531-14536.

Liman, E. R., Corey, D. P., and Dulac, C. (1999). TRP2: a candidate transduction channel for mammalian pheromone sensory signaling. Proc Natl Acad Sci USA *96*, 5791-5796.

Liu, D., and Liman, E. R. (2003). Intracellular Ca2+ and the phospholipid PIP2 regulate the taste transduction ion channel TRPM5. Proc Natl Acad Sci U S A *100*, 15160-15165.

Liu, K. S., and Sternberg, P. W. (1995). Sensory regulation of male mating behavior in *Caenorhabditis elegans*. Neuron *14*, 79-89.

Lucas, P., Ukhanov, K., Leinders-Zufall, T., and Zufall, F. (2003). A diacylglycerol-gated cation channel in vomeronasal neuron dendrites is impaired in TRPC2 mutant mice: mechanism of pheromone transduction. Neuron *40*, 551-561.

Luo, Y., Vassilev, P. M., Li, X., Kawanabe, Y., and Zhou, J. (2003). Native polycystin 2 functions as a plasma membrane Ca2+-permeable cation channel in renal epithelia. Mol Cell Biol *23*, 2600-2607.

McKemy, D. D., Neuhausser, W. M., and Julius, D. (2002). Identification of a cold receptor reveals a general role for TRP channels in thermosensation. Nature *416*, 52-58.

Mezey, E., Toth, Z. E., Cortright, D. N., Arzubi, M. K., Krause, J. E., Elde, R., Guo, A., Blumberg, P. M., and Szallasi, A. (2000). Distribution of mRNA for vanilloid receptor subtype 1 (VR1), and VR1-like immunoreactivity, in the central nervous system of the rat and human. Proc Natl Acad Sci U S A *97*, 3655-3660.

Mizuno, A., Matsumoto, N., Imai, M., and Suzuki, M. (2003). Impaired osmotic sensation in mice lacking TRPV4. Am J Physiol Cell Physiol *285*, C96-101.

Mochizuki, T., Wu, G., Hayashi, T., Xenophontos, S. L., Veldhuisen, B., Saris, J. J., Reynolds, D. M., Cai, Y., Gabow, P. A., Pierides, A., *et al.* (1996). PKD2, a gene for polycystic kidney disease that encodes an integral membrane protein. Science *272*, 1339-1342.

Montell, C. (2003). The venerable inveterate invertebrate TRP channels. Cell Calcium *33*, 409-417.

Montell, C., Birnbaumer, L., Flockerzi, V., Bindels, R. J., Bruford, E. A., Caterina, M. J., Clapham, D. E., Harteneck, C., Heller, S., Julius, D., *et al.* (2002). A unified nomenclature for the superfamily of TRP cation channels. Mol Cell *9*, 229-231.

Montell, C., and Rubin, G. M. (1989). Molecular characterization of the *Drosophila trp* locus: a putative integral membrane protein required for phototransduction. Neuron *2*, 1313-1323.

Newby, L. J., Streets, A. J., Zhao, Y., Harris, P. C., Ward, C. J., and Ong, A. C. (2002). Identification, characterization, and localization of a novel kidney polycystin-1-polycystin-2 complex. J Biol Chem *277*, 20763-20773.

Nilius, B. (2004). Store-operated Ca2+ entry channels: still elusive! Sci STKE *2004*, pe36.

Okada, T., Inoue, R., Yamazaki, K., Maeda, A., Kurosaki, T., Yamakuni, T., Tanaka, I., Shimizu, S., Ikenaka, K., Imoto, K., and Mori, Y. (1999). Molecular and functional characterization of a novel mouse transient receptor potential protein homologue TRP7. Ca(2+)-permeable cation channel that is constitutively activated and enhanced by stimulation of G protein-coupled receptor. J Biol Chem *274*, 27359-27370.

Peier, A. M., Moqrich, A., Hergarden, A. C., Reeve, A. J., Andersson, D. A., Story, G. M., Earley, T. J., Dragoni, I., McIntyre, P., Bevan, S., and Patapoutian, A. (2002a). A TRP channel that senses cold stimuli and menthol. Cell *108*, 705-715.

Peier, A. M., Reeve, A. J., Andersson, D. A., Moqrich, A., Earley, T. J., Hergarden, A. C., Story, G. M., Colley, S., Hogenesch, J. B., McIntyre, P., *et al.* (2002b). A heat-sensitive TRP channel expressed in keratinocytes. Science *296*, 2046-2049.

Perez, C. A., Huang, L., Rong, M., Kozak, J. A., Preuss, A. K., Zhang, H., Max, M., and Margolskee, R. F. (2002). A transient receptor potential channel expressed in taste receptor cells. Nat Neurosci *5*, 1169-1176.

Phillips, A. M., Bull, A., and Kelly, L. E. (1992). Identification of a *Drosophila* gene encoding a calmodulin-binding protein with homology to the *trp* phototransduction gene. Neuron *8*, 631-642.

Portman, D. S., and Emmons, S. W. (2004). Identification of *C. elegans* sensory ray genes using whole-genome expression profiling. Dev Biol *270*, 499-512.

Prawitt, D., Enklaar, T., Klemm, G., Gartner, B., Spangenberg, C., Winterpacht, A., Higgins, M., Pelletier, J., and Zabel, B. (2000). Identification and characterization of MTR1, a novel gene with homology to melastatin (MLSN1) and the trp gene family located in the BWS-WT2 critical region on chromosome 11p15.5 and showing allele-specific expression. Hum Mol Genet *9*, 203-216.

Prawitt, D., Monteilh-Zoller, M. K., Brixel, L., Spangenberg, C., Zabel, B., Fleig, A., and Penner, R. (2003). TRPM5 is a transient Ca2+-activated cation channel responding to rapid changes in [Ca2+]i. Proc Natl Acad Sci U S A *100*, 15166-15171.

Prescott, E. D., and Julius, D. (2003). A modular PIP2 binding site as a determinant of capsaicin receptor sensitivity. Science *300*, 1284-1288.

Qin, H., Rosenbaum, J. L., and Barr, M. M. (2001). An autosomal recessive polycystic kidney disease gene homolog is involved in intraflagellar transport in *C. elegans* ciliated sensory neurons. Curr Biol *11*, 457-461.

Raghu, P., Colley, N. J., Webel, R., James, T., Hasan, G., Danin, M., Selinger, Z., and Hardie, R. C. (2000). Normal phototransduction in *Drosophila* photoreceptors lacking an InsP(3) receptor gene. Mol Cell Neurosci *15*, 429-445.

Raychowdhury, M. K., Gonzalez-Perrett, S., Montalbetti, N., Timpanaro, G. A., Chasan, B., Goldmann, W. H., Stahl, S., Cooney, A., Goldin, E., and Cantiello, H. F. (2004). Molecular pathophysiology of mucolipidosis type IV: pH dysregulation of the mucolipin-1 cation channel. Hum Mol Genet *13*, 617-627.

Roayaie, K., Crump, J. G., Sagasti, A., and Bargmann, C. I. (1998). The Ga protein ODR-3 mediates olfactory and nociceptive function and controls cilium morphogenesis in *C. elegans* olfactory neurons. Neuron *20*, 55-67.

Runnels, L. W., Yue, L., and Clapham, D. E. (2002). The TRPM7 channel is inactivated by PIP(2) hydrolysis. Nat Cell Biol *4*, 329-336.

Sawin, E. R., Ranganathan, R., and Horvitz, H. R. (2000). *C. elegans* locomotory rate is modulated by the environment through a dopaminergic pathway and by experience through a serotonergic pathway. Neuron *26*, 619-631.

Sengupta, P., Chou, J. H., and Bargmann, C. I. (1996). *odr-10* encodes a seven transmembrane domain olfactory receptor required for responses to the odorant diacetyl. Cell *84*, 899-909.

Sengupta, P., Colbert, H. A., and Bargmann, C. I. (1994). The *C. elegans* gene *odr-7* encodes an olfactory-specific member of the nuclear receptor superfamily. Cell *79*, 971-980.

Sidi, S., Friedrich, R. W., and Nicolson, T. (2003). NompC TRP channel required for vertebrate sensory hair cell mechanotransduction. Science *301*, 96-99.

Simmer, F., Tijsterman, M., Parrish, S., Koushika, S. P., Nonet, M. L., Fire, A., Ahringer, J., and Plasterk, R. H. (2002). Loss of the putative RNA-directed RNA polymerase RRF-3 makes *C. elegans* hypersensitive to RNAi. Curr Biol *12*, 1317-1319.

Smith, G. D., Gunthorpe, M. J., Kelsell, R. E., Hayes, P. D., Reilly, P., Facer, P., Wright, J. E., Jerman, J. C., Walhin, J. P., Ooi, L., *et al.* (2002). TRPV3 is a temperature-sensitive vanilloid receptor-like protein. Nature *418*, 186-190.

Story, G. M., Peier, A. M., Reeve, A. J., Eid, S. R., Mosbacher, J., Hricik, T. R., Earley, T. J., Hergarden, A. C., Andersson, D. A., Hwang, S. W., *et al.* (2003). ANKTM1, a TRP-like channel expressed in nociceptive neurons, is activated by cold temperatures. Cell *112*, 819-829.

Stowers, L., Holy, T. E., Meister, M., Dulac, C., and Koentges, G. (2002). Loss of sex discrimination and male-male aggression in mice deficient for TRP2. Science *295*, 1493-1500.

Strotmann, R., Harteneck, C., Nunnenmacher, K., Schultz, G., and Plant, T. D. (2000). OTRPC4, a nonselective cation channel that confers sensitivity to extracellular osmolarity. Nat Cell Biol *2*, 695-702.

Strubing, C., Krapivinsky, G., Krapivinsky, L., and Clapham, D. E. (2001). TRPC1 and TRPC5 form a novel cation channel in mammalian brain. Neuron *29*, 645-655.

Sun, A. Y., and Lambie, E. J. (1997). *gon-2*, a gene required for gonadogenesis in *Caenorhabditis elegans*. Genetics *147*, 1077-1089.

Sun, M., Goldin, E., Stahl, S., Falardeau, J. L., Kennedy, J. C., Acierno, J. S., Jr., Bove, C., Kaneski, C. R., Nagle, J., Bromley, M. C., *et al.* (2000). Mucolipidosis type IV is caused by mutations in a gene encoding a novel transient receptor potential channel. Hum Mol Genet *9*, 2471-2478.

Suzuki, M., Mizuno, A., Kodaira, K., and Imai, M. (2003). Impaired pressure sensation in mice lacking TRPV4. J Biol Chem *278*, 22664-22668.

Tobin, D., Madsen, D., Kahn-Kirby, A., Peckol, E., Moulder, G., Barstead, R., Maricq, A., and Bargmann, C. (2002). Combinatorial expression of TRPV channel proteins defines their sensory functions and subcellular localization in *C. elegans* neurons. Neuron *35*, 307-318.

Tominaga, M., Caterina, M. J., Malmberg, A. B., Rosen, T. A., Gilbert, H., Skinner, K., Raumann, B. E., Basbaum, A. I., and Julius, D. (1998). The cloned capsaicin receptor integrates multiple pain-producing stimuli. Neuron *21*, 531-543.

Tracey, W. D., Jr., Wilson, R. I., Laurent, G., and Benzer, S. (2003). *painless*, a *Drosophila* gene essential for nociception. Cell *113*, 261-273.

Treusch, S., Knuth, S., Slaugenhaupt, S. A., Goldin, E., Grant, B. D., and Fares, H. (2004). *Caenorhabditis elegans* functional orthologue of human protein h-mucolipin-1 is required for lysosome biogenesis. Proc Natl Acad Sci U S A *101*, 4483-4488.

Tsavaler, L., Shapero, M. H., Morkowski, S., and Laus, R. (2001). Trp-p8, a novel prostate-specific gene, is up-regulated in prostate cancer and other malignancies and shares high homology with transient receptor potential calcium channel proteins. Cancer Res *61*, 3760-3769.

Viswanath, V., Story, G. M., Peier, A. M., Petrus, M. J., Lee, V. M., Hwang, S. W., Patapoutian, A., and Jegla, T. (2003). Opposite thermosensor in fruitfly and mouse. Nature *423*, 822-823.

Voets, T., Droogmans, G., Wissenbach, U., Janssens, A., Flockerzi, V., and Nilius, B. (2004). The principle of temperature-dependent gating in cold- and heat-sensitive TRP channels. Nature *430*, 748-754.

Walker, R. G., Willingham, A. T., and Zuker, C. S. (2000). A *Drosophila* mechanosensory transduction channel. Science *287*, 2229-2234.

Ward, S. M., Bayguinov, J., Won, K. J., Grundy, D., and Berthoud, H. R. (2003). Distribution of the vanilloid receptor (VR1) in the gastrointestinal tract. J Comp Neurol *465*, 121-135.

Watanabe, H., Davis, J. B., Smart, D., Jerman, J. C., Smith, G. D., Hayes, P., Vriens, J., Cairns, W., Wissenbach, U., Prenen, J., *et al.* (2002). Activation of TRPV4 channels (hVRL-2/mTRP12) by phorbol derivatives. J Biol Chem *277*, 13569-13577.

Watanabe, H., Vriens, J., Prenen, J., Droogmans, G., Voets, T., and Nilius, B. (2003). Anandamide and arachidonic acid use epoxyeicosatrienoic acids to activate TRPV4 channels. Nature *424*, 434-438.

Watnick, T. J., Jin, Y., Matunis, E., Kernan, M. J., and Montell, C. (2003). A flagellar polycystin-2 homolog required for male fertility in *Drosophila*. Curr Biol *13*, 2179-2184.

West, R. J., Sun, A. Y., Church, D. L., and Lambie, E. J. (2001). The *C. elegans gon-2* gene encodes a putative TRP cation channel protein required for mitotic cell cycle progression. Gene *266*, 103-110.

White, J. G., Southgate, E., Thomson, J. N., and Brenner, S. (1986). The Structure of the Nervous System of the Nematode *Caenorhabditis elegans*. Phil Trans Royal Soc London Series B, Biol Scien *314*, 1-340.

Wu, J., Duggan, A., and Chalfie, M. (2001). Inhibition of touch cell fate by *egl-44* and *egl-46* in *C. elegans*. Genes Dev *15*, 789-802.

Xu, H., Ramsey, I. S., Kotecha, S. A., Moran, M. M., Chong, J. A., Lawson, D., Ge, P., Lilly, J., Silos-Santiago, I., Xie, Y., *et al.* (2002). TRPV3 is a calcium-permeable temperature-sensitive cation channel. Nature *418*, 181-186.

Xu, X. Z., and Sternberg, P. W. (2003). A *C. elegans* sperm TRP protein required for sperm-egg interactions during fertilization. Cell *114*, 285-297.

Yoder, B. K., Hou, X., and Guay-Woodford, L. M. (2002). The polycystic kidney disease proteins, polycystin-1, polycystin-2, polaris, and cystin, are co-localized in renal cilia. J Am Soc Nephrol *13*, 2508-2516.

Yu, H., Pretot, R. F., Burglin, T. R., and Sternberg, P. W. (2003). Distinct roles of transcription factors EGL-46 and DAF-19 in specifying the functionality of a polycystin-expressing sensory neuron necessary for *C. elegans* male vulva location behavior. Development *130*, 5217-5227.

Zahner, M. R., Li, D. P., Chen, S. R., and Pan, H. L. (2003). Cardiac vanilloid receptor 1-expressing afferent nerves and their role in the cardiogenic sympathetic reflex in rats. J Physiol *551*, 515-523.

Zhang, H., He, C., Yan, X., Mirshahi, T., and Logothetis, D. E. (1999). Activation of inwardly rectifying K+ channels by distinct PtdIns(4,5)P2 interactions. Nat Cell Biol *1*, 183-188.

Zhang, S., Sokolchik, I., Blanco, G., and Sze, J. Y. (2004). *Caenorhabditis elegans* TRPV ion channel regulates 5HT biosynthesis in chemosensory neurons. Development *131*, 1629-1638.

Zhang, Y., Hoon, M. A., Chandrashekar, J., Mueller, K. L., Cook, B., Wu, D., Zuker, C. S., and Ryba, N. J. (2003). Coding of sweet, bitter, and umami tastes: different receptor cells sharing similar signaling pathways. Cell *112*, 293-301.

Zygmunt, P. M., Petersson, J., Andersson, D. A., Chuang, H.-h., Sorgard, M., Marzo, V. D., Julius, D., and Hogestatt, E. D. (1999). Vanilloid receptors on sensory nerves mediate the vasodilator action of anandamide. Nature *400*, 452-457.

Figure 1-1: Chemosensory transduction pathways in *C. elegans*

A. Sensory transduction pathway for volatile attractants in the AWC neuron. Activation of a GPCR stimulates the Gα ODR-3, which couples to ODR-1/DAF-11 guanylyl cyclase. Production of cyclic GMP gates the TAX-2/TAX-4 channel, leading to neuronal depolarization and chemotaxis behavior. B. Sensory transduction pathway for volatile attractants in the AWA neuron. Activation of the ODR-10 GPCR by its ligand, the buttery bacterial metabolite diacetyl, stimulates ODR-3 Gα. The signaling molecules downstream of *odr-3* are discussed in chapters 2 and 3 of this dissertation. OSM-9 and OCR-2 are subunits in the TRPV transduction channel; channel activation leads to depolarization, chemotaxis behavior, and transcription of *odr-10*.

Figure 1-1

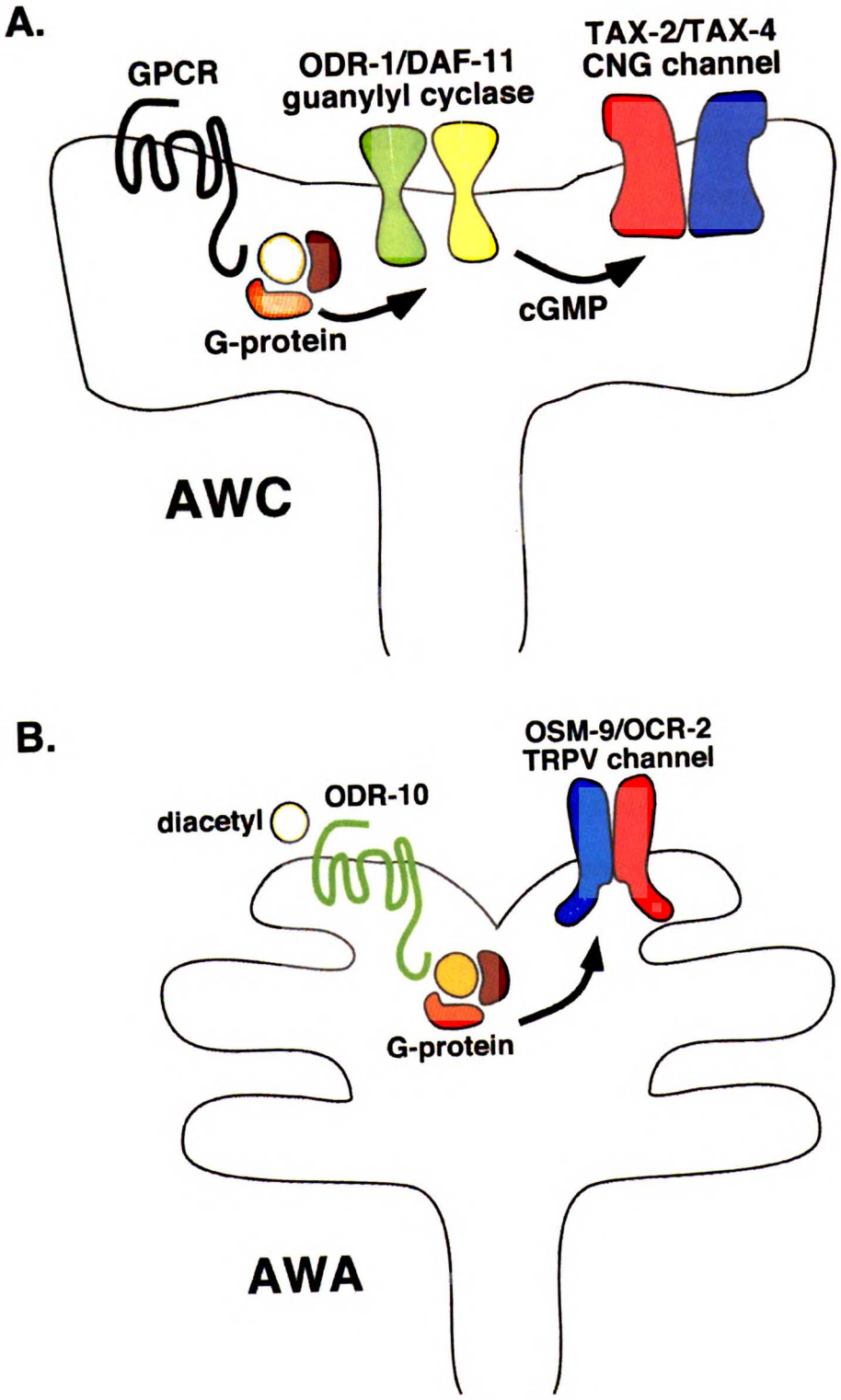
A.
GPCR
ODR-1/DAF-11
guanylyl cyclase
TAX-2/TAX-4
CNG channel
G-protein
cGMP
AWC
B.
OSM-9/OCR-2
TRPV channel
diacetyl
ODR-10
G-protein
AWA

Figure 1-2: Analogous sensory transduction pathways

A. Sensory transduction in mammalian olfactory neurons. Binding of an odorant ligand to a GPCR stimulates an olfactory G protein, which activates adenylyl cyclase. Increased levels of cyclic AMP gate the transduction channel, leading to depolarization, Ca^{2+} entry, and olfactory responses. B. Sensory transduction in mammalian rod and cone photoreceptors. Light activates rhodopsin, stimulating the G-protein transducin. Activation of phosphodiesterase reduces the levels of cyclic GMP, closing a cyclic nucleotide gated channel. C. Sensory transduction in rodent vomeronasal neurons. Pheromones bind to V1R and V2R receptors, stimulating a G protein. Activation of phospholipase C cleaves membrane PIP_2 into IP_3 and diacylglycerol (DAG). DAG (or a metabolite) stimulates the TRP2 channel, leading to depolarization and sex-specific behavioral responses. D. Phototransduction in *Drosophila* photoreceptors. Light activates *ninaA* rhodopsin, stimulating a G protein. Activation of *norpA* phospholipase C generates IP_3 and DAG. DAG (or a metabolite) stimulates the TRP/TRPL channels, leading to depolarization and visual responses.

Figure 1-2

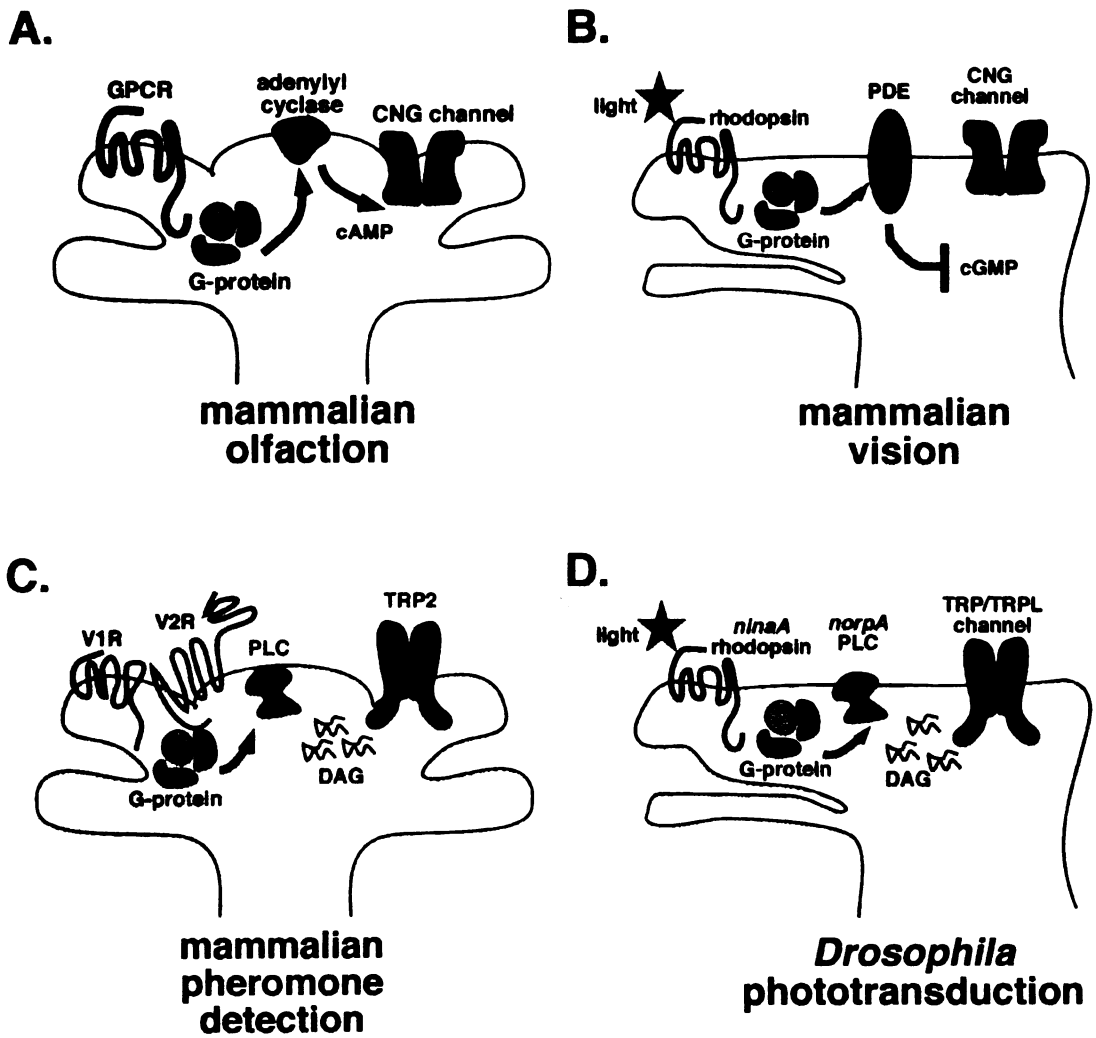
A.
GPCR
adenylyl cyclase
CNG channel
cAMP
G-protein
mammalian olfaction
B.
light
rhodopsin
PDE
CNG channel
G-protein
cGMP
mammalian vision
C.
V1R
V2R
PLC
TRP2
DAG
G-protein
mammalian pheromone detection
D.
light
ninaA rhodopsin
norpA PLC
TRP/TRPL channel
G-protein
DAG
Drosophila phototransduction

Figure 1-3: TRP structure and select *C. elegans* TRP channels

A. Representative TRP channel structure. The cytoplasmic N′ region of most TRP subfamilies contains a variable number of ankyrin repeats. Channels have 6 transmembrane domains, with S5 and S6 gate domains flanking a pore loop selectivity filter. The transmembrane domains and pore loop have the strongest conservation among TRP family channels. The cytoplasmic C′ region varies among subfamilies, and may contain lipid binding motifs, coiled-coil domains, Ca^{2+} binding regions, kinase domains, PDZ recognition motifs, or other functional structures. B. Alignment of *C. elegans* TRP channels. Conserved transmembrane regions were identified with SMART analysis and refined with NCBI CDD/reverse psi-BLAST. ClustalW was used to align transmembrane domains, and the results are presented as a phylogram. Note clustering of TRPP, TRPC, TRPM, and TRPV subfamilies. Also shown are single members of TRPA, TRPML, and TRPN subfamilies. *C. elegans* has 6 other candidate TRP channels which are uncharacterized; those are omitted from the figure for clarity, and are not discussed in the text.

Figure 1-3

A.

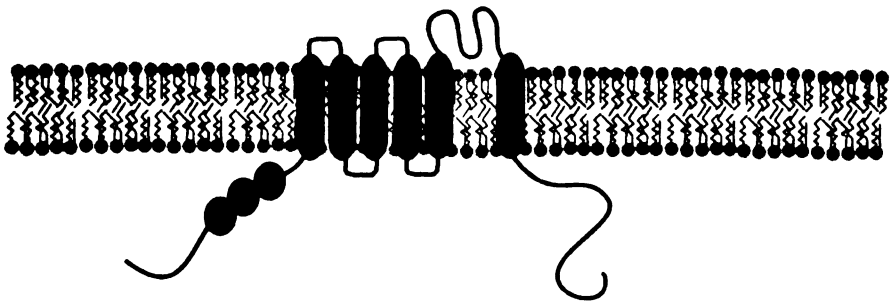

B.

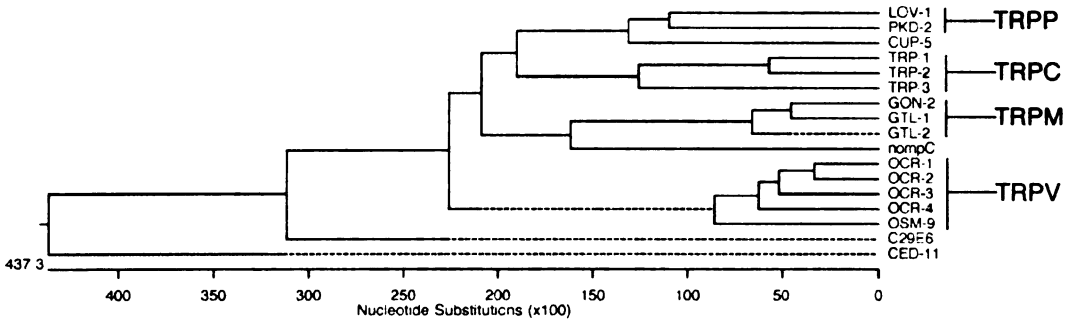
LOV-1
PKD-2
CUP-5
TRP 1
TRP-2
TRP 3
GON-2
GTL-1
GTL-2
nompC
OCR-1
OCR-2
OCR-3
OCR-4
OSM-9
C29E6
CED-11
TRPP
TRPC
TRPM
TRPV
437 3
400
350
300
250
200
150
100
50
0
Nucleotide Substituticns (x100)

Figure 1-4: Natural and synthetic ligands for mammalian TRPV channels

Chemical structures for candidate TRPV ligands; note that many contain an unsaturated lipid tail. Capsaicin is a vanilloid synthesized by chili peppers. Arachidonic acid (AA) is a polyunsaturated fatty acid. Anandamide and oleoyl ethanolamide are endocannabinoids, endogenous brain ligands for cannabinoid receptors. N-arachidonoyl dopamine and N-oleoyl dopamine are endovanilloids, endogenous brain ligands for TRPV1. 5′,6′-epoxy eicosatrienoic acid is an epoxygenase-derived ligand for TRPV4. 4α-PDD is a synthetic TRPV4 ligand; its acyl tails are not shown for simplicity. Diagrams courtesy of Cayman Chemical and LC Laboratories.

Figure 1-4

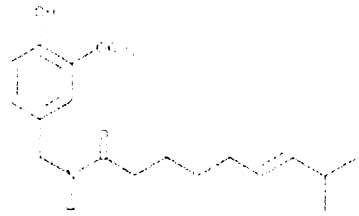

capsaicin

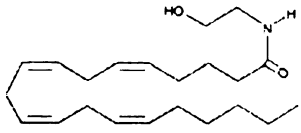

anandamide
(arachidonoyl ethanolamide)

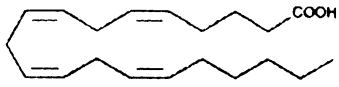

arachidonic acid

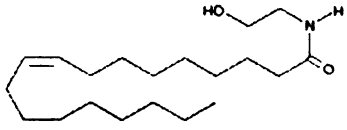

oleoyl ethanolamide

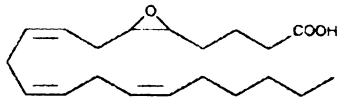

5',6'-epoxyeicosatrienoic acid

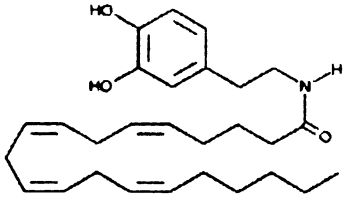

N-arachidonoyl dopamine

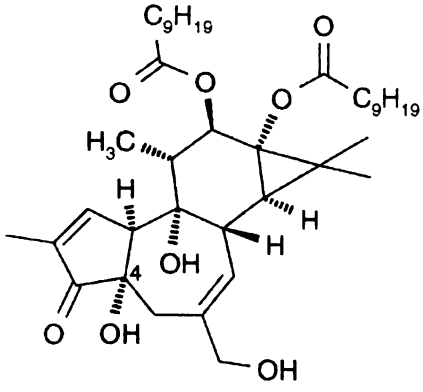

4α-phorbol didecanoate

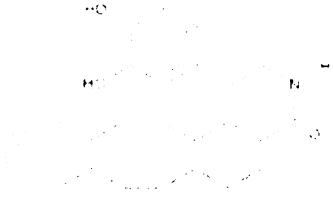

N-oleoyl dopamine

Figure 1-5: Expression patterns of *C. elegans* TRPV subunits

All *ocr* subunits are co-expressed with *osm-9*. *osm-9* is expressed widely in sensory neurons and select non-sensory tissue, including neurons that primarily sense volatile odors (green), repellents (red), mechanical stimuli (blue), water-soluble compounds (orange), or dauer development-related stimuli (purple). Each of the *ocr* channels is expressed in a partially-overlapping set of *osm-9*-containing cells. In neurons coexpressing *osm-9* and an *ocr*, TRPV channels serve as the major sensory transduction channel. In cells expressing *osm-9* only, other channels function in primary transduction. Figure adapted from Tobin et al., 2002.

Figure 1-5

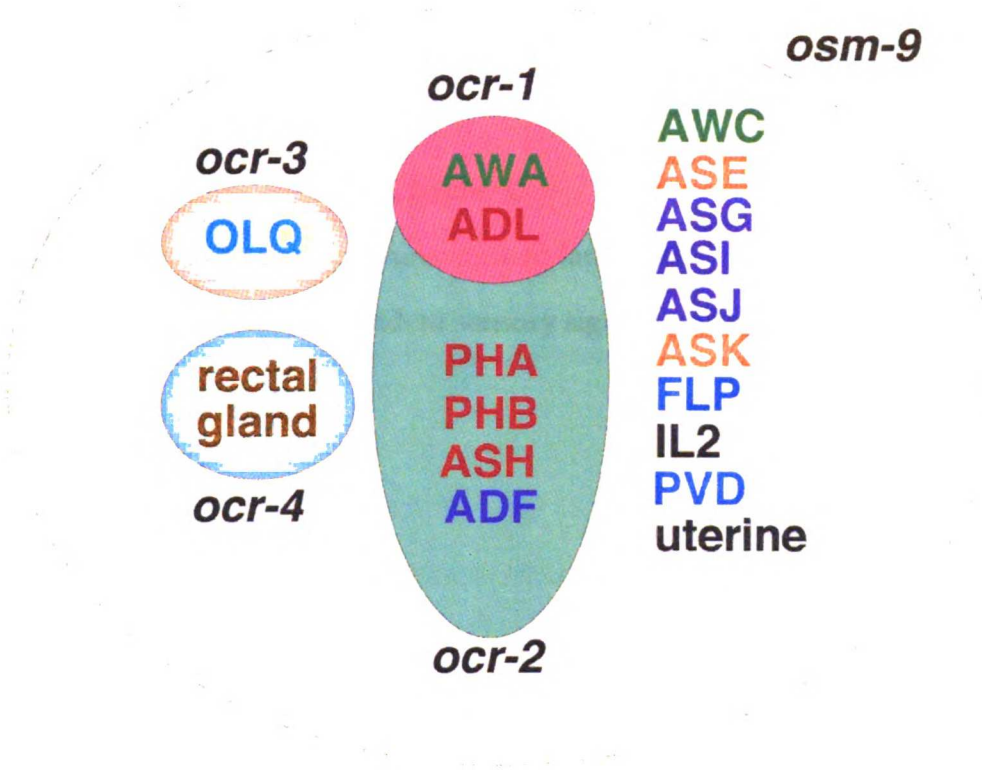
osm-9
ocr-1
ocr-3
OLQ
AWA
ADL
AWC
ASE
ASG
ASI
ASJ
ASK
FLP
IL2
PVD
uterine
rectal gland
PHA
PHB
ASH
ADF
ocr-4
ocr-2

Chapter 2:

Specific polyunsaturated fatty acids

drive TRPV-dependent sensory signaling *in vivo*

Statement of contributions:

A revised version of this chapter is published as Kahn-Kirby et al., Cell *119* (2004), 889-900.

My work contributed substantially to all the figures in the paper. Jenny Watts at Washington State University performed the gas chromatography analysis, the nose touch avoidance experiments, and the dietary rescue experiment in Figure 2-6C, D, E. Jami Dantzker performed the G-CaMP calcium imaging experiments in Figure 2-4, and conducted preliminary cameleon calcium imaging experiments in collaboration with Alfonso Apicella at UCSD.

Specific polyunsaturated fatty acids drive TRPV-dependent sensory signaling *in vivo*

by

Amanda H. Kahn-Kirby[1,2], Jami L.M. Dantzker[2], Alfonso J. Apicella[3], William R. Schafer[3], John Browse[4], Cornelia I. Bargmann[1,2*], Jennifer L. Watts[4*]

[1]Neuroscience Graduate Program [2]HHMI and Department of Anatomy, 513 Parnassus, University of California San Francisco, San Francisco CA 94143-0452. Telephone: 415-476-3558, Fax: 415-476-3493.

[3]Division of Biology, University of California, San Diego, California 92093-0349

[4]Institute of Biological Chemistry, Washington State University, Pullman, Washington 99164-6340. Telephone: 509-335-8554, Fax: 509-335-7643.

*Correspondence may be addressed to CIB (cori@itsa.ucsf.edu) or JLW (jwatts@mail.wsu.edu).

Running Title: Lipids modulate TRPV signaling *in vivo*.

keywords: PUFA, TRPV ion channel, *C. elegans*, eicosapentaenoic acid, calcium imaging.

Abstract:

A variety of lipid and lipid-derived molecules can modulate TRP cation channel activity, but the identity of the lipids that affect TRP channel function *in vivo* is unknown. Here, we use genetic and behavioral analysis in the nematode *C. elegans* to implicate a subset of 20-carbon polyunsaturated fatty acids (PUFAs) in TRPV channel-dependent olfactory and nociceptive behaviors. Olfactory TRPV signaling and nociceptive TRPV signaling are sustained by overlapping but non-identical sets of 20-carbon PUFAs including eicosapentaenoic acid (EPA) and arachidonic acid (AA). PUFAs act upstream of TRPV family channels in sensory transduction. Short-term dietary supplementation with PUFAs can rescue PUFA biosynthetic mutants, and exogenous PUFAs can generate rapid TRPV-dependent calcium transients in sensory neurons, bypassing the normal requirement for PUFA synthesis. These results demonstrate that a subset of PUFAs act as endogenous modulators of TRPV channel pathways, and suggest that lipid-modulated signal transduction pathways are tuned to specific omega-3 and omega-6 acyl groups.

Introduction

Cell membranes contain a rich variety of phospholipids that vary in their head groups, fatty acid chain lengths, and saturation. Lipids affect membrane fluidity, compartmentalization, and signal transduction, but the relationship between specific lipids and discrete cellular functions is often unknown, especially for the fatty acid component. Humans obtain long-chain polyunsaturated fatty acids (PUFAs) from their diet, and human PUFA deficiencies result in neurodevelopmental, neurological and cardiovascular defects through pathways that are poorly characterized (Innis, 2003; Mata Lopez and Ortega, 2003). An opportunity to define PUFA function is provided by *C. elegans*, which synthesizes 18- and 20-carbon PUFAs from dietary precursors through the action of endogenous lipid biosynthetic enzymes encoded by the *fat* (*fat*ty acid desaturase) and *elo* (fatty acid *elo*ngation) genes. A gas chromatography (GC)-based genetic screen led to the identification of the *fat* and *elo* mutations, which disrupt the synthesis of long-chain PUFAs from dietary precursors (Fig.1a)(Watts and Browse, 2002). The ability to manipulate PUFA composition using these mutants permits a dissection of the roles of specific PUFAs *in vivo*.

Among the signal transduction molecules that are modulated by lipids are members of the transient receptor potential (TRP) ion channel family. TRP channels play a prominent role in sensory signaling, as first recognized in *Drosophila* phototransduction (Montell and Rubin, 1989), and subsequently in vertebrate and invertebrate nociception, thermosensation, olfaction, pheromone sensation, osmosensation, and mechanosensation (Clapham, 2003). The TRP superfamily is divided into TRPC, TRPV, TRPM, TRPP, TRPML and TRPA subfamilies, based on overall domain structure and sequence similarity

(Clapham, 2003). Individual TRP channels may respond directly to physical stimuli such as temperature, or to signal transduction pathways downstream of G protein-coupled receptors (GPCRs) or tyrosine kinase receptors. In *Drosophila* photoreceptors, rhodopsin-mediated activation of phospholipase Cβ generates a lipid messenger that triggers TRP activation (Hardie, 2001, Hardie et al, 2003). Although the nature of the endogenous lipid messenger is unknown, polyunsaturated fatty acids (PUFAs) can activate TRP and the related TRPL channel in isolated *Drosophila* photoreceptors (Chyb et al., 1999). Other TRP channels can be modulated by DAG and its analogues (Hofmann et al., 1999; Lucas et al., 2003, Grimaldi et al., 2003), the endocannabinoid anandamide (Zygmunt et al., 1999), phosphatidylinositol diphosphate (PIP_2) (Chuang et al., 2001; Prescott and Julius, 2003; Runnels et al., 2002), prostaglandins (Alessandri-Haber et al., 2003), and epoxyeicosatrienoic acids (Watanabe et al., 2003). TRP channels have been found to be inhibited by the lipid PIP_2, inhibited by PIP_2 hydrolysis, or otherwise responsive to the products of PIP_2 hydrolysis.

The *C. elegans* genome encodes predicted members of each subgroup in the TRP superfamily. There are three TRPC genes, one of which acts in sperm during fertilization (Xu et al, 2003), two TRPP genes that act in male mating (Barr and Sternberg, 1999), three TRPM genes including one that acts in gonadogenesis (West et al., 2001), members of the TRPML, TRPN, and TRPA subfamilies, and five TRPV genes, *osm-9* and *ocr-1,2,3,* and *4* (Goodman and Schwarz, 2003). The TRPV gene *osm-9* is expressed and required in a subset of olfactory, chemosensory, osmosensory, and mechanosensory neurons (Colbert et al., 1997). The four *ocr* TRPV genes are each expressed in a subset of the cells that express *osm-9,* suggesting that they cooperate with *osm-9* in specific sensory

functions. *ocr-2* is coexpressed with *osm-9* in the polymodal ASH sensory neurons and the AWA olfactory neurons, and acts with *osm-9* in AWA olfaction and in ASH mechanosensation, osmosensation, and chemosensation (Tobin et al., 2002).

Here we show that *C. elegans* strains defective in PUFA synthesis display cell-specific and modality-specific sensory deficits in TRPV-dependent neurons. These behavioral defects originate upstream of the TRPV sensory transduction channel. Our results suggest that specific PUFAs function as endogenous modulators of TRPV channels in sensory neurons.

Results

C. elegans PUFA synthesis mutants have selective olfactory defects

To ask whether PUFAs have specific roles in sensory signaling, we examined olfactory chemotaxis behaviors mediated by the AWA and AWC olfactory neurons. These sensory neurons detect attractive volatile odors through ciliated dendrites at the tip of the nose, and mediate long-range chemotaxis responses. AWA senses diacetyl and 2-methylpyrazine, AWC senses benzaldehyde, butanone, isoamyl alcohol, and 2,3-pentanedione, and both neurons sense trimethylthiazole. The chemotaxis behaviors mediated by AWA and AWC are similar, but the signal transduction pathways within these neurons are distinct. Both cells initiate olfactory signaling with G protein-coupled olfactory receptors and the Gi-like G_α protein ODR-3, but AWA sensory transduction relies on the TRPV proteins OSM-9 and OCR-2 (Colbert et al., 1997; Tobin et al, 2002), whereas AWC sensory transduction relies on guanylate

cyclases and the cGMP-dependent channel proteins TAX-2 and TAX-4 (Coburn et al., 1996; Komatsu et al., 1996).

To study the *in vivo* effects of PUFA depletion on TRPV signaling pathways, we employed the *fat* lipid desaturase mutants. *fat-1(wa9), fat-3(wa22),* and *fat-4(wa14)* mutants are viable under laboratory conditions in which they are fed on *E. coli* OP50, a bacterium that does not synthesize or require polyunsaturated fatty acids (Tanaka et al., 1996). *fat-1* mutants and *fat-4* mutants are healthy, active, fertile, and superficially indistinguishable from wild-type *N2* animals in their appearance and development (Watts et al., 2002); *fat-4(wa14) fat-1(wa9)* double mutants are similarly robust (data not shown). *fat-3* mutants have a slightly dumpy body size, a reduced brood size due to defects in oocyte development, and impaired mating behavior (Watts et al., 2003). *fat-3* locomotion is sluggish, probably because of decreased synaptic transmission at the neuromuscular junction (Lesa et al., 2003). Each of the single and double mutants exhibits a unique biochemical lipid profile as measured by gas chromatography (GC) analysis (Fig. 2-1b).

fat-4 fat-1 double mutants were defective in chemotaxis to standard dilutions of the AWA-sensed odors diacetyl and pyrazine, but proficient in chemotaxis to benzaldehyde and other AWC-sensed odorants (Fig. 2-2a,b,e). *fat-1* and *fat-4* single mutants were proficient in chemotaxis to all odors. To characterize the *fat-4 fat-1* double mutant defects further, we examined chemotaxis at different concentrations of diacetyl and benzaldehyde. *fat-4 fat-1* mutants were specifically defective in chemotaxis at low diacetyl concentrations (≤ 1 nl), and normal in benzaldehyde responses at all concentrations (Fig. 2-2c,d). The *fat-4 fat-1* pattern of chemotaxis defects is similar to that associated with

TRPV *osm-9* mutations (Fig. 2-2)(Colbert et al., 1997) or mutations that affect cell fate of the AWA olfactory neurons (Sengupta et al., 1994). These results suggest that AWA sensory function, but not AWC sensory function, is disrupted in the *fat-4 fat-1* double mutant.

fat-3 mutants also exhibited a strong chemotaxis defect to AWA-sensed odors (Fig. 2-2a,c,e). In addition, they exhibited diminished chemotaxis to several odors sensed by AWC, especially when odors were presented at low concentrations (Fig. 2-2d). These results suggest that AWA function is strongly impaired in the *fat-3* mutant, whereas AWC-dependent behaviors are mildly impaired.

Based on the pattern of PUFA accumulation in different *fat* mutants (Fig. 2-1b), these results suggest that any one of the PUFAs AA, EPA or O3AA is required for AWA olfaction. The slight but statistically significant diacetyl chemotaxis defect of *fat-4* single mutants (Fig. 2-2c) further suggests that AA and EPA are most effective for AWA sensory function. The mild defect in AWC chemotaxis in *fat-3* mutants could suggest a minor PUFA requirement in AWC, but is also consistent with slight general sensory or motor defects and the apparent sluggishness of *fat-3* mutants.

PUFA synthesis mutants have defects in TRPV-dependent nociception

Like AWA neurons, the ASH polymodal nociceptive neurons use the TRPV channels OSM-9 and OCR-2 for sensory transduction (Colbert et al., 1997; Tobin et al., 2002). The two ASH neurons generate rapid escape behaviors to noxious stimuli including high osmolarity, nose touch, heavy metal ions, and volatile repellents (Hilliard et al., 2002; Kaplan and Horvitz, 1993; Troemel et al.,

1995). We examined ASH-mediated behaviors to determine whether *fat* genes are specifically required for certain sensory modalities, certain behavioral outputs, or OSM-9/OCR-2 signal transduction.

fat-3 animals were highly defective for nose touch avoidance (Fig. 2-3a). *fat-4* mutants and *fat-4 fat-1* double mutants had milder defects, and *fat-1* mutants were unaffected (Fig. 2-3a). These behavioral results suggest that ASH-mediated mechanosensation, like AWA olfaction, is supported by AA and EPA PUFAs. Light touch and nose touch are detected by different mechanosensory neurons, but transduced through the same interneurons and motor neurons (Chalfie and Sulston, 1981; Chalfie et al., 1985; Kaplan et al., 1993). Avoidance of light touch to the body was intact in *fat* mutants, indicating that the defect in nose touch was likely to result from a defect in the sensory neurons rather than the downstream motor circuit (Fig. 2-3b).

ASH-mediated avoidance of high osmolarity, heavy metals, and volatile repellents was also defective in *fat-3* mutants (Fig. 2-3c-e). *fat-4 fat-1* double mutants had milder but significant defects in these behaviors. Avoidance of high osmolarity, heavy metals, and volatile repellents was much more robust in *fat* mutants than in *osm-9* mutants, indicating that some TRPV signaling persisted in the absence of C20 PUFAs (Fig. 2-3c-e).

ASH nociceptive function was also disrupted in the fatty acid elongation mutant *elo-1(wa7)*, which encodes one of several elongases in the *C. elegans* genome. *elo-1* mutants have reduced levels of all C20 PUFAs (Fig. 2-supplementary 1a) and exhibited defects in ASH-mediated avoidance of nose touch, high osmolarity, and heavy metals (Fig. 2-supplementary 1b-d). AWA olfactory signaling was normal in *elo-1* mutants except at very low odorant

concentrations, perhaps because of redundancy among the elongase enzymes (Fig. 2-supplementary 1e) (Kniazeva et al., 2003).

Gq and PLCβ activate TRPC in *Drosophila* photoreceptors and in other contexts (Montell, 2003). The *C. elegans* Gqα mutant *egl-30* and phospholipase Cβ mutant *egl-8* have defects at the neuromuscular junction (Lackner et al., 1999; Miller et al., 1999) and are too sluggish to be assayed for olfactory chemotaxis, but they reverse to escape noxious stimuli. To ask whether TRPV signaling in ASH requires Gq/PLCβ signaling, *egl-8(md1971)* and *egl-30(n686sd)* mutants were tested for ASH-mediated escape behaviors. In spite of their locomotor defects, both *egl-8* and *egl-30* mutants avoided high osmolarity (Fig. 2-3f). Thus classical Gq signaling is unlikely to be central to TRPV signaling in ASH. Moreover, the ability of *egl-8* and *egl-30* mutants to avoid ASH stimuli indicates that moderate sluggishness and moderate neuromuscular defects are unlikely to explain the ASH sensory defects in *fat-3(wa22)* mutants.

fat-3 is required for sensory Ca^{2+} mobilization in ASH

To ask directly whether *fat-3* affects sensory signaling in ASH, we imaged neuronal Ca^{2+} *in vivo* using a transgenic calcium reporter protein. Stimulus-induced activity in *C. elegans* neurons has been measured previously with the ratiometric Ca^{2+} indicator cameleon (Suzuki et al., 2003, Miyawaki et al. 1999, Hilliard et al., in press). In *Drosophila*, measurements of odor-evoked activity in the antennal lobe exhibit a greater dynamic range when probed with the genetically encodable Ca^{2+} sensor G-CaMP than with cameleon (Nakai et al., 2001, Fiala et al., 2002, Wang et al., 2003). Therefore, we expressed G-CaMP (kindly provided by Junichi Nakai) in ASH under the *sra-6* promoter. Ca^{2+}

transients were measured in the ASH cell body as changes in background subtracted fluorescence intensity values (ΔF) relative to baseline (Fig. 2-4a).

High osmotic strength glycerol stimulation of wild-type animals gave a robust increase in G-CaMP fluorescence in the ASH cell body, with a mean maximum ΔF/F of 68%±4%(SEM) (Fig. 2-4b,e). This signal appeared to be selective for nociceptive signaling in ASH: no reliable Ca^{2+} transients were observed in ASH neurons of wild-type animals in response to a control ethanol solution (Fig. 2-4c,e), nor were glycerol-evoked Ca^{2+} signals observed in mutants for the *osm-9* sensory channel (n=4 and Hilliard et al., in press).

We next asked whether the osmotic avoidance defect in *fat-3* mutants reflects a defect in primary detection by ASH. Ca^{2+} transients evoked by 1 M glycerol were significantly diminished in *fat-3* (15%±3%) compared to wild-type (Fig. 2-4b,e). These results directly demonstrate that *fat-3* mutants are impaired in ASH sensory signal transduction. Similar results with smaller signals were obtained using cameleon for Ca^{2+} imaging in ASH (data not shown).

ASH synaptic function is retained in *fat-3* mutants

The behavioral and sensory defects in *fat-3* mutants are consistent with a defect in ASH sensory signaling, cilium development or morphology, or propagation of a calcium signal from the cilium to the cell body. To establish the step at which *fat-3* affects sensory functions of ASH, we used a heterologous channel that bypasses ASH sensory transduction molecules. Wild-type *C. elegans* does not respond to the chili pepper irritant capsaicin, but animals expressing the rat TRPV1 channel in ASH respond to capsaicin with an escape behavior that is similar to endogenous ASH avoidance responses (Tobin et al., 2002). TRPV1-

dependent capsaicin avoidance behavior bypasses the upstream Gα protein ODR-3 as well as OSM-9 and OCR-2 TRPV channels, presumably because capsaicin directly activates TRPV1 to depolarize ASH (Tobin et al., 2002). However, TRPV1-dependent capsaicin avoidance does require glutamatergic neurotransmission from ASH to downstream neurons. We found that *fat-3(wa22)* animals expressing a *sra-6::TRPV1* transgene in ASH avoided capsaicin to the same extent as *fat-3(+); sra-6::TRPV1* animals across a range of capsaicin concentrations (Fig. 2-5). This result indicates that *fat-3* is not required for effective signal propagation in ASH or synaptic communication between ASH and its downstream targets, and localizes the most important requirement for *fat-3* upstream of the step at which sensory signals depolarize ASH.

fat-3 mutations are associated with decreased numbers of synaptic vesicles and slightly impaired synaptic transmission at neuromuscular junctions (Lesa et al., 2003). To ask whether this level of synaptic dysfunction could account for the chemosensory and mechanosensory deficits in *fat-3* mutants, we examined AWA, AWC, and ASH behavior in the synaptic vesicle trafficking mutant *rab-3* (Nonet et al, 1997). *rab-3* has defects in cholinergic vesicle biogenesis and neurotransmission that are similar to those of *fat-3* mutants (Lesa *et al.*, 2003), but *rab-3(y250)* mutants were normal in AWA diacetyl chemotaxis and ASH high osmolarity avoidance (Fig. 2-supplementary 2a,c) and in AWC benzaldehyde chemotaxis (Fig. 2-supplementary 2b). These results indicate that the sensory defects in *fat-3* are not explained by the *fat-3* defect in synaptic transmission. Moreover, even strong defects in synaptic transmission do not diminish stimulus-evoked Ca^{2+} transients in ASH (Hilliard et al., in press), but the *fat-3* mutation does.

ASH signaling is sensitive to the structure of the sensory cilia, so we asked whether *fat-3* might be important in cilia biogenesis. The ASH sensory neurons take up the lipophilic dye DiI through exposed sensory cilia, and dye uptake is disrupted by defects in cilia morphogenesis or transport (Hedgecock et al., 1985, Perkins et al., 1986). The ASH neurons of *fat* mutants stained normally with DiI, suggesting that the sensory neurons and their cilia were structurally and functionally intact (data not shown). Similarly, ASH and AWA neurons of *fat-3* animals had superficially normal cilia, dendrites, cell bodies, and axons when examined using cell type-specific GFP markers (data not shown).

PUFAs can act in adults to rescue sensory behaviors

fat genes are expressed at high levels in intestinal cells, which probably serve as the main site of endogenous PUFA synthesis from dietary precursors, although *fat::gfp* transgenes are also expressed in some neurons (J.L.W. and C.I.B., unpublished observations). A functional green fluorescent protein (GFP)-tagged *fat-3* genomic fragment (Watts et al., 2003) partially restored PUFA biosynthesis in *fat-3* mutants when expressed under the *sra-6* promoter, which directs expression in the ASH, ASI, and PVQ neurons (Fig. 2-6a). Osmotic avoidance behavior was restored in transgenic animals expressing *sra-6::fat-3::GFP*, but not in sibling animals that lost the *sra-6::fat-3::GFP* transgene (Fig. 2-6b). *fat-3; sra-6::fat-3::GFP* animals also had improved body size, male mating, and locomotion relative to *fat-3* mutants (data not shown). These results indicate that the behavioral defects as well as the more general defects in the *fat-3* strain are specifically associated with the *fat-3* mutation.

To ask when lipids were required for sensory behavior, we supplemented *fat* mutants with OP50 bacteria grown in the presence of free fatty acids (Watts et al., 2003). The bacteria typically accumulated the exogenous PUFA to an extent that 8-15% of their total fatty acids consisted of the dietary PUFA, as determined by GC analysis (data not shown). Animals were transferred to PUFA-supplemented plates at the L4 or young adult stage, and assayed 4-24 hours later as adults. After this dietary supplementation, *fat-3* animals had improved locomotion and body shape, providing straightforward visual confirmation that the lipid plates delivered fatty acids to internal tissues. *fat-1* and *fat-4* desaturase activities and the *elo-1* and *elo-2* elongase activities in the *fat-3* mutant converted exogenous GLA, DGLA, and AA into downstream PUFAs, but did not modify ALA and EPA (Fig. 2-1a,b). GC of lipid-supplemented *fat-3* mutants confirmed rescue of systemic C20 PUFA levels, which was often accompanied by accumulation of the supplemental fatty acid (Fig. 2-1b).

fat-3 AWA diacetyl chemotaxis behavior was rescued by 24-hour dietary supplementation with AA or EPA, but not by supplementation with ALA, GLA, or DGLA (Fig. 2-6c). Diacetyl chemotaxis of wild-type animals was unaffected by supplementation by AA, EPA, and ALA, but a reduction in chemotaxis was seen with DGLA or GLA supplementation. Dietary supplementation with the same panel of PUFAs neither enhanced nor impaired AWC benzaldehyde chemotaxis in wild-type or *fat-3* mutants (Fig. 2-6d). These results suggest first, that AA and EPA facilitate AWA function in adults, and second, that elevated levels of DGLA or GLA fatty acids could have a deleterious effect on AWA function.

fat-3 ASH nose touch avoidance and osmotic avoidance were rescued by 24-hour dietary supplementation with AA, EPA, DGLA, or GLA, but not rescued

by ALA (Fig. 2-6e,f). Lipid supplementation for four hours caused partial rescue of nose touch avoidance behavior (data not shown). Nose touch avoidance and osmotic avoidance in wild-type animals were unaffected by dietary lipid supplementation. These results reveal a difference between the lipids that are required for ASH function and those that are required for AWA function.

Dietary lipid supplementation did not rescue the osmotic avoidance defects of *osm-9* mutants (Fig. 2-6f). These results suggest that dietary PUFAs act either upstream of or parallel to the TRPV channel.

Exogenous PUFAs elicit TRPV-dependent, *fat-3*-independent avoidance behavior

Electrophysiological analysis of mammalian TRP channels has demonstrated that lipids can either stimulate or inhibit TRP activity (Chuang et al., 2001; Prescott and Julius, 2003; Runnels et al., 2002). The *fat* mutant data do not distinguish between these opposite possibilities, since long-term depletion of either an activator or an inhibitor could result in defective neuronal function. To ask how PUFAs might act as acute regulators of TRPV channel activity in *C. elegans*, we exposed animals directly to PUFA solutions and monitored their behavior in avoidance assays. Remarkably, EPA elicited a robust, rapid avoidance behavior in wild-type worms that is characteristic of activation of the ASH neuron (Fig. 2-7a). A different PUFA, LA, elicited minimal avoidance behavior, demonstrating lipid specificity of ASH activation (Fig. 2-7b). Since the avoidance behavior was observed within seconds, these results suggest that PUFAs can act as direct activators of sensory neurons. They are consistent with a potential role of PUFAs as activators, but not inhibitors, of ASH TRPV channels.

EPA-evoked avoidance responses were not present in *osm-9* or *ocr-2* animals across a 2,000-fold concentration range, suggesting that PUFA avoidance is generated by ASH signaling upstream of the OSM-9/OCR-2 sensory channel (Fig. 2-7a and data not shown). By contrast, EPA avoidance was maintained in *fat-3* mutants, which do not avoid natural ASH stimuli effectively. These genetic results suggest that the cellular target of exogenous PUFAs does not require lipid synthesis, but does require TRPV channel function. One interpretation of these observations is that PUFA lipids could act directly on TRPV channels, leading to ASH activation.

Imaging PUFA-induced activity in ASH sensory neurons

To ask directly whether PUFAs stimulate ASH sensory signaling, we delivered PUFAs to immobilized animals and imaged ASH calcium responses using G-CaMP. At all concentrations tested, the PUFA EPA reliably elicited robust ASH Ca^{2+} transients in wild-type animals (Fig. 2-4d,e). The mean Ca^{2+} response to EPA in wild-type animals was slightly less than the ASH response to high osmolarity glycerol (mean ± sem of maximum $\Delta F/F$: 68%±4% to glycerol versus 48%±3% to EPA); the magnitude of the response appeared to be saturated, since it did not vary significantly when EPA concentrations were increased. The ratiometric Ca^{2+} indicator cameleon detected reliable, but smaller ASH signals in response to the PUFAs EPA and AA (data not shown). Thus EPA is likely to function directly on ASH to generate sensory responses. No reliable Ca^{2+} transients were observed in ASH neurons of *osm-9* mutants in response to EPA (n=6) or AA (*osm-9 ocr-2*, n=7), indicating that the lipids act through the TRPV OSM-9 and OCR-2 channels.

fat-3 ASH neurons were defective in their response to standard ASH nociceptive stimuli such as high osmotic strength, but remarkably the ASH neurons in *fat-3* mutants were robustly activated by EPA at a level comparable to wild-type ASH neurons (Fig. 2-4d,e). Thus exogenous EPA directly and rapidly bypasses the requirement for the PUFA biosynthetic enzyme FAT-3 in ASH activation.

Discussion

Our results demonstrate that PUFAs synthesized by the *fat* genes are required for TRPV-dependent AWA olfactory signaling, and for TRPV-dependent ASH avoidance of nose touch, high osmolarity, heavy metals, and volatile repellents. Three lines of evidence place the PUFA requirement at an early step of sensory processing, upstream of TRPV channels. First, *fat-3* PUFA biosynthetic mutants had diminished stimulus-evoked sensory Ca^{2+} transients in ASH neurons. Second, exogenous PUFAs elicited ASH Ca^{2+} transients and avoidance behaviors, bypassing the PUFA biosynthetic defect. Third, the PUFA requirement in ASH was bypassed by depolarization with a ligand for the artificially expressed rat TRPV1 channel, arguing against general defects in membrane formation, vesicle biogenesis, and synaptic transmission. These results implicate C20 PUFAs as specific *in vivo* regulators of TRPV channel activity.

The absence of certain PUFAs in *fat-3*, *fat-4 fat-1*, or *elo-1* mutants resulted in specific behavioral defects; dietary supplementation of adult *fat-3* animals with specific PUFAs alleviated those defects. Different lipids were preferentially associated with AWA or ASH functions, a result that was most striking in dietary

supplementation experiments: ASH function was rescued by a broad set of dietary C20 PUFAs, whereas AWA function was selectively restored by EPA or AA. Unexpectedly, some dietary PUFAs inhibited AWA signaling in wild-type animals. These results suggest that different sensory cells rely upon different PUFAs to function. The difference between AWA and ASH could arise from distinct subunit compositions of their OSM-9, OCR-2, and OCR-1 TRPV channels, distinct kinetics of sensory signaling, or the actions of other lipid-signaling enzymes such as protein kinase C or diacylglycerol lipase.

Although they had general effects on viability and fertility, PUFAs were not required during early development for behavioral rescue, consistent with an acute sensory function in ASH and AWA. Interestingly, altered dietary lipid intake can result in mammalian behavioral and signal transduction defects, in addition to affecting human retinal and brain development (Innis, 2003, Moriguchi et al., 2000, Niu et al., 2004).

Exogenous PUFAs evoked rapid avoidance behaviors when delivered to sensory cilia. Moreover, Ca^{2+} imaging showed that exogenously applied PUFAs directly increased Ca^{2+} levels in ASH, probably in association with depolarization, in a fraction of a second. Applied PUFAs evoked avoidance behavior and Ca^{2+} responses in the ASH signal transduction mutant *fat-3*, but not in *osm-9*, raising the possibility that these PUFAs act directly on TRP channels downstream of essential G protein signaling components. This result is consistent with mammalian and *Drosophila* electrophysiology and imaging studies suggesting that PUFAs, PIP_2, DAG, endocannabinoids, and epoxyeicosatrienoic acids can act as modulators and ligands of TRP family channels. However, our results do not exclude the possibility that PUFAs regulate neuronal activity by interacting with

additional targets upstream of the TRPV channels (Oliver et al., 2004, Rohacs et al., 1999, Hilgemann et al., 2001).

Normal AWA signaling is associated with the activation of G protein-coupled receptors (GPCRs) such as the diacetyl receptor ODR-10, whereas ASH signaling probably involves both GPCRs for chemical stimuli and channel-associated mechanisms for sensing mechanical and osmotic stimuli (Sengupta et al., 1996, Liedtke et al., 2003, Fukuto et al., 2004). We suggest that sensory GPCRs regulate levels of a PUFA-containing lipid agonist of OSM-9/OCR-2 channels in AWA and ASH. The FAT and ELO-1 enzymes are required to synthesize the PUFA-containing membrane phospholipids, but the dietary rescue of *fat-3* mutants with lipids indicates that *fat-3* cannot be the enzyme that rapidly mobilizes lipid second messengers in response to sensory stimuli. Instead, *fat* enzymes must synthesize substrate lipids for an unidentified phospholipase or second messenger-generating enzyme downstream of G protein signaling. This proposed lipid mobilizing activity is not the canonical phospholipase Cβ EGL-8, but the *C. elegans* genome encodes a wide variety of alternative lipid-mobilizing enzymes.

Dietary intake of omega-3 fatty acids in humans is associated with a protective effect on cardiovascular health and a less-defined positive effect on neuronal function. The relevant targets of the omega-3 fatty acids are unknown, but at least some of their positive effects are thought to be mediated by vasodilation and improved endothelial function (von Schacky, 2004). Our results indicate that an important class of omega-3 fatty acid targets in *C. elegans* are TRPV channels. Mammalian TRPV4, which is functionally orthologous to *C. elegans* OSM-9, is expressed in endothelial cells and activated by PUFA

derivatives, conferring a potential vasodilatory effect (Watanabe et al., 2003; Liedtke et al., 2003). Other TRP channels including TRPC4 are also implicated in vessel relaxation (Freichel et al., 2001). We speculate that the importance of dietary omega-3 fatty acids may be directly related to the ability of PUFAs and their derivatives to modulate TRP function in diverse cellular contexts.

Experimental Procedures

Strains and Genetics

Wild-type animals were *C. elegans* variety Bristol, strain N2. Worms were grown at 20°C and maintained using standard methods (Brenner, 1974). Strains used in this work included *N2*, CX3260 *kyIs37* II, BX24 *fat-1(wa9)* IV, BX74 *kyIs37* II; *fat-1(wa9)* IV, BX17 *fat-4(wa14)* IV, BX77 *kyIs37* II; *fat-4(wa14)* IV, BX14 *elo-1(wa7)* IV, BX78 *kyIs37* II; *elo-1(wa7)* IV, BX52 *fat-4(wa14) fat-1(wa9)* IV, BX82 *kyIs37* II; *fat-4(wa14) fat-1(wa9)* IV, BX30 *fat-3(wa22)*, BX83 *kyIs37* II; *fat-3(wa22)* IV, CX4366 *kyIs37* II; *osm-9(n2743)* IV, CX10 *osm-9(ky10)* IV, CX4544 *ocr-2(ak47)* IV, CX5342 *kyIs37* II; *osm-9(ky10) ocr-2(ak47)* IV, MT1434 *egl-30(n686sd)* I, RM2221 *egl-8(md1971)* V, CB1339 *mec-4(e1339)* X, CX5569 *osm-9(ky10) ocr-2(ak47)* IV; *kyIs200* X, CX5075 *kyIs200* X, CX6636 *fat-3(wa22)* IV; *kyIs200* X , CX6637 *fat-3(wa22)* IV; *kyIs200* X, CX6625 *kyIs37* II; *fat-3(wa22)* IV; *kyEx726*, CX6627 *kyIs37* II; *fat-3(wa22)* IV; *kyEx729*, CX6626 *kyIs37* II; *fat-3(wa22)* IV; *kyEx727*, CX6632 *kyEx728*, CX6635 *fat-3(wa22)* IV; *kyEx728*,CX6633 *osm-9(ky10) ocr-2(ak47)* IV; *kyEx728*. Some strains contained the AWA::GFP transgene *kyIs37*, which does not affect AWA, AWC, or ASH behavior (A.K.-K. and C.I.B., unpublished observations). For double mutant strains or transgene-marked strains, the presence of all mutant alleles was confirmed by PCR analysis or by GC analysis of candidate mutants. Some nematode strains used in this study were provided by the Caenorhabditis Genetics Center, which is funded by the NIH National Center for Research Resources (NCRR).

fat-1(wa9) and *fat-4(wa14)* mutations result in premature stop codons that are predicted to eliminate biochemical activity. *fat-3(wa22)* and two other alleles derived from the same screen (Watts and Browse, 2002) result in the biochemical

absence of Δ6 desaturase products. *elo-1(wa7)* is a 1 base pair deletion that causes a frameshift, eliminating the last 50 amino acids of the protein, including residues predicted to be important for endoplasmic reticulum retention and recycling (Watts and Browse, 2002).

Gas Chromatography

Methods were similar to those in Watts and Browse, 2002. To determine nematode fatty acid composition, at least 200 well-fed worms were washed, rapidly frozen at –80°, or immediately flushed with 1 mL 2.5% H_2SO_4 in methanol to extract fatty acids from tissues and transmethylate them. Samples were capped and incubated at 80° for one hour. After the addition of 0.2 mL of hexane and 1.5 mL H_2O, the fatty acid methyl esters were extracted into the hexane layer by shaking and centrifuging the tubes at low speed. 1 mL samples of the organic phase were analyzed by GC using an Agilent 6890 series GC equipped with a 30-m x 0.25-mm SP-2380 column (Supelco, Bellefonte, PA), helium as the carrier gas at 1.4 ml/min and a flame ionization detector. The GC was programmed for an initial temperature of 120°C for 1 min followed by an increase of 10°C/min to 190°C followed by an increase of 2°C/min to 200°.

Behavioral Assays

Chemotaxis assays were performed on populations of animals in a binary choice between odorant and diluent essentially as described (Bargmann et al., 1993), except that the boundaries of the "attractant" and "diluent" zones were enlarged on all assay plates to accommodate the decreased motility of *fat-3* animals. Nose touch assays were performed as described (Kaplan and Horvitz, 1993); a positive

response was defined as a reversal within 2 seconds of encountering an eyelash. All assays were done blind to genotype. ASH avoidance assays of 2-octanone presented in a glass capillary pipette were performed as described (Tobin et al., 2002). Touch cell mechanosensory avoidance assays were performed using a dog hair mounted on a glass capillary, as described in Chalfie and Sulston, 1981.

Osmotic avoidance was measured using glycerol in modified drop test assays (Hilliard et al., 2002). 30-50 well-fed, uncrowded adult animals were picked away from food onto a dry, unseeded, uncovered nematode growth medium plate, and allowed to acclimate to their surroundings for at least 10 minutes. Individual, forward-moving animals were then challenged with drops of M13 buffer or 1M glycerol in M13, delivered adjacent to the tail from a 10 μL capillary mouth pipette. The repellent reached the nose of the animal by capillary action, and an avoidance response was scored if the animal reversed at least one body bend within 5 seconds of the stimulus delivery. Each assay consisted of at least 25 drops distributed across the plate population. A similar method was used for heavy metal avoidance assays with $CuCl_2$ (Sigma) diluted from a 0.5M stock. Capsaicin drop test assays were performed in an identical fashion, using 100 μM capsaicin in 1% ethanol/M13 as the repellent and 1% ethanol in M13 as control.

For lipid drop test assays, fresh 200 mM stock PUFA solutions in ethanol were diluted M13 immediately prior to the assay, vortexed for 30 seconds, and flushed with nitrogen. Animals were tested with M13, 1M glycerol, and ethanol/M13 controls prior to lipid exposure. Two lipid solutions were tested during each assay, and the investigator was blind to lipid identity. Positive (*N2*) and negative (*osm-9*) control strains were assayed along mutant strains each day,

and mutant data was collected only if positive and negative control animals displayed normal performance on M13 and 1M glycerol assays.

M13 buffer contains 30 mM TRIS pH 7.0, 100 mM NaCl, and 10 mM KCl. Free fatty acids were obtained from Nu-Chek Prep (Elysian, MN), stored at –20° in the dark, and prepared as fresh 200 mM stocks prior to assays. Capsaicin was purchased from Tocris Cookson (Ellisville, MO).

Dietary Lipid Supplementation

PUFA stocks were prepared by diluting fatty acid salts (Nu-Chek Prep, Elysian, MN) to 100 mM in ddH_20 immediately prior to making plates. NGM solution was prepared with the addition of 0.1% tergitol (NP-40, Sigma). Once the agar was cooled to 45-50°C, lipids were added slowly, with stirring, to a final concentration of 160 μM or 80 μM. Plates were poured immediately, then dried in the dark at room temperature for 24 hours, seeded with OP50 *E. coli* for 48 hours, and stored in the dark at 4 degrees until ready for use. After behavioral assays were completed, at least 200 animals were washed off the plates and prepared for gas chromatography analysis of lipid content, as described above.

Construction of Transgenic Animals

The *sra-6::fat-3::GFP* plasmid was made by PCR-amplifying a full-length *fat-3* genomic fragment, and fusing it in-frame to the SalI and KpnI sites of the promoterless *C. elegans* GFP expression vector pSM::GFP (a gracious gift of Steven McCarroll). 3.8 kb of the *sra-6* promoter, which directs expression to ASH, ASI, and PVQ, was then cloned between NotI and XmaI sites. *fat-3(wa22)* animals were injected with 50 ng/μL *sra-6::fat-3::GFP* along with 25 ng/μL *odr-*

1::RFP as a coinjection marker, using conventional methods for germline transformation (Mello et al., 1991).

The *sra-6::G-CaMP* plasmid was made by cutting the mammalian G-CaMP vector pN1-G-CaMP with NotI, filling in with Klenow, and cutting again with NheI. The resulting blunted G-CaMP fragment was cloned into the NheI/EcoRV sites of pSM to make a promoterless G-CaMP *C. elegans* expression vector. The 3.8 kb *sra-6* promoter was cloned into the FseI and AscI sites of *G-CaMP::pSM*. *N2* animals were injected with 50 ng/μL *sra-6::G-CaMP*, and selected by G-CaMP fluorescence under a dissecting microscope. The transgene was subsequently crossed into different genetic backgrounds using standard approaches.

In vivo Ca^{2+} Imaging and Data Analysis

Imaging methods were adapted from Kerr et al., 2000, and Hilliard et al., in press. Young adult hermaphrodites with dim *sra-6::G-CaMP* expression were removed from plates with food and immediately glued with 2-octyl cyanoacrylate adhesive onto a chilled, hydrated 2% agarose pad on a glass coverslip. The coverslip was attached with silicone grease to a perfusion chamber (Warner Instruments RC-26GLP) that promotes laminar flow. The chamber was perfused with saline buffer (in mM: NaCl 80, KCl 5, D-glucose 20, HEPES 10, MgCl2 5, CaCl2 1, sucrose 25, pH 7.3) at a rate of ~1.5ml/min.

PUFAs used for stimulation were first dissolved in ethanol and further dissolved in saline buffer to a ten-fold range of final PUFA concentrations (2mM to 0.1mM) similar to what was used in the behavioral experiments. Usually, imaging experiments were done on the same days with the same PUFA stock as

the behavioral experiments. The amplitude of PUFA-evoked Ca^{2+} transients did not vary systematically within the ten-fold concentration range tested.

Stimulants dissolved in saline buffer were delivered under light pressure through a borosilicate glass needle (World Precision Instruments O.D. 1mm, I.D. 0.58mm) that had been pulled to a 50 micron diameter opening. Stimulants were kept under nitrogen pressure in 30ml syringes at room temperature. During stimulation, the needle was positioned perpendicular to the tip of the animal's head at a distance of about 150 μm. When not stimulating, the needle was moved ~1mm away from the animal to minimize unintended leakage of stimulants onto the preparation. Movement of the needle was computer controlled by a motorized stage (Polytec/PI M-111.1DG micro translation stage with C-862 Mercury II controller).

Each imaging trial lasted for 30 sec with the following temporal sequence: ~6 sec baseline, 4 sec stimulation, 10 sec interstimulus interval, 4 sec stimulation, and ~6 sec recovery. To minimize neuronal adaptation from repeated stimulus exposure, the inter-trial interval was 3-5 minutes. Animals were stimulated for a maximum of 10 trials and were healthy throughout the experiment.

Optical recordings were performed on a Zeiss Axioskop 2 FS upright compound microscope fitted with epifluorescence, a variable intensity controller (Opti-Quip), and a CoolSNAP HQ CCD camera (Photometrics). Images were taken at 10Hz with 2x2 binning using a 63x/0.95NA Zeiss Achroplan water immersion objective. Filter/dichroic pairs were: excitation, 470/20 plus 0.6 neutral density; dichroic, 510; emission, 520 LP (Chroma). Fluorescence images were acquired using Metamorph software (Universal Imaging). Lateral movements of a region of interest were tracked offline using custom Java

software written by Rex Kerr (Kerr et al., 2000) and changes in fluorescence intensity over time were calculated from background subtracted images relative to averaged prestimulus baseline ($\Delta F/F$). To minimize signal variations due to G-CaMP expression, only animals within a narrow window of expression were used. Noise artifacts such as movement and bleaching were minimal relative to signal.

Acknowledgements

We thank Eric Phillips, Katharine Griffing, Hai Nguyen, Dianne Parry, Joe Hill, and Ricky Meñeses for excellent technical assistance, Massimo Hilliard and David Tobin for helpful discussions, Makoto Tsunozaki, Hang Lu, Yun Zhang, Jesse Gray, and Sreekanth Chalasani for comments on the manuscript, Giovanni Lesa for sharing data prior to publication, Rex Kerr for sharing software and unpublished cameleon imaging data, Junichi Nakai for pN1-G-CaMP, and Steven McCarroll for the pSM vector. This work was supported by a NSF Predoctoral Fellowship and a University of California Mentorship Award (A.K.-K.), the Helen Hay Whitney Foundation (J.L.M.D.), NIH R01 GM62521 (J.B.) and DC04089 (C.I.B.), and the Human Frontiers Science Program. C.I.B. is an Investigator with the Howard Hughes Medical Institute.

References

Alessandri-Haber, N., Yeh, J. J., Boyd, A. E., Parada, C. A., Chen, X., Reichling, D. B., and Levine, J. D. (2003). Hypotonicity induces TRPV4-mediated nociception in rat. Neuron *39*, 497-511.

Bargmann, C. I., Hartwieg, E., and Horvitz, H. R. (1993). Odorant-selective genes and neurons mediate olfaction in *C. elegans*. Cell *74*, 515-527.

Barr, M. M., and Sternberg, P. W. (1999). A polycystic kidney-disease gene homologue required for male mating behaviour in *C. elegans*. Nature *401*, 386-389.

Brenner, S. (1974). The genetics of *Caenorhabditis elegans*. Genetics *77*, 71-94.

Chalfie, M., and Sulston, J. (1981). Developmental genetics of the mechanosensory neurons of *Caenorhabditis elegans*. Dev Biol *82*, 358-70.

Chalfie, M., Sulston, J. E., White, J. G., Southgate, E., Thomson, J. N., and Brenner, S. (1985). The neural circuit for touch sensitivity in *Caenorhabditis elegans*. J Neurosci. *5*, 956-964.

Chuang, H. H., Prescott, E. D., Kong, H., Shields, S., Jordt, S. E., Basbaum, A. I., Chao, M. V., and Julius, D. (2001). Bradykinin and nerve growth factor release the capsaicin receptor from PtdIns(4,5)P2-mediated inhibition. Nature *411*, 957-962.

Chyb, S., Raghu, P., and Hardie, R. C. (1999). Polyunsaturated fatty acids activate the *Drosophila* light-sensitive channels TRP and TRPL. Nature *397*, 255-259.

Clapham, D. E. (2003). TRP channels as cellular sensors. Nature *426*, 517-524.

Coburn, C. M., and Bargmann C. I. (1996). A putative cyclic nucleotide-gated channel is required for sensory development and function in *C. elegans*. Neuron *17*, 695-706.

Colbert, H. A., Smith, T. L., and Bargmann, C. I. (1997). OSM-9, a novel protein with structural similarity to channels, is required for olfaction, mechanosensation, and olfactory adaptation in *Caenorhabditis elegans*. J Neurosci *17*, 8259-8269.

Fiala, A., Spall, T., Diegelmann, S., Eisermann, B., Sachse, S., Devaud, J. M., Buchner, E., and Galizia C. G. (2002). Genetically expressed cameleon in *Drosophila melanogaster* is used to visualize olfactory information in projection neurons. Curr Biol *12*, 1877-1884.

Friechel, M., Suh, S.H., Pfeifer, A., Schweig, U., Trost, C., Weissgerber, P., Biel, M., Philipp, S., Freise, D., Droggmans, G., Hofmanss, F., Fockerzi, V., and Nilus, B. (2001). Lack of an endothelial store-operated Ca2+ current impairs agonist-dependent vasorelaxation in TRP4-/- mice. Nat Cell Biol *3*, 121-127.

Fukuto, H. S., Ferkey, D. M., Apicella, A. J., Lans, H., Sharmeen, T., Chen, W., Lefkowitz, R. J., Jansen, G., Schafer, W. R., and Hart, A. C. (2004). G protein-coupled receptor kinase function is essential for chemosensation in *C. elegans*. Neuron *42*, 581-593.

Goodman, M. B., and Schwarz, E. M. (2003). Transducing touch in *Caenorhabditis elegans*. Annu Rev Physiol *65*, 429-452.

Grimaldi, M., Maratos, M., and Verma, A. (2003). Transient receptor potential channel activation causes a novel form of [Ca 2+]I oscillations and is not involved in capacitative Ca 2+ entry in glial cells. J Neurosci *23*, 4737-4745.

Hardie, R. C. (2001). Phototransduction in *Drosophila melanogaster*. J Exp Biol *204*, 3403-3409.

Hardie, R. C., Martin, F., Chyb, S., and Raghu, P. (2003). Rescue of light responses in the *Drosophila* "null" phospholipase C mutant, norpAP24, by the diacylglycerol kinase mutant, rdgA, and by metabolic inhibition. J Biol Chem *278*, 18851-18858.

Hedgecock, E. M., Culotti, J. G., Thomson, J. N., and Perkins L. A. (1985). Axonal guidance mutants of *Caenorhabditis elegans* identified by filling sensory neurons with fluorescein dyes. Dev Biol *111*, 158-170.

Hilgemann, D. W., Feng, S., and Nasuhoglu, C. (2001). The complex and intriguing lives of PIP2 with ion channels and transporters. Sci STKE *2001*, RE19.

Hilliard, M. A., Apicella, A. J., Kerr, R., Suzuki, H., Bassicalupo, P., and Schafer, W. R. (2004). *In vivo* imaging of *C. elegans* aversive taste neurons reveals a role for G-protein γ subunit heterogeneity in repellent taste adaptation. In press.

Hilliard, M. A., Bargmann, C. I., and Bazzicalupo, P. (2002). *C. elegans* responds to chemical repellents by integrating sensory inputs from the head and the tail. Curr Biol *12*, 730-734.

Hofmann, T., Obukhov, A. G., Schaefer, M., Harteneck, C., Gudermann, T., and Schultz, G. (1999). Direct activation of human TRPC6 and TRPC3 channels by diacylglycerol. Nature *397*, 259-263.

Innis, S. M. (2003). Perinatal biochemistry and physiology of long-chain polyunsaturated fatty acids. J Pediatr *143*, S1-8.

Kaplan, J. M., and Horvitz, H. R. (1993). A dual mechanosensory and chemosensory neuron in *Caenorhabditis elegans*. Proc Natl Acad Sci USA *90*, 2227-2231.

Kerr, R., Lev-Ram, V., Baird, G., Vincent, P., Tsien, R. Y., and Schafer, W. R. (2000). Optical imaging of calcium transients in neurons and pharyngeal muscle of *C. elegans*. Neuron *26*, 583-594.

Kniazeva, M., Sieber, M., McCauley, S., Zhang, K., Watts, J.L., and Han, M. (2003). Suppression of the ELO-2 FA elongation activity results in alterations of the fatty acid composition and multiple physiological defects, including abnormal ultradian rhythms, in *Caenorhabditis elegans*. Genetics *163*, 159-169.

Komatsu, H., Mori, I., Rhee, J.S., Akaike, N., and Ohshima, Y. (1996). Mutations in a cyclic nucleotide-gated channel lead to abnormal thermosensation and chemosensation in *C. elegans*. Neuron *17*, 707-718.

Lackner, M. R., Nurrish, S. J., and Kaplan, J. M. (1999). Facilitation of synaptic transmission by EGL-30 Gqalpha and EGL-8 PLCbeta: DAG binding to UNC-13 is required to stimulate acetylcholine release. Neuron *24*, 335-346.

Lesa, G. M., Palfreyman, M., Hall, D. H., Clandinin, M. T., Rudolph, C., Jorgensen, E. M., and Schiavo, G. (2003). Long chain polyunsaturated fatty acids are required for efficient neurotransmission in *C. elegans*. J Cell Sci *116*, 4965-4975.

Liedtke, W., Tobin, D. M., Bargmann, C. I., and Friedman, J. M. (2003). Mammalian TRPV4 (VR-OAC) directs behavioral responses to osmotic and mechanical stimuli in *Caenorhabditis elegans*. Proc Natl Acad Sci USA *100*, 14531-14536.

Lucas, P., Ukhanov, K., Leinders-Zufall, T., and Zufall, F. (2003). A diacylglycerol-gated cation channel in vomeronasal neuron dendrites is impaired in TRPC2 mutant mice: mechanism of pheromone transduction. Neuron *40*, 551-561.

Mata Lopez, P., and Ortega, R.M. (2003). Omega-3 fatty acids in the prevention and control of cardiovascular disease. Eur J Clin Nutr *57*, S22-S25.

Mello, C. C., Kramer, J.M., Stinchcomb, D., and Ambros, V. (1991). Efficient gene transfer in *C. elegans*: extrachromosomal maintenance and integration of transforming sequences. EMBO J 10, 3959-3970.

Miller, K. G., Emerson, M. D., and Rand, J. B. (1999). Goalpha and diacylglycerol kinase negatively regulate the Gqalpha pathway in *C. elegans*. Neuron *24*, 323-333.

Miyawaki, A., Griesbeck, O., Heim, R., and Tsien, R. Y. (1999). Dynamic and quantitative Ca2+ measurements using improved cameleons. Proc Natl Acad Sci USA *96*, 2135-2140.

Montell, C. (2003). The venerable inveterate invertebrate TRP channels. Cell Calcium *33*, 409-417.

Montell, C., and Rubin, G. M. (1989). Molecular characterization of the *Drosophila* trp locus: a putative integral membrane protein required for phototransduction. Neuron *2*, 1313-1323.

Moriguchi, T., Greiner, R. S., and Salem, N., Jr. (2000). Behavioral deficits associated with dietary induction of decreased brain docosahexaenoic acid concentration. J Neurochem *75*, 2563-2573.

Nakai, J., Ohkura, M., and Imoto, K. (2001). A high signal-to-noise Ca(2+) probe composed of a single green fluorescent protein. Nat Biotechnol *19*, 137-141.

Niu, S. L., Mitchell, D. C., Lim, S. Y., Wen, Z. M., Kim, H. Y., Salem, N., Jr., and Litman, B. J. (2004). Reduced G protein-coupled signaling efficiency in retinal rod outer segments in response to N-3 fatty acid deficiency. J Biol Chem *279*, 31098-31104.

Nonet, M.L., Staunton, J.E., Kilgard, M.P., Fergestad, T., Hartwieg, E., Horvitz, H.R., Jorgensen, E.M., and Meyer, B.J. (1997). *Caenorhabditis elegans rab-3* mutant synapses exhibit impaired function and are partially depleted of vesicles. J Neurosci *21*, 8061-8073.

Oliver, D., Lien, C. C., Soom, M., Baukrowitz, T., Jonas, P., and Fakler, B. (2004). Functional conversion between A-type and delayed rectifier K+ channels by membrane lipids. Science *304*, 223-224.

Perkins, L. A., Hedgecock, E. M., Thomson, J. N., and Culotti, J. G. (1986). Mutant sensory cilia in the nematode *Caenorhabditis elegans*. Dev Biol *117*, 456-487.

Prescott, E. D., and Julius, D. (2003). A modular PIP2 binding site as a determinant of capsaicin receptor sensitivity. Science *300*, 1284-1288.

Rohacs, T., Chen, J., Prestwich, G. D., and Logothetis, D. E. (1999). Distinct specificities of inwardly rectifying K(+) channels for phosphoinositides. J Biol Chem *274*, 36065-36072.

Runnels, L. W., Yue, L., and Clapham, D. E. (2002). The TRPM7 channel is inactivated by PIP(2) hydrolysis. Nat Cell Biol *4*, 329-336.

Sengupta, P., Colbert, H. A., and Bargmann, C. I. (1994). The *C. elegans* gene *odr-7* encodes an olfactory-specific member of the nuclear receptor superfamily. Cell *79*, 971-980.

Sengupta, P., Chou, J. H., and Bargmann, C. I. (1996). *odr-10* encodes a seven transmembrane domain olfactory receptor required for responses to the odorant diacetyl. Cell *84*, 899-909.

Suzuki, H., Kerr, R., Bianchi, L., Frokjaer-Jensen, C., Slone, D., Xue, J., Gerstbrein, B., Driscoll, M., and Schafer, W. R. (2003). *In vivo* imaging of *C. elegans* mechanosensory neurons demonstrates a specific role for the MEC-4 channel in the process of gentle touch sensation. Neuron *39*, 1005-1017.

Tanaka, T., Ikita, K., Ashida, T., Motoyama, Y., Yamaguchi., Y., and Satouchi, K. (1996). Effects of growth temperature on the fatty acid composition of the free-living nematode *Caenorhabditis elegans*. Lipids *31*, 1173-1178.

Tobin, D., Madsen, D., Kahn-Kirby, A., Peckol, E., Moulder, G., Barstead, R., Maricq, A., and Bargmann, C. (2002). Combinatorial expression of TRPV channel proteins defines their sensory functions and subcellular localization in *C. elegans* neurons. Neuron *35*, 307-318.

Troemel, E. R., Chou, J. H., Dwyer, N. D., Colbert, H. A., and Bargmann, C. I. (1995). Divergent seven transmembrane receptors are candidate chemosensory receptors in *C. elegans*. Cell *83*, 207-218.

Von Schacky, C. (2004). Omega-3 fatty acids and cardiovascular disease. Curr Opin Clin Nutr Metab Care *7*, 131-136.

Wang, J. W., Wong, A. M., Flores, J, Vosshall, L. B., and Axel, R. (2003). Two-photon calcium imaging reveals an odor-evoked map of activity in the fly brain. Cell *112*, 271-282.

Watanabe, H., Vriens, J., Prenen, J., Droogmans, G., Voets, T., and Nilius, B. (2003). Anandamide and arachidonic acid use epoxyeicosatrienoic acids to activate TRPV4 channels. Nature *424*, 434-438.

Watts, J. L., and Browse, J. (2002). Genetic dissection of polyunsaturated fatty acid synthesis in *Caenorhabditis elegans*. Proc Natl Acad Sci USA *99*, 5854-5859.

Watts, J. L., Phillips, E., Griffing, K. R., and Browse, J. (2003). Deficiencies in C20 Polyunsaturated Fatty Acids Cause Behavioral and Developmental Defects in *Caenorhabditis elegans fat-3* Mutants. Genetics *163*, 581-589.

West, R.J., Sun, A.Y., Church, D.L., and Lambie, E.J. (2001). The *C. elegans gon-2* gene encodes a putative TRP cation channel protein required for mitotic cell cycle progression. Gene *266*, 103-110.

Xu, X. Z., and Sternberg, P. W. (2003). A *C. elegans* sperm TRP protein required for sperm-egg interactions during fertilization. Cell *114*, 285-297.

Zygmunt, P. M., Petersson, J., Andersson, D. A., Chuang, H.-h., Sorgard, M., Marzo, V. D., Julius, D., and Hogestatt, E. D. (1999). Vanilloid receptors on sensory nerves mediate the vasodilator action of anandamide. Nature *400*, 452-457.

Figure 2-1. Lipid synthesis pathways in *C. elegans*.

A. Schematic diagram of *C. elegans* lipid synthesis from saturated fatty acids found in bacteria. Desaturation by the Δ9 and Δ12 desaturase activities yields the substrates for the n-3 desaturase *fat-1*, the Δ6 desaturase *fat-3*, and the Δ5 desaturase *fat-4*. The *elo-1* and *elo-2* activities elongate 18-carbon PUFAs into 20-carbon PUFAs. Lipid structures are abbreviated as in 20:5n-3, which has 20 carbons and 5 double bonds, the first occurring at the n-3 position. PUFAs measured in this study are denoted as follows: LA, linoleic acid; ALA, linolenic acid; GLA, gamma-linolenic acid; STA, stearidonic acid; DGLA, dihomo-gamma-linolenic acid; O3AA, omega-3 arachidonic acid; AA, arachidonic acid; EPA; eicosapentaenoic acid.

B. *fat* single and double mutants are depleted in specific PUFAs, as measured by gas chromatography (N2, wild-type strain). Note that in the absence of a specific desaturase activity, the immediate precursor accumulates to excess. Dietary supplementation of *fat-3(wa22)* worms with specific PUFAs results in the accretion of that PUFA and its downstream products, and negligible retroconversion into upstream PUFAs. The diameter of each circle represents the ratio of specific PUFA content to the total PUFA content. Data shown are representative examples from multiple gas chromatography experiments. Portions of representative GC traces for single mutants were published in Watts and Browse, 2002.

Figure 2-1

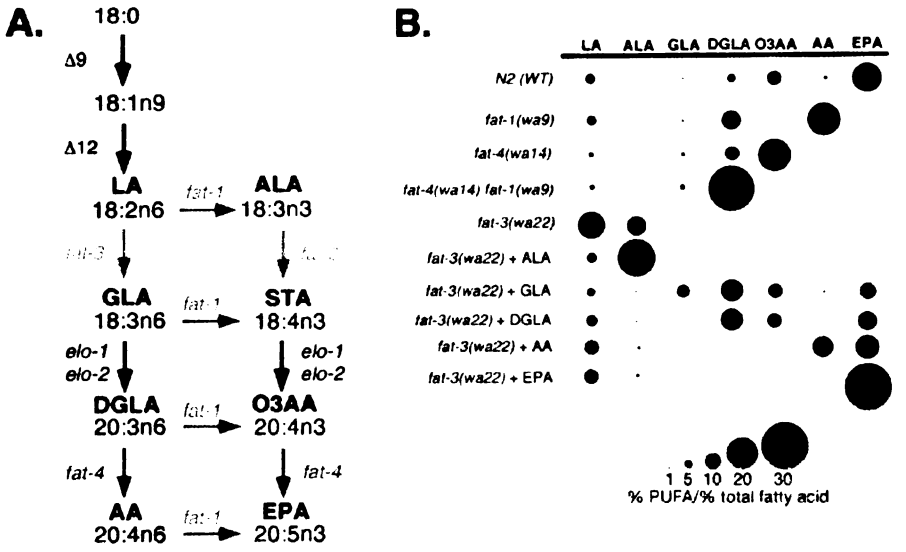
A.
18:0
Δ9
18:1n9
Δ12
LA
18:2n6
fat-1
ALA
18:3n3
GLA
18:3n6
STA
18:4n3
elo-1
elo-2
DGLA
20:3n6
O3AA
20:4n3
fat-4
AA
20:4n6
EPA
20:5n3
B.
LA ALA GLA DGLA O3AA AA EPA
N2 (WT)
fat-1(wa9)
fat-4(wa14)
fat-4(wa14) fat-1(wa9)
fat-3(wa22)
fat-3(wa22) + ALA
fat-3(wa22) + GLA
fat-3(wa22) + DGLA
fat-3(wa22) + AA
fat-3(wa22) + EPA
1 5 10 20 30
% PUFA/% total fatty acid

Figure 2-2. *fat-3* mutants show cell-specific chemotaxis defects.

A. Chemotaxis to the AWA-sensed odorant diacetyl (1 nl).

B. Chemotaxis to the AWC-sensed odorant benzaldehyde (5 nl).

C. Diacetyl chemotaxis across a range of concentrations.

D. Benzaldehyde chemotaxis across a range of concentrations.

E. Chemotaxis to the AWA-sensed odorant 2-methylpyrazine (2MP), the AWC-sensed odorants butanone (Bu), isoamyl alcohol (IAA) and 2,3-pentanedione (2,3-PD), and the AWA / AWC-sensed odorant trimethylthiazole (TMT).

For all panels, each bar represents the mean + s.e.m. of at least 5 independent assays. Statistical analysis by ANOVA and t-test with Bonferroni correction for multiple comparisons, Different from wild-type at * $P<0.05$, ** $P<0.01$. Alleles tested were *osm-9(ky10)*, *osm-9(n2743)*, *fat-1(wa9)*, *fat-4(wa14)*, *fat-3(wa22)*, and the double mutant *fat-4(wa14) fat-1(wa9)*.

Figure 2-2

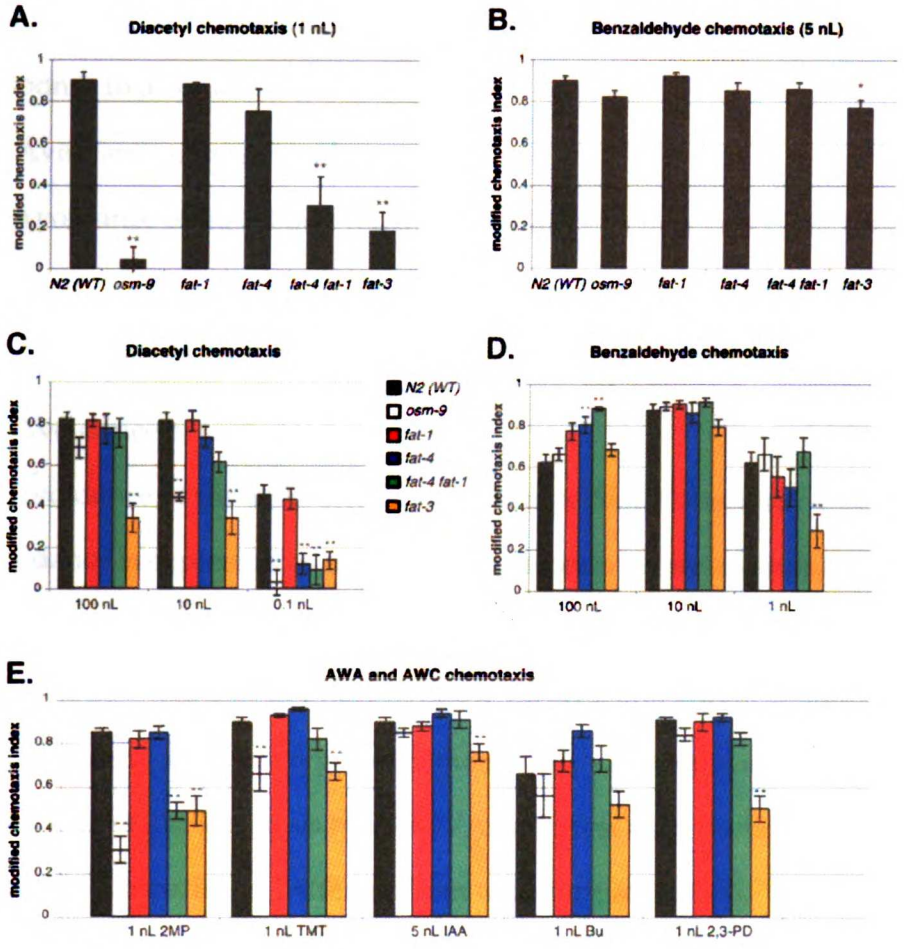
A.
Diacetyl chemotaxis (1 nL)
modified chemotaxis index
N2 (WT)
osm-9
fat-1
fat-4
fat-4 fat-1
fat-3
B.
Benzaldehyde chemotaxis (5 nL)
C.
Diacetyl chemotaxis
100 nL
10 nL
0.1 nL
D.
Benzaldehyde chemotaxis
1 nL
E.
AWA and AWC chemotaxis
1 nL 2MP
1 nL TMT
5 nL IAA
1 nL Bu
1 nL 2,3-PD

Figure 2-3. Defective nociception in *fat-3* mutants.

For A,C,D,F, avoidance is expressed as percentage of animals reversing in response to a noxious stimulus.

A. Avoidance of nose touch.

B. Avoidance of light body touch, scored as percent reversing in response to anterior touch, or percent accelerating in response to posterior body touch.

C. Avoidance of high osmolarity across a range of concentrations.

D. Avoidance of Cu^{2+} ions.

E. Avoidance of the ASH-sensed volatile repellent 2-octanone. 2-octanone avoidance is expressed as mean time in seconds before an animal reverses movement.

F. Osmotic avoidance in phospholipase Cβ *egl-8* and Gq *egl-30* mutants.

For all panels, each bar represents the mean + s.e.m. of at least 4 independent assays. Statistical analysis by ANOVA and t-test with Bonferroni correction for multiple comparisons, Different from wild-type at *P<0.05, ** P<0.01. Alleles tested were *osm-9(ky10), osm-9(n2743), fat-1(wa9), fat-4(wa14), fat-3(wa22), egl-8(md1971), egl-30(n686sd), mec-4(e1339),* and the double mutant *fat-4(wa14) fat-1(wa9).*

Figure 2-3

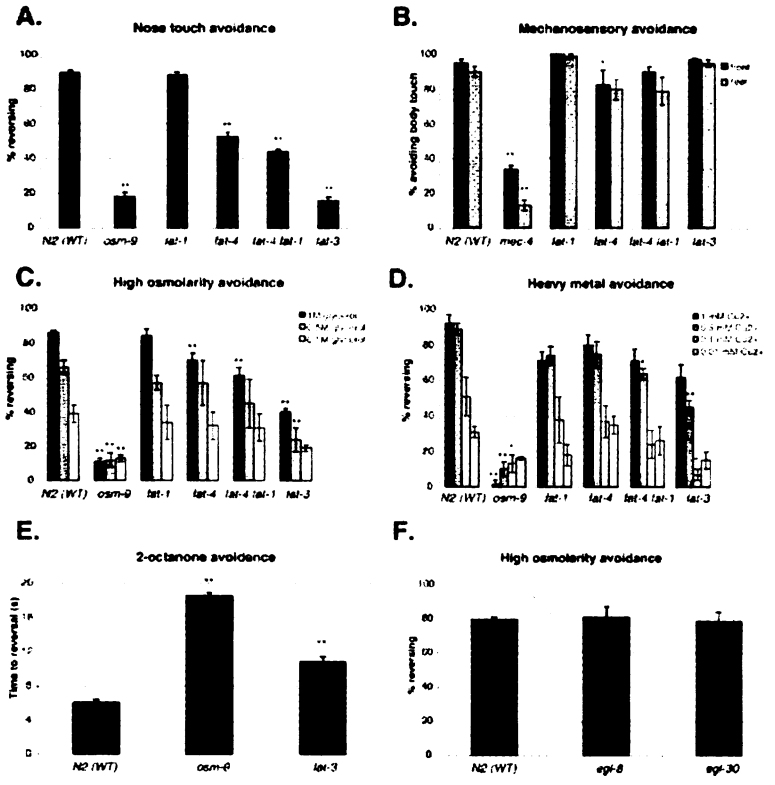
A.
Nose touch avoidance
% reversing
N2 (WT)
osm-9
tat-1
tat-4
tat-4 tat-1
tat-3
B.
Mechanosensory avoidance
% avoiding body touch
N2 (WT)
mec-4
tat-1
tat-4
tat-4 tat-1
tat-3
C.
High osmolarity avoidance
% reversing
N2 (WT)
osm-9
tat-1
tat-4
tat-4 tat-1
tat-3
D.
Heavy metal avoidance
% reversing
N2 (WT)
osm-9
tat-1
tat-4
tat-4 tat-1
tat-3
E.
2-octanone avoidance
Time to reversal (s)
N2 (WT)
osm-9
tat-3
F.
High osmolarity avoidance
% reversing
N2 (WT)
egl-8
egl-30

Figure 2-4. Sensory stimuli elicit calcium transients in ASH neurons.

A. Resting G-CaMP fluorescence in ASH and maximum ΔF/F response to 100μM EPA. Pseudocolor scale from 0 to 95% of maximum ΔF. Scale bar is 5 μm.

B.-D. Time-course of stimuli-evoked G-CaMP fluorescence changes shown relative to averaged prestimulus baseline for individual imaging trials.

B. Glycerol evoked a larger Ca^{2+} transient in N2 than *fat-3*.

C. M13-ethanol buffer control did not evoke robust Ca^{2+} transients in any animal.

D. EPA evoked robust, similar Ca^{2+} transients in N2 and *fat-3*.

Data were collected at 10 Hz and are presented with no temporal filtering or photobleaching correction. Stimuli were given in two 4 sec pulses (dash under trace) during each trial. For all stimuli tested, the second Ca^{2+} response during each trial was invariably smaller than the first. This reduction likely represents sensory adaptation; responses recovered after several minutes.

E. The maximum ΔF/F plotted for individual imaging trials with N2 and *fat-3* animals. Responses did not systematically vary with concentration over a range of 0.1- 2 mM EPA or 0.1-1% ethanol, suggesting that they are saturated. *osm-9* animals did not exhibit Ca^{2+} transients in response to any stimuli tested (n=6 for 1M glycerol, n=7 for 0.1M EPA, n=4 for 1% ethanol control; data not shown). *osm-9* mutants also failed to respond to glycerol or PUFAs when examined with the ratiometric Ca^{2+} indicator cameleon (data not shown).

Figure 2-4

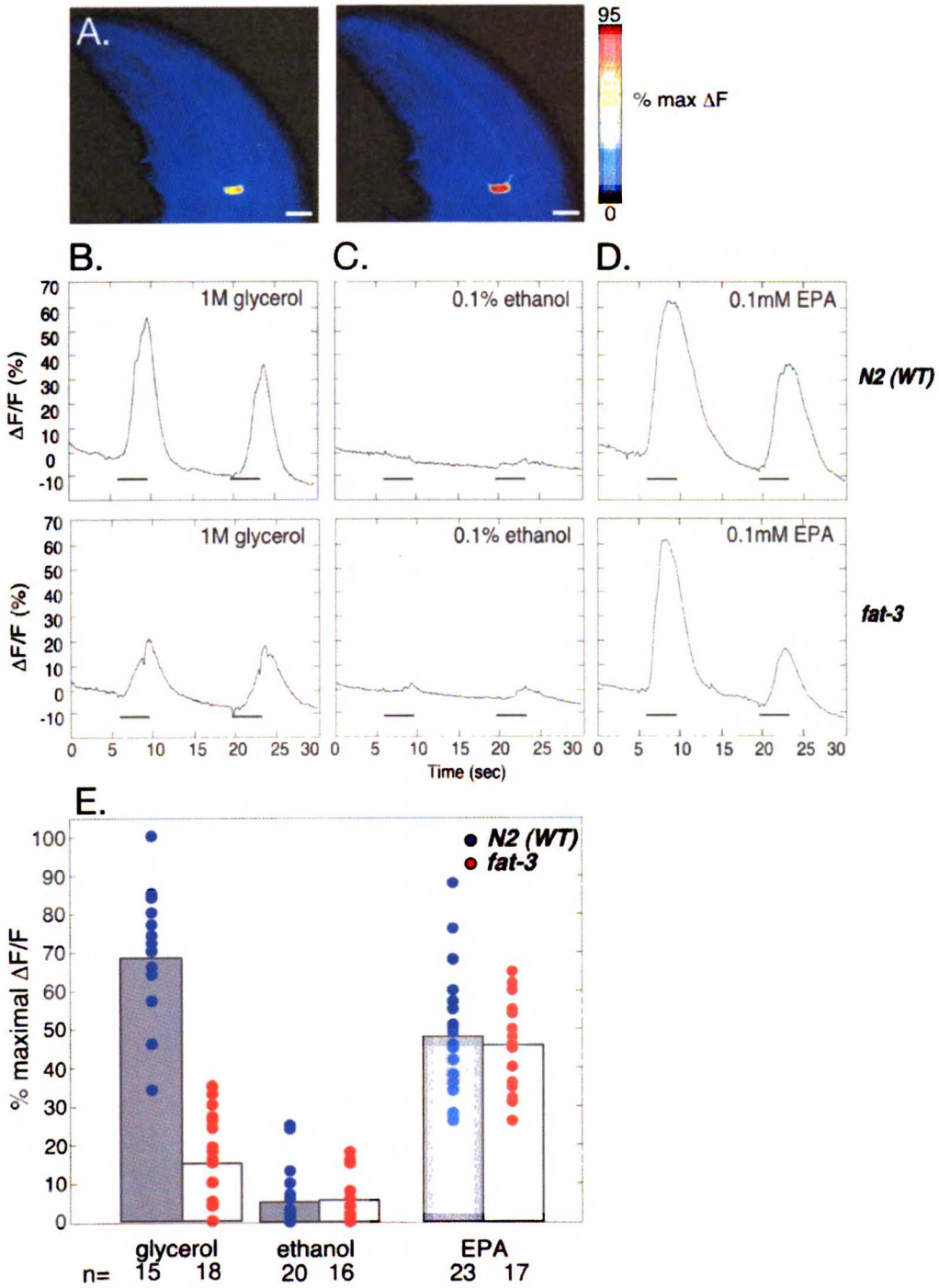
A.
95
% max ΔF
0
B.
C.
D.
1M glycerol
0.1% ethanol
0.1mM EPA
N2 (WT)
fat-3
ΔF/F (%)
Time (sec)
E.
N2 (WT)
fat-3
% maximal ΔF/F
glycerol
ethanol
EPA
n= 15 18 20 16 23 17

Figure 2-5. ASH synaptic transmission is spared in *fat-3; sra-6::TRPV1* animals. Drop test avoidance assays to 100 μM, 50 μM, and 10 μM capsaicin application, with percentage of animals reversing as an index of avoidance. The *sra-6::TRPV1* transgene expresses the rat TRPV1 channel in ASH and two other neurons, and has been shown to generate avoidance through ASH (Tobin et al., 2002). Each bar represents the mean + s.e.m. of at least 3 independent assays. Statistical analysis by ANOVA and t-test with Bonferroni correction for multiple comparisons, *P<0.05, ** P<0.01 relative to *sra-6::TRPV1*.

Figure 2-5

A.

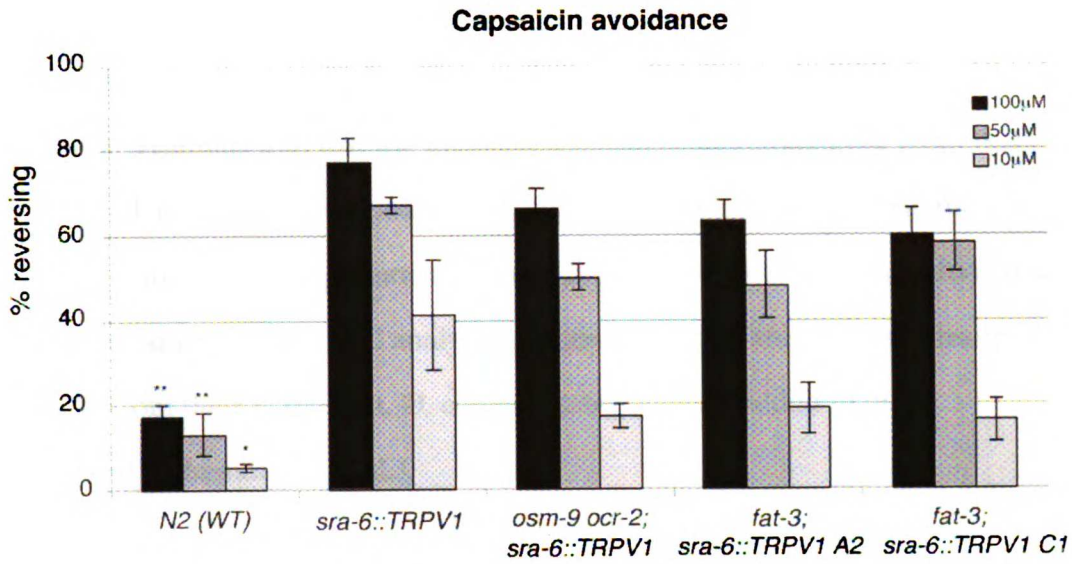
Capsaicin avoidance
% reversing
100
80
60
40
20
0
100μM
50μM
10μM
N2 (WT)
sra-6::TRPV1
osm-9 ocr-2; sra-6::TRPV1
fat-3; sra-6::TRPV1 A2
fat-3; sra-6::TRPV1 C1

Figure 2-6. Rescue of *fat-3* behavioral defects by restoring PUFAs.

A. *sra-6::fat-3::GFP* partially rescues systemic PUFA levels. Diameter of circles represents the ratio of specific PUFA content to the total fatty acid content.

B. Transgenic rescue of *fat-3* osmotic avoidance defects by the FAT-3::GFP chimera. Animals that lost the unstable *sra-6::fat-3::GFP* transgene from ASH (indicated as -) are not rescued. Data from three independent transgenic lines.

C.-F. 24 hour dietary supplementation with lipids was followed by behavioral assays of adult animals. GC analysis confirmed that all animals had absorbed PUFAs from their *E. coli* diet. Ø, control plates without added PUFA.

C. Diacetyl chemotaxis (1 nL).

D. Benzaldehyde chemotaxis (5 nL).

E. ASH nose touch avoidance.

F. ASH osmotic avoidance of 1M glycerol.

For all graphs, each bar represents the mean + s.e.m. of at least 3 independent assays. Statistical analysis by ANOVA and t-test with Bonferroni correction for multiple comparisons. Panels C-F, comparisons within genotype of PUFA-supplemented animals to tergitol-fed controls. Panel B, comparison of transgenic strains vs. siblings that lost the transgene. * $P<0.05$, ** $P<0.01$.

Figure 2-6

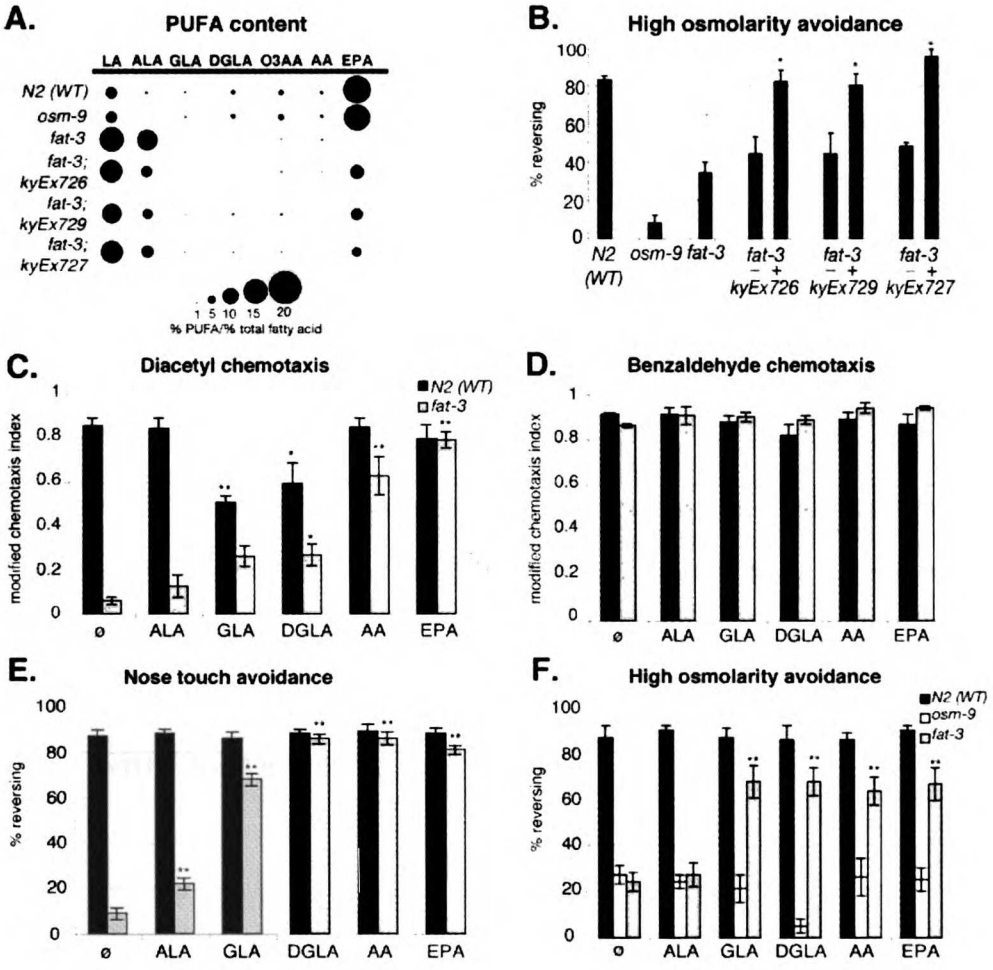
A.
PUFA content
LA ALA GLA DGLA O3AA AA EPA
N2 (WT)
osm-9
fat-3
fat-3; kyEx726
fat-3; kyEx729
fat-3; kyEx727
1 5 10 15 20
% PUFA/% total fatty acid
B.
High osmolarity avoidance
% reversing
N2 (WT)
osm-9
fat-3
fat-3 − +
kyEx726
fat-3 − +
kyEx729
fat-3 − +
kyEx727
C.
Diacetyl chemotaxis
N2 (WT)
fat-3
modified chemotaxis index
ø ALA GLA DGLA AA EPA
D.
Benzaldehyde chemotaxis
modified chemotaxis index
ø ALA GLA DGLA AA EPA
E.
Nose touch avoidance
% reversing
ø ALA GLA DGLA AA EPA
F.
High osmolarity avoidance
N2 (WT)
osm-9
fat-3
% reversing
ø ALA GLA DGLA AA EPA

Figure 2-7. Exogenous PUFAs elicit avoidance responses.

A. Percentage of animals avoiding drops of EPA in a modified drop test (Hilliard et al., 2002).

B. Percentage of animals avoiding drops of LA in a modified drop test. LA, like M13-ethanol buffer, elicits modest avoidance responses in wild-type and *osm-9* animals.

Diameters of circles represent the fraction of animals showing no avoidance response (0-20% reversing), low avoidance (21-40% reversing), or high avoidance (41-100% reversing). For all panels, the total number of animals tested is given, as well as the number of independent experiments conducted on different days. Statistical analysis by ANOVA and t-test or t-test with Bonferroni correction for multiple comparisons. Shaded areas represent responses significantly different from wild-type (for 0.1 mM EPA, $P<0.0005$, for 1 mM and 2 mM EPA, $P<0.05$, for 4 mM EPA, $P<0.01$).

Figure 2-7

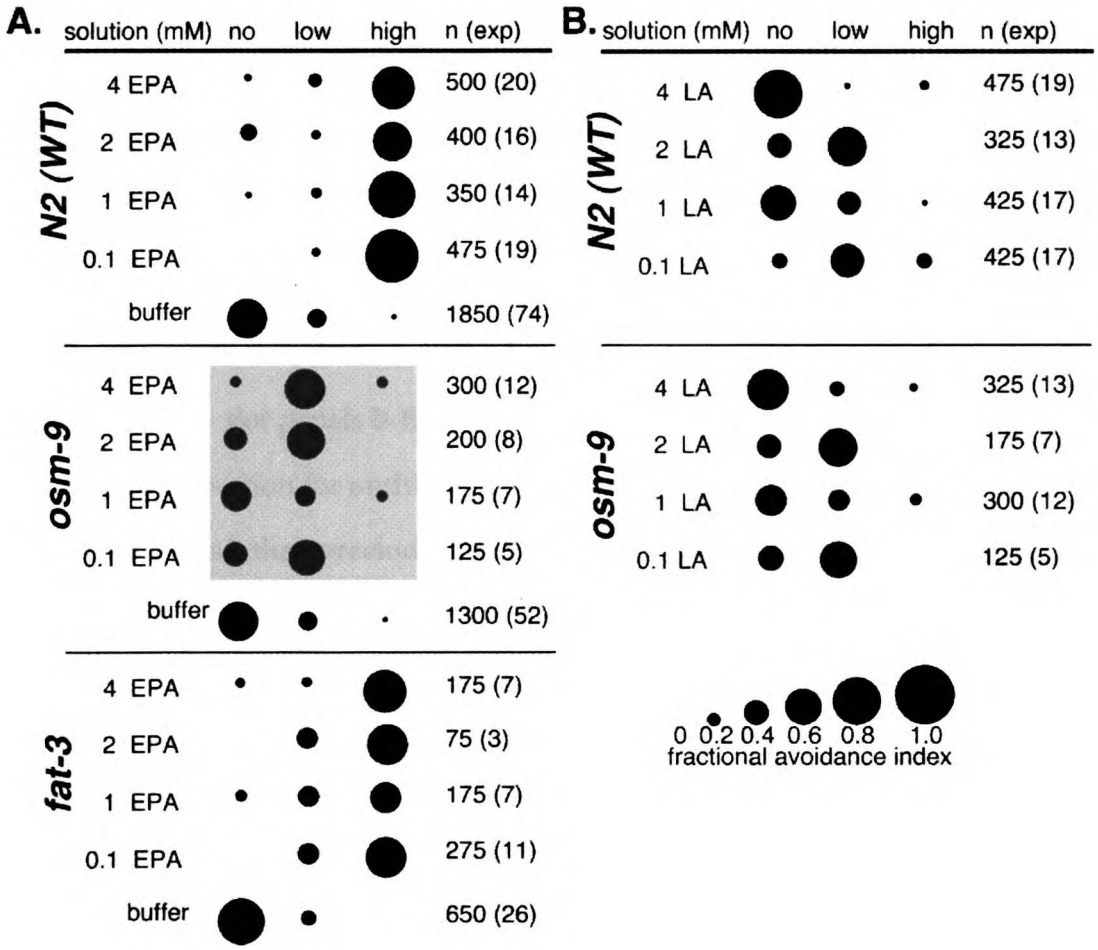
A.
solution (mM) no low high n (exp)
N2 (WT)
4 EPA 500 (20)
2 EPA 400 (16)
1 EPA 350 (14)
0.1 EPA 475 (19)
buffer 1850 (74)
osm-9
4 EPA 300 (12)
2 EPA 200 (8)
1 EPA 175 (7)
0.1 EPA 125 (5)
buffer 1300 (52)
fat-3
4 EPA 175 (7)
2 EPA 75 (3)
1 EPA 175 (7)
0.1 EPA 275 (11)
buffer 650 (26)
B.
solution (mM) no low high n (exp)
N2 (WT)
4 LA 475 (19)
2 LA 325 (13)
1 LA 425 (17)
0.1 LA 425 (17)
osm-9
4 LA 325 (13)
2 LA 175 (7)
1 LA 300 (12)
0.1 LA 125 (5)
0 0.2 0.4 0.6 0.8 1.0
fractional avoidance index

Figure 2-supplementary 1. Cell-specific sensory defects in *elo-1(wa7)* mutants.

A. Representative GC data for PUFA composition of *N2* and *elo-1(wa7)* animals. Portions of this data were reported in Watts and Browse (2002) and in Fig. 2-1b.

B. Defective avoidance of ASH nose touch.

C. Defective avoidance of high osmolarity solutions.

D. Defective avoidance of certain concentrations of heavy metals.

E. Chemotaxis to the AWA-sensed odorant diacetyl across a range of concentrations. For panels B-E, statistical analysis by ANOVA and t-test with Bonferroni correction for multiple comparisons, *$P<0.05$, **$P<0.01$. RNAi against the *elo-2* locus is lethal, precluding behavioral analysis (Kniazeva et al, 2003).

Figure 2-supplementary 1

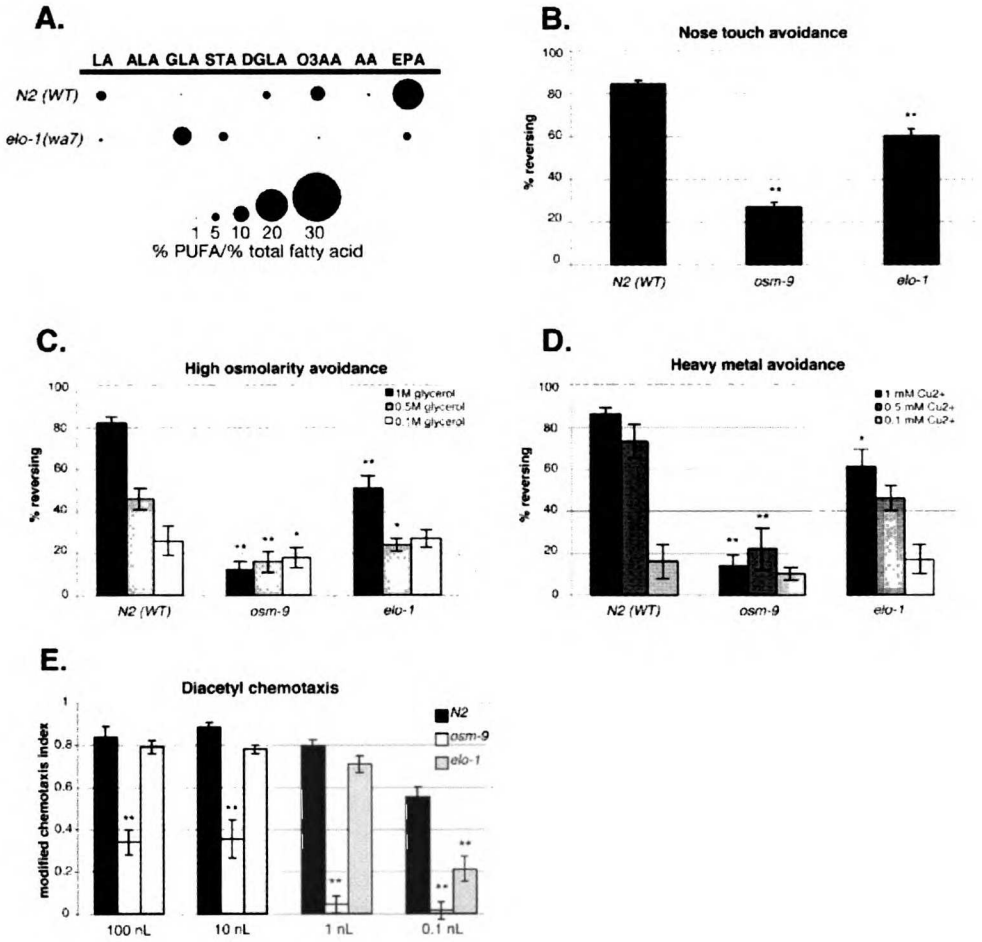

Figure 2-supplementary 2. Absence of sensory defects in the synaptic neurotransmission mutant *rab-3(y250)*.

A. Chemotaxis to a standard concentration of the AWA-sensed odorant diacetyl.

B. Chemotaxis to a standard concentration of the AWC-sensed odorant benzaldehyde.

C. Avoidance of high osmolarity solutions.

D. Avoidance of nose touch, showing a very mild but statistically significant defect in *rab-3*. Statistical analysis by ANOVA and t-test with Bonferroni correction for multiple comparisons, *$P<0.05$, **$P<0.01$.

Figure 2-supplementary 2

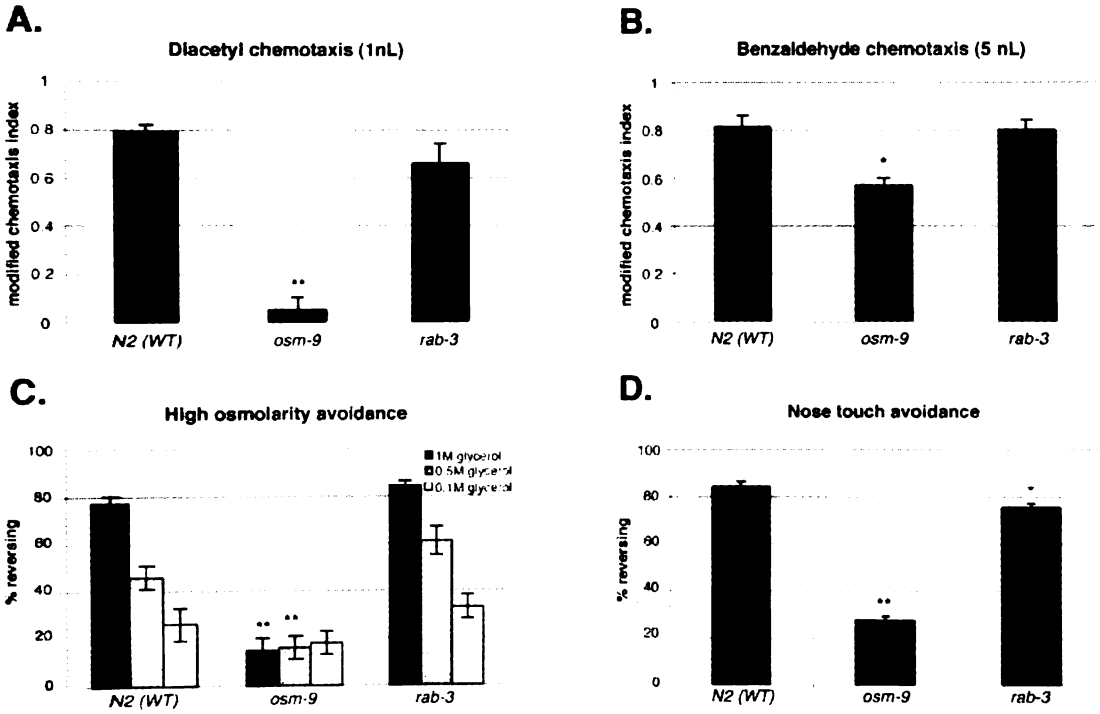

Chapter three:

TRPV-dependent regulation

of gene expression in sensory neurons

The ensemble of receptors expressed on a sensory neuron's cell surface determines its capacity to detect and subsequently respond to environmental cues. How does a neuron determine which receptors it should express? One possibility is that receptor expression is rigidly specified in development, and remains static through the life of the organism. A second possibility is that receptor expression is dynamic, tuned to the changing environmental conditions faced by an organism. Here, I describe genetic studies directed towards understanding how TRPV ion channel signaling pathways regulate G-protein coupled receptor (GPCR) expression in *C. elegans* sensory neurons.

In *C. elegans,* sensory receptors include GPCRs (Sengupta et al., 1996) and perhaps guanylyl cyclases (Gray et al., 2004; Yu et al., 1997). Evidence suggests that the initial specification of receptor expression is regulated by elaborate developmental cascades; I will illustrate two particularly elegant examples here. In the AWC olfactory neuron pair, stochastic expression of the *str-2* GPCR in either the left or right cell is determined by a lateral signaling pathway that ultimately impinges upon a MAP kinase signaling cassette (Sagasti et al., 2001). While the molecular details of this process are an ongoing subject of study, a favored model is that the two AWC cells are initially equivalent, but fluctuations in Ca^{2+} signaling are amplified into a transcriptional difference between the left and right AWC neurons. Expression of a specific suite of GPCRs endows each individual AWC neuron with the ability to respond to a different ensemble of odorants, showing that receptor choice has functional chemosensory consequences (Wes and Bargmann, 2001). Similarly, the salt-sensing ASE neuron pair expresses different sets of guanylyl cyclases in the left or right cell (Yu et al.,

1997), and the left and right cells have different neuronal sensitivities to ions (Pierce-Shimomura et al., 2001). ASE receptor choice is not stochastic; two micro-RNAs gate the function of alternative transcriptional pathways leading to the expression of different transcription factors and different receptors in the ASEL and ASER neurons (Chang et al., 2004; Johnston and Hobert, 2003).

Sensory receptor expression may be under tight initial control, but is still capable of modification. Chemosensory receptor expression can be modified bidirectionally in postembryonic stages, as demonstrated by studies of gene expression in the ASI neuron pair. ASI is involved in sensing water-soluble attractants, and has a major role in regulating entry into the dauer diapause state. Worms enter into dauer in response to harsh environmental conditions. Dauer entry and exit are regulated by information including food levels, the presence of lipid pheromones, and ambient temperature (Riddle and Albert, 1997). Upon dauer entry, ASI expression of the *srd-1* GPCR is decreased, and ASI *str-2* expression is induced (Peckol et al., 2001). Similarly, in the constitutive dauer formation mutant *daf-7*, ASI expression of *str-3* and ASH/ASI expression of *sra-6* were reduced (Nolan et al., 2002). An interesting possibility emerges, namely that sensory stimulation feeds back upon the types of receptors expressed by neurons. If so, do worms with altered sensory signaling also exhibit altered receptor expression?

Analysis of AWC *str-2* expression indicated that fluctuations in cyclic GMP (cGMP) signaling could influence GPCR expression. In AWC neurons, *str-2* expression is diminished at mid-larval stages in animals with mutations in the *odr-1* or *daf-11* guanylyl cyclases, or in *tax-2* and *tax-4* cyclic nucleotide gated ion channel subunits (Troemel et al., 1999). Initial specification of AWC asymmetry

is only mildly affected in *odr-1* and *daf-11*, suggesting the model that AWC chemosensory activity elevates cGMP levels, leading to the maintenance of *str-2* expression. In the absence of adequate cGMP signaling, *str-2* expression is extinguished.

Are other chemosensory neurons subject to GPCR expression regulation through discrete signal transduction pathways? Like AWC, the AWA chemosensory neuron pair mediates chemotaxis towards certain volatile odorants, including the bacterial metabolite diacetyl. A model for diacetyl detection is shown in Figure 3-1, where diacetyl interacts with the *odr-10* GPCR and *odr-3* Gα proteins to promote depolarization via a heteromeric *osm-9/ocr-2* TRPV ion channel (Colbert et al., 1997; Roayaie et al., 1998; Sengupta et al., 1996; Tobin et al., 2002). This molecular framework for AWA signal transduction made it an attractive subject for studying TRPV-dependent GPCR expression regulation.

Initial observations of the TRPV channel mutant *osm-9* suggested that defects in signal transduction could indeed affect AWA *odr-10* GPCR expression. Erin Peckol noted that AWA expression of a GFP reporter driven by the *odr-10* GPCR promoter was strongly decreased in *osm-9* mutants (Figure 3-2). Weak *odr-10*::GFP expression in the CEP neurons and nonspecific transgene expression in the tail were unaffected by mutations in *osm-9*, indicating that this mode of regulation might be specific to AWA. Subsequently, David Tobin showed that *odr-10*::GFP expression was reduced in *ocr-2* single mutants and an *ocr-2; ocr-1* double mutant (Tobin et al., 2002). Together, this work suggested for the first time that TRP channels could regulate gene expression.

In addition, these results suggested a strategy for forward genetic screens for additional signal transduction components, namely visual inspection of *odr-10*::GFP levels. Such screens could reveal additional signal transduction components in AWA, molecules specifically involved in receptor expression regulation in AWA, or molecules expressed in other neurons with an ability to regulate AWA gene expression non-cell autonomously.

In this portion of my dissertation, I will describe two approaches to understanding how sensory activity influences receptor expression, focusing on the AWA neuron and its TRPV-dependent expression of the *odr-10*::GFP reporter. One approach was to examine signal transduction mutants predicted to interact with *osm-9*/*ocr-2* TRPV pathways on the basis of their function in other organisms. From these experiments, several groups of signaling molecules emerged as regulators of *osm-9*-dependent *odr-10*::GFP expression, including G proteins, Ca^{2+} signaling components, lipid synthesis genes, and insulin signaling pathways. A second approach was a forward genetic suppressor screen in *osm-9(n2743)* loss-of-function mutants. The screen successfully generated a handful of mutants with intriguing phenotypes, but the genes affected by these mutants have yet to be cloned.

TRPV mutants have defects in maintenance of AWA *odr-10*::GFP expression

Expression of *str-2*::GFP in AWC is initially specified by a Ca^{2+}/MAP kinase signaling cascade, and maintained by cGMP-dependent neuronal activity (Sagasti et al., 2001; Troemel et al., 1999). Similarly, AWA *odr-10*::GFP expression defects in TRPV mutants could be due to a lack of embryonic gene expression, or due to a failure in postembryonic maintenance of gene expression. To

distinguish among these possibilities, I examined *odr-10*::GFP expression in wild-type, *osm-9(n2743)*, *ocr-2(ak47)*, and *osm-9(ky10) ocr-2(ak47)* animals at discrete embryonic and larval stages, grown at 20°C on HB101 *E. coli*. *odr-10*::GFP expression was apparent within 30 minutes of hatching in wild-type and *osm-9/ocr-2* mutant animals, although embryonic expression was occasionally seen as well at the 3-fold and 2-fold stages (Figure 3-2). Cells tentatively identified as AWA and CEP showed the most consistent expression of *odr-10*::GFP, but some expression was noted in additional, unidentified head cells (which had sizes and positions consistent with amphid neurons). At 24 hours after egg laying, wild-type and *osm-9/ocr-2* mutant larvae had brighter expression in AWA and faint expression in CEP and other cells. At 44 hours after egg laying, *N2*, *osm-9* and *ocr-2* single and double mutants showed a similar degree and pattern of *odr-10*::GFP expression. By the adult stage, *osm-9* and *ocr-2* single and double mutants had strong defects in AWA *odr-10*::GFP expression (Figures 3-2, 3-3, 3-4; Tobin et al., 2002). Thus, TRPV signaling is not required for expression of *odr-10*::GFP in AWA, CEP, and unidentified head cells at L1 and L3 larval stages, but is required for maintenance of *odr-10*::GFP expression into adulthood.

Candidate regulators of AWA *odr-10*::GFP expression

By analogy with other TRP signal transduction pathways such as the canonical *Drosophila* phototransduction cascade (Hardie, 2003), *osm-9* and *ocr-2* signaling in the AWA chemosensory neurons was predicted to function downstream of G-proteins and upstream of neuronal depolarization and calcium influx (Figure 3-1). If *osm-9* and *ocr-2* affect AWA expression through the same signaling pathway, other genes that function as positive effectors of AWA

signaling should have reduced AWA *odr-10*::GFP expression as a loss-of-function phenotype, like *osm-9* or *ocr-2* mutants (Figure 3-2; Tobin et al., 2002). Alternately, mutations that enhance signaling through this pathway might be expected to suppress weak *osm-9* (or *ocr-2*) mutations. Such genes could represent novel effectors of TRPV signaling pathways. Within this framework, members of multiple signaling families were tested for their effects on AWA GFP expression in either an *osm-9(+)* or *osm-9* mutant background.

Multiple G-proteins of the G_i class regulate AWA *odr-10*::GFP expression

The *C. elegans* genome encodes 20 predicted Gα subunits, including 14 G_i-like proteins expressed in specific subsets of sensory neurons (Jansen et al., 1999). Mutations that affect the G_i-like Gα ODR-3 result in defective AWA, AWC, and ASH signal transduction (Roayaie et al., 1998), but the role of *odr-3* in regulating gene expression was unknown. Moreover, although the activity of the TRPV channel encoded by *osm-9* and *ocr-2* was predicted to lie downstream of G-protein activation, direct evidence for this model was lacking. The roles of other G-proteins expressed in AWA were also unknown. To address these points, I examined *odr-10*::GFP expression in both gain-of-function and loss-of-function G-protein mutants.

Animals with mutations in *odr-3* had diminished expression of *odr-10*::GFP (Figure 3-3). Results were quantified by scoring the percentage of animals with high, low, or no expression of *odr-10*::GFP in AWA. By these criteria, *odr-3* mutants were less defective than *osm-9* null mutants. Mutations in the closely-related Gα *gpa-3* did not affect *odr-10*::GFP expression, but an *odr-3 gpa-3* double

mutant had slightly lower *odr-10*::GFP than the *odr-3* single mutant, suggesting that *gpa-3* plays a minor role in regulating AWA activity. The *odr-3 gpa-3* double mutant is still less defective than *osm-9*, suggesting that additional G-proteins or parallel genetic pathways upstream of the TRPV channels contribute to *odr-10*::GFP expression regulation. Studies by the Jansen lab suggest that *gpa-5* and *gpa-6* negatively regulate *odr-3* and *gpa-3* olfactory signaling pathways (Lans et al., 2004). An *odr-3 gpa-3; gpa-5 gpa-6* quadruple mutant had strong AWA *odr-10*::GFP expression (Figure 3-3), supporting the model that *gpa-5* and *gpa-6* antagonize the activity of *odr-3* and *gpa-3*, and, more generally, that G-proteins can have positive and negative regulatory roles in AWA signaling.

To address whether TRPV channels function downstream of G-protein signaling in AWA, we employed a gain-of-function approach. High copy over-expression of the *odr-3* Gα (abbreviated as *odr-3(XS)*) causes morphological defects in AWA as well as defects in AWA-mediated behaviors (Roayaie et al., 1998). Enhanced activity of a positive G-protein effector would be predicted to stimulate TRPV channel function, perhaps leading to enhanced *odr-10*::GFP expression. Consistent with this hypothesis, *odr-3(XS)* animals had uniformly strong AWA *odr-10*::GFP expression (Figure 3-3)[1]. If *odr-3(XS)* functions through TRPV pathways to enhance *odr-10*::GFP expression, then mutations that inactivate TRPV channels should suppress *odr-3(XS)*. Initial results were ambiguous: *osm-9; odr-3(XS)* double mutants had intermediate levels of *odr-10*::GFP expression (Figures 3-3 and 3-4). Thus, *odr-3(XS)* partly suppressed the

[1] Figure 3-3 does not adequately reflect that most *odr-3(XS)* animals had extremely bright *odr-10*::GFP expression in AWA, visible under a 10X objective and filling the cilia, dendrite, and axon.

odr-10::GFP expression defect of *osm-9(n2743)* missense mutants or *osm-9(ky10)* null mutants, and *osm-9* partly suppressed the strong *odr-10*::GFP expression of *odr-3(XS)* animals. One interpretation of these results is that residual G-protein signaling persists through the *ocr-2* and/or *ocr-1* TRPV subunits in an *osm-9; odr-3(XS)* double mutant, leading to moderate levels of AWA *odr-10*::GFP expression. To test this possibility, I constructed an *osm-9 ocr-2; odr-3(XS)* triple mutant strain, which is predicted to have greatly diminished TRPV function in AWA. Indeed, *osm-9(ky10) ocr-2(ak47); odr-3(XS)* animals had further reductions in *odr-10*::GFP expression (Figure 3-4). Some *odr-10*::GFP expression remained in the *osm-9 ocr-2; odr-3(XS)* triple mutant, suggesting that *odr-3(XS)* can act through additional targets to modulate *odr-10*::GFP expression. One strong candidate is the *ocr-1* TRPV subunit, which is still present in AWA neurons of *osm-9 ocr-2* double mutants, although it is possible that *odr-3(XS)* can signal through non-TRPV ion channels as well. These results are consistent with a model where the AWA sensory transduction channel is composed of the TRPV subunits *osm-9, ocr-2,* and *ocr-1,* which individually and in combination function downstream of *odr-3* Gα activity.

odr-3(XS) modulation of TRPV signaling pathways was also explored in the ASH nociceptive neuron, which mediates avoidance of aversive stimuli as discussed in Chapter 2 of this thesis. *osm-9, ocr-2,* and *ocr-1* single, double, and triple mutants have defects in avoidance of high osmolarity glycerol solutions (Figure 3-4; Colbert et al., 1997; Tobin et al., 2002). *odr-3(XS)* exhibits wild-type avoidance of ASH aversive stimuli (Roayaie et al., 1998), and potently suppresses the glycerol avoidance defect of *osm-9(n2743)* or *osm-9(ky10)* animals (Figure 3-4). Suppression of an *osm-9 ocr-2* double mutant was less effective. *osm-9* and *ocr-2*

are the only TRPV subunits known to be expressed in ASH neurons, unlike AWA which also expresses the *ocr-1* TRPV subunit. These results further support a model where *odr-3* G-protein activity functions upstream of an *osm-9/ocr-2* TRPV channel.

Classical G_q signaling is not required for *odr-10*::GFP expression regulation

The residual *odr-10*::GFP expression seen in *odr-3 gpa-3* double mutants suggested that additional G-proteins could influence TRPV-dependent gene expression regulation. In *Drosophila* photoreceptors, activation of rhodopsin leads to stimulation of a $G_q\alpha$ protein, and subsequent activity of a phospholipase Cβ (PLCβ) and TRP channel (Figure 1-2) (Hardie, 2003). We hypothesized that a similar $G_q\alpha$-PLCβ pathway could regulate TRPV signaling in AWA.

Worms have a single $G_q\alpha$, encoded by the *egl-30* gene; multiple viable *egl-30* loss-of-function mutant alleles are available, and all have weak semidominant phenotypes (Brundage et al., 1999). Predicted null alleles are essentially lethal, and cannot be used for studies of postembryonic gene expression regulation or behavior. *egl-30* is essential for synaptic transmission at the *C. elegans* neuromuscular junction (NMJ), but is expressed more broadly in the nervous system (Brundage et al., 1996; Miller et al., 1999). The role of *egl-30* in mediating TRPV-dependent chemosensory behaviors was unknown. To determine if G_q signaling was involved in TRPV-dependent AWA *odr-10*::GFP regulation, I crossed *odr-10*::GFP and *osm-9(n2743)* into the reference allele *egl-30(n686sd)*, a splice acceptor mutant which exhibits mild semidominant egg-laying defects. *egl-30(n686sd)* mutant animals had normal levels of *odr-10*::GFP expression in

AWA, and failed to suppress *osm-9(n2743)* mutations (Figure 3-3). Thus, $G_q\alpha$ is unlikely to play a central signaling role in AWA neurons.

The signaling target of *egl-30* $G_q\alpha$ is *egl-8*, which encodes a PLCβ required for neuromuscular junction signaling but also expressed in most neurons (Lackner et al., 1999; Miller et al., 1999). Multiple viable alleles of *egl-8* are available, including the nonsense mutant *egl-8(md1971)* which eliminates key catalytic domains, and the *egl-8(n488)* deletion mutant (Miller et al., 1999). To determine if PLCβ mutants had a role in TRPV-dependent AWA *odr-10*::GFP expression regulation, *odr-10*::GFP was crossed into *egl-8* mutants. *egl-8(md1971)* mutants had slightly reduced AWA *odr-10*::GFP expression in one cross, and strongly reduced expression in a second cross (Figure 3-3). The basis for this difference in results is unclear, but likely due to an uncharacterized background mutation in one of the isolates. *egl-8(n488)* mutants have no defect in *odr-10*::GFP expression (D. Paskowitz and C.I.B., personal communication). At present, the role of PLCβ in TRPV-dependent *odr-10*::GFP expression regulation is unresolved. *egl-8(md1971)* and *egl-30(n686sd)* mutants are unambiguously wild-type for TRPV-dependent ASH avoidance behavior (see Chapter 2), showing that $G_q\alpha$/PLCβ signaling is not required for TRPV function in that sensory context.

Our results described in Chapter 2 demonstrate that lipid signaling is essential for TRPV-dependent chemosensory behaviors. The involvement of TRPV channels in AWA *odr-10*::GFP expression regulation suggests that lipid signaling may be important in that context, as well. The *egl-8* PLCβ may or may not be involved in *odr-10*::GFP expression regulation, but the *C. elegans* genome encodes additional phospholipase proteins which could generate diacylglycerol

(DAG), PUFAs, and other potential lipid second messengers downstream of G_i activity. The *C. elegans* gene knockout consortium has generated deletion alleles in some phospholipase genes, and made them available to the worm research community. Preliminary experiments with putative deletion alleles of *pld-1* phospholipase D and *plc-4* phospholipase C were performed to determine their involvement in TRPV-dependent sensory signaling. *plc-4(ok1215)* deletion mutants have wild-type AWA *odr-10*::GFP expression (40/43 with bright GFP), and variable ASH high osmolarity avoidance (avoidance indexes 0.40, 0.72, 0.88; n=75 animals). *pld-1(ok986)* deletion mutants have wild-type AWA *odr-10*::GFP expression (50/50 with bright GFP) and consistently defective ASH high osmolarity avoidance (avoidance indexes 0.44, 0.40, 0.40; n=75 animals). These results must be interpreted with caution, as neither *pld-1(ok986)* nor *plc-4(ok1215)* was adequately outcrossed prior to double mutant construction and analysis. Still, the moderate defect in ASH avoidance seen in *pld-1(ok986)* mutants hints at an involvement in TRPV-dependent sensory signaling pathways.

Lipid second messenger levels could also be modulated by the activity of enzymes such as the DAG kinase *dgk-1*, which metabolizes the lipid second messenger DAG, and is essential for NMJ signaling (Nurrish et al., 1999). Animals singly mutant in the DAG kinase genes *dgk-1* (data not shown) and *dgk-2* had normal levels of AWA *odr-10*::GFP expression (Figure 3-3), and *dgk-1* failed to suppress the AWA GFP expression phenotype of *osm-9* (data not shown). These two genes may function redundantly with one another or with other DAG/triacylglycerol kinases to regulate levels of lipid second messengers in AWA. Alternately, DAG kinases may not be involved in TRPV-dependent AWA *odr-10*::GFP expression regulation pathways. Later in chapter 3, I discuss other

potential lipid modulators of TRPV pathways and some possible experiments to identify them.

CaMKII modulation of *odr-10*::GFP expression

As TRPV channels are Ca^{2+} permeable (Clapham, 2003), they may exert their effects on neurons either through depolarization or by activating Ca^{2+} signaling pathways, or perhaps through both mechanisms. A key Ca^{2+} signaling integrator in many cells is the calcium-calmodulin dependent kinase CaMKII, which links Ca^{2+} influx to receptor trafficking, transcription, and activity modulation pathways (Colbran and Brown, 2004). The worm genome encodes a single CaMKII, *unc-43* (Reiner et al., 1999). Animals bearing an *unc-43(n1186)* null mutation had no defect in AWA *odr-10*::GFP expression (Figure 3-3). However, the constitutively-active gain-of-function mutation *unc-43(n498sd)* completely suppressed the AWA *odr-10*::GFP expression defect of *osm-9(n2743)* or *osm-9(ky10)* mutants. These results suggest that CaMKII could function redundantly with other Ca^{2+} effectors downstream of Ca^{2+} entry through *osm-9*, but enhanced CaMKII function is sufficient to boost signaling in an *osm-9* mutant background. The strong *osm-9* suppression seen with *unc-43(n498sd)* contrasts with the intermediate suppression seen in *odr-3(XS)* (Figures 3-3 and 3-4). This is consistent with *unc-43(n498sd)* acting downstream of the additional AWA TRPV subunits *ocr-2* and *ocr-1*, although that hypothesis has not been tested. *unc-43(n498sd)* was recently shown to moderately suppress an *osm-9*-dependent decrease in expression of the *tph-1* tryptophan hydroxylase enzyme in ADF neurons (Zhang et al., 2004), supporting a genetic interaction between CaMKII and TRPV channels in multiple *C. elegans* chemosensory neurons.

Several other Ca^{2+} signaling components did not appear to have a significant role in AWA *odr-10*::GFP expression regulation. Animals mutant in the P/Q-type voltage-gated calcium channel alpha subunit *unc-2(e55)* had normal AWA *odr-10*::GFP expression (Figure 3-3), demonstrating that AWA gene expression regulation is not a general function of all Ca^{2+} channels. Some TRPV channel alleles did not have AWA *odr-10*::GFP expression defects: the *ocr-2(yz5)* point mutant had normal AWA *odr-10*::GFP expression, even though it was strongly defective for ASH high osmolarity avoidance (data not shown) and AWA chemotaxis (J. Sze, personal communication). Analysis of this mutant may provide structural insight into TRPV channel domains required for different cellular functions, or for cell-specific roles. The calcineurin phosphatase encoded by *tax-6* functions in sensory signaling and regulation of *gcy-8*::GFP expression in *C. elegans* thermosensory neurons (Kuhara et al., 2002). *tax-6(p675)* loss-of-function mutants had no discernible effects on *odr-10*::GFP expression in an *osm-9(+)* or *osm-9(n2743)* background.

The *C. elegans* cGMP-dependent protein kinase *egl-4* promotes adaptation in the AWC neuron downstream of Ca^{2+} entry, a property that it shares with *osm-9* (L'Etoile et al., 2002). *egl-4(n479)* null mutants had no defects in AWA *odr-10*::GFP expression, and failed to suppress *osm-9(n2743)* defects in *odr-10*::GFP expression.

PUFA synthesis mutants have diet-dependent *odr-10*::GFP expression defects

As discussed in Chapter 2, *C. elegans* strains mutant for PUFA synthesis pathways have specific sensory defects in TRPV-dependent neurons. If loss of a PUFA-containing lipid second messenger reduces TRPV channel activity, then

PUFA synthesis mutants would also be expected to have defects in AWA *odr-10*::GFP expression.

Unexpectedly, PUFA synthesis mutants exhibited AWA *odr-10*::GFP expression phenotypes that depended on their *E. coli* diet. *fat-1(wa9), fat-4(wa14), fat-3(wa22)*, and *elo-1(wa7)* mutants maintained on *E. coli* HB101 had normal levels of *odr-10*::GFP expression (Figure 3-5). *fat-4 fat-1* or *fat-3 fat-1* double mutants fed HB101 also had no apparent AWA *odr-10*::GFP expression defects. By contrast, *fat-1, fat-4,* and *fat-3* single mutants fed an *E. coli* OP50 diet had decreased *odr-10*::GFP expression. *fat-4 fat-1* and *fat-3 fat-1* double mutants were similarly affected by an OP50 diet. *elo-1* mutants had no AWA *odr-10*::GFP expression defects when fed OP50, perhaps due to functional redundancy with the *elo-2* enzyme. Many other signal transduction mutants have been tested on OP50 and HB101, and do not show this diet-dependent phenotype[2]. AWA and ASH behaviors of *fat* and *elo* mutants, as well as wild-type animals and other mutant strains, are not obviously sensitive to OP50 vs. HB101 diet (data not shown).

By thin layer chromatography and GC analysis, the two different types of bacteria have different lipid compositions (Figure 3-5) (J. Watts and E. Phillips, personal communication). OP50 phospholipids tend to contain more 17:delta and 19:delta cyclopropane acyl chains, while HB101 phospholipids tend to contain the monounsaturated acyl chain 16:1. OP50 bacterial lipids have higher levels of phosphatidyl glycerol head groups (12.0% vs. 6.8% of total lipids), while

[2] A potentially interesting exception was the *egl-8* PLCβ, which showed diminished *odr-10*::GFP expression on OP50 in a small number of experiments. Given the inconsistencies in my *odr-10*::GFP; *egl-8* phenotypes, this result should be reproduced independently before interpretation.

a fraction of HB101 lipids have cardiolipin head groups (5.2% vs. undetectable in OP50). Differences in bacterial lipid acyl chain composition could translate into differences in *C. elegans* membrane phospholipids, which in turn could affect the synthesis of lipid second messengers required for TRPV-dependent *odr-10*::GFP expression. Alternately, HB101 and OP50 bacteria may secrete distinct volatile odorants (of lipid and/or non-lipid origin) capable of modulating AWA neuronal activity. As discussed below, further genetic experiments and lipid analysis could clarify the basis of this difference in *odr-10*::GFP expression.

Insulin signaling pathways modulate *odr-10*::GFP expression

When a young *C. elegans* is faced with adverse environmental conditions such as high temperature, crowding, or starvation, it can enter into a nematode alternative lifestyle called dauer development. Dauer larvae have a thickened cuticle which acts as a barrier against environmental hazards, and do not feed or reproduce. Unlike an adult animal that lives only about 2-3 weeks, a *C. elegans* dauer larva can survive 6 months or longer in the laboratory. While examining a plate of *odr-10*::GFP; *osm-9* dauers, David Tobin noticed dauer formation restored *odr-10*:: GFP expression in AWA, and that the AWA cilia in those dauer larvae had lost their typical branched morphology. Strong *odr-10*::GFP expression was also seen in *ocr-2* and *osm-9 ocr-2; ocr-1* dauers induced by starvation (data not shown), suggesting that dauer regulation of *odr-10*::GFP expression occurs downstream of or parallel to TRPV activity. Dauer development proceeds by the action of a complex genetic network illustrated in Figure 3-6. There are two principal input pathways into dauer development: a cGMP-dependent pathway that acts largely in the ASJ sensory neurons, and a TGFβ signaling pathway that

is initiated mainly in the ASI sensory neurons (Li et al., 2003). Both pathways impinge on insulin receptor signaling and upon the nuclear hormone receptor *daf-12*. Ultimately, the FOXO transcription factor *daf-16* promotes dauer formation; activity of the worm insulin receptor homologue DAF-2 blocks *daf-16* function, and thus favors reproductive development, perhaps through formation of a sterol signaling molecule (Matyash et al., 2004; Ogg et al., 1997).

To determine which branch(es) of the dauer development pathway might be relevant to AWA *odr-10*::GFP gene expression, I constructed single and double mutant strains with genes in the dauer pathway, *osm-9*, and the *odr-10*::GFP reporter. Mutations in the ASJ/cGMP and ASI/TGFβ branches did not have strong AWA GFP expression defects, although some had intriguing genetic interactions with *osm-9* (Figure 3-7). Animals mutant in the *daf-11(m47ts)* guanylyl cyclase normally form dauers at 25°C; this phenotype was suppressed by an *osm-9(n2743)* mutation. *daf-7(e1372ts)* TGFβ null mutant animals also form dauers at higher cultivation temperatures and associate in aggregates. *daf-7(e1372ts); osm-9(n2743)* double mutants formed dauers but were suppressed for aggregation behavior. *daf-7(e1372ts); osm-9(n2743)* non-dauer double mutants are weakly suppressed for AWA *odr-10*::GFP expression, suggesting that TGFβ signaling may modulate TRPV signaling pathways. Despite repeated attempts, it was not possible to isolate a *osm-9* or *ocr-2* double mutant strain with the TGFβ receptor mutant *daf-4(m63ts)*, suggesting a synthetic constitutive dauer formation or larval arrest phenotype.

Mutations in the insulin signaling branch of the dauer pathway had strong effects on *odr-10*::GFP expression. *daf-2(e1370)* loss-of-function mutants

had no intrinsic change in AWA *odr-10*::GFP expression, but consistently suppressed the *osm-9(n2743) odr-10*::GFP expression defect (Figure 3-11). The suppression seen in *daf-2(e1370); osm-9(n2743)* double mutants was substantially less than that seen in *osm-9(n2743)* dauer animals, suggesting that additional, unknown genes act in parallel with *daf-2* to modulate TRPV-dependent *odr-10*::GFP expression (or, highlighting that *daf-2(e1370)* is not a null allele). Like dauer formation, lifespan regulation, and other known *daf-2* phenotypes, this effect required the FOXO transcription *daf-16*. *daf-16* mutants and the *daf-16; daf-2* double mutant both had normal AWA GFP expression, but the null allele *daf-16(mu86)* eliminated *odr-10*::GFP expression in *daf-2(e1370); osm-9(n2743)* double mutants. *daf-2* activity is antagonized by the PTEN lipid phosphatase *daf-18*, which dephosphorylates the lipid second messenger PIP_3. The *daf-18(nr2037)* allele deletes the catalytic domain, and is a candidate null. Mutations in *daf-18(nr2037)* both decreased AWA *odr-10*::GFP expression and moderately suppressed the *odr-10*::GFP expression defects in *osm-9(n2743)* mutants. *daf-18(nr2037)* failed to suppress *osm-9(ky10) ocr-2(ak47)* mutants, indicating that it functions genetically upstream of or parallel to TRPV channels.

The ASI/TGFβ, ASJ/cGMP, and insulin branches of the dauer pathway converge upon *daf-12*, a lipid-responsive nuclear hormone receptor. *daf-12(m20)* mutant animals had reduced AWA *odr-10*::GFP expression, slightly more severe than the reduction seen in *daf-18*.

How might TRPV pathways regulate *odr-10*::GFP expression?

The data presented here provide a framework for understanding how TRPV signaling regulates postembryonic AWA *odr-10*::GFP expression through

cell-autonomous and cell non-autonomous mechanisms. A model for TRPV-dependent regulation of AWA *odr-10*::GFP expression does not simply recapitulate the classical $G_q\alpha$/PLCβ/TRP channel signaling pathway of *Drosophila* phototransduction. Instead, it incorporates genes implicated in G-protein signaling, lipid signaling, and the insulin-dependent dauer pathway.

Multiple $G_i\alpha$ proteins serve as positive and negative effectors of TRPV signaling in AWA, although *odr-3* and *gpa-3* do not account for the full excitatory drive in the signaling pathway leading to *odr-10*::GFP expression. Additional G-proteins expressed in AWA may serve as positive effectors, or there could be a basal level of G-protein-independent signaling through TRPV channels. The $G_q\alpha$ protein *egl-30* is not a positive effector of TRPV signaling in AWA. My experiments with *odr-3(XS)* are consistent with the expected function of G-proteins upstream of TRPV ion channels in AWA and ASH, but the persistence of some *odr-10*::GFP expression in *osm-9 ocr-2; odr-3(XS)* triple mutants raises the possibility of additional, non-TRPV ion channel targets in AWA. Analysis of *odr-10*::GFP expression in the *osm-9 ocr-2; ocr-1 odr-3(XS)* quadruple mutant strain would clarify this issue. An alternate explanation is that disruption of $G_i\alpha$ and TRPV sensory signaling in multiple amphid neurons could feed back upon AWA neurons, altering gene expression through cell non-autonomous means.

Multiple lines of genetic evidence suggest that lipid molecules are involved in TRPV-dependent sensory signaling, but do not reveal the precise identity of the relevant molecule(s). PUFA synthesis mutants had intriguing diet-dependent defects in *odr-10*::GFP expression, as well as the AWA and ASH behavioral phenotypes addressed in Chapter 2. As discussed below, further

experiments are needed to determine if this expression difference can be attributed to differences in bacterial lipid composition or volatile odorants. *egl-8* PLCβ and *pld-1* phospholipase D may function in AWA *odr-10*::GFP expression regulation and ASH avoidance behavior, respectively, but those data should be independently verified due to the likely presence of background mutations. *daf-18* lipid phosphatase activity both positively and negatively interacted with TRPV-dependent *odr-10*::GFP expression pathways, suggesting multiple layers of regulation. It is interesting that *daf-18* suppressed the *odr-10*::GFP defect in *osm-9* mutants but not in *osm-9 ocr-2* mutants; a lipid product of *daf-18* activity could act as or serve as precursor to a second messenger ligand of TRPV channels.

Additional components of the dauer developmental pathway modulate *odr-10*::GFP expression through TRPV-dependent and –independent means. Starvation-induced dauer formation caused bright AWA *odr-10*::GFP expression independent of TRPV ion channels, demonstrating a downstream or parallel mechanism for regulating *odr-10*::GFP expression. Dauer formation caused by mutations in ASJ/cGMP signaling failed to suppress the *odr-10*::GFP expression defect in *osm-9* mutants, while dauer formation caused by reduced ASI/TGFβ signaling offered weak suppression. Mutations in the *daf-2* insulin receptor and in *daf-18* caused moderate suppression, but still fell short of the strong suppression seen in starvation-induced dauers. Multiple branches of the dauer signaling pathway may synergize to confer full suppression of the *odr-10*::GFP expression defect in TRPV mutants. Alternately, the changing gustatory, olfactory, and neuroendocrine cues associated with starvation-induced dauer formation may have independent effects on AWA *odr-10*::GFP expression.

A limitation of these studies is that my data do not coalesce into a single model for TRPV-dependent AWA *odr-10*::GFP regulation. One future line of inquiry could investigate the role of additional G-proteins in regulating AWA function, although such questions are no longer novel (Lans et al., 2004). A second set of experiments would address the nature of the diverse lipids acting in AWA *odr-10*::GFP expression pathways, including bacterial lipids, PUFAs, and the products of *daf-18* activity. A third set of experiments would extend the links between dauer developmental pathways and TRPV-dependent gene expression, and address the cell non-autonomous aspects of *odr-10*::GFP regulation. Finally, additional forward and reverse genetic approaches could be used to identify other components of TRPV-dependent *odr-10*::GFP expression pathways, perhaps including Ca^{2+} signaling molecules and transcriptional regulators. Below, I discuss some ideas for potential extensions of my work.

A key future direction: investigating diet-dependent phenotypes

What might cause the apparent difference in PUFA-dependent gene expression for worms fed an HB101 or OP50 diet? One possibility is that the lipid composition of the OP50 bacterial diet is permissive for revealing PUFA-dependent gene expression defects. A related possibility is that HB101 is somehow protective, and prevents the manifestation of PUFA-dependent expression defects. To determine if one of these differences may be responsible for the expression phenotypes of PUFA synthesis mutants, one could manipulate the lipid head group or acyl group composition of a laboratory *E. coli* strain. Bacterial lipid synthesis mutants are available in the *E. coli* K-12 genetic background (Cronan and Rock, 1996), the background of HB101 (but not OP50).

One could also manipulate bacterial lipid composition by growing the bacteria in the presence of free fatty acids or defined lipid precursors.

A provocative alternative possibility is that OP50 and HB101 secrete different AWA-sensed odiferous metabolites, and that reduced AWA activity in OP50-fed PUFA synthesis mutant animals results in *odr-10*::GFP downregulation. If HB101 emits an odor that stimulates AWA activity, then OP50-grown PUFA mutants exposed to HB101 odorants – perhaps by spotting a small HB101 lawn on the lid of a plate – should have restored AWA GFP expression. Conversely, if OP50 secretes a molecule which *decreases* AWA activity, then HB101-grown PUFA mutants exposed to OP50 odorants may have decreased *odr-10*::GFP expression. The most parsimonious scenario would have all odors detected by and acting upon AWA, but it is also possible that an interaction among chemosensory neurons could regulate AWA chemosensory receptor expression non-cell autonomously. These further experiments could clarify whether bacterial lipid composition, odorant secretion, or additional factors are involved in diet-dependent chemosensory receptor gene expression regulation. Whatever the molecular mechanism, these observations show that interaction of diet and genotype dynamically regulates an organism's sensory capacity. These experiments could provide an opportunity to explore an exciting area: how benign environmental conditions can alter an organism's sensory capacity, thereby fundamentally changing its understanding of the world.

A future direction: cell non-autonomous regulation of *odr-10*::GFP expression

The dauer developmental pathway regulates neuronal function and gene expression through the concerted action of multiple genes acting in diverse

neurons and tissues. How does the dauer pathway impinge upon TRPV-dependent AWA transcription?

A first step would be to determine if multiple dauer pathway branches can synergize to produce strong suppression of the TRPV-dependent defect in AWA *odr-10*::GFP expression, as seen in starvation-induced dauers. For example, a *daf-7 daf-2; osm-9* triple mutant might recapitulate the starvation-induced dauer suppression of *osm-9*, and suggest that the TGFβ and insulin branches of the dauer pathway are most relevant for AWA *odr-10*::GFP regulation.

A second, challenging goal would be to identify which neurons are involved in cell non-autonomous regulation of AWA gene expression. TGFβ and insulin receptors are expressed widely in the *C. elegans* nervous system. *daf-7* and a *daf-2* ligand (which is unknown) could exert their effects directly on AWA, or by acting through other neurons in a direct or neuroendocrine circuit. If AWA cell-specific rescue of *daf-2* in a *daf-2; osm-9* double mutant eliminates *odr-10*::GFP expression, it would suggest that DAF-2 receptors on AWA directly feed into gene expression regulation pathways. If not, additional cell-specific rescue experiments or mosaic analysis could reveal the relevant neuron(s) for cell non-autonomous regulation of AWA transcription.

Finally, it would be interesting to determine if insulin modulation of TRPV signaling pathways proceeds via a lipid second messenger. *daf-2* receptor tyrosine kinase activity is transduced through the *age-1* phosphatidylinositol 3-kinase, and antagonized by *daf-18* lipid phosphatase. The balance of *daf-2/age-1* and *daf-18* activity within AWA may regulate a pool of phosphoinositide lipids,

which could directly modulate TRPV channel activity. Precedent is provided by studies of mammalian TRPV channels: the TRPV1 capsaicin receptor is directly modulated by PIP_2 signaling downstream of the receptor tyrosine kinase TrkA (Chuang et al., 2001; Prescott and Julius, 2003). Perhaps study of the *daf-2/daf-18/osm-9* genetic interaction will suggest additional general mechanisms for TRP channel modulation by receptor tyrosine kinases.

Further directions: filling in the genetic web

Generation, cloning, and analysis of behavioral mutants by previous members of the Bargmann lab created a framework for understanding AWA sensory transduction. The candidate screens methods described here provide hints about additional mechanisms of signal transduction and gene regulation in AWA sensory neurons.

A promising methodology for exploring new candidate regulators of *odr-10*::GFP expression is RNA interference (RNAi). Selection of candidates has been hampered to some degree by the limited availability of EMS or knockout alleles. With the recent identification of genetic backgrounds which are more permissive for neuronal RNAi (Kennedy et al., 2004; Simmer et al., 2002), it may be possible to use this approach to screen for additional components of TRPV signaling pathways. An initial neuronal RNAi screen for TRPV regulatory genes would focus on uncharacterized components of lipid signaling pathways, given that the lipid ligands for TRPV channels *in vivo* are still not known (Figure 3-8). One could rapidly screen for animals mutant in AWA gene expression and ASH high osmolarity avoidance, providing an opportunity to compare and contrast TRPV-dependent signaling mechanisms across sensory neurons. The identification of

lipid signaling cassettes beyond the canonical PLCβ pathway would be a valuable addition to the TRPV signaling field.

A screen for new genes involved in TRPV-dependent transcriptional regulation

In addition to screening known candidates for altered AWA expression of *odr-10*::GFP, I also performed a forward genetic screen for genes involved in AWA *odr-10*::GFP regulation. The objective of my suppressor screen was two-fold: first, to identify genes involved in receptor expression regulation, and second, to find genes involved in TRP signal transduction pathways. I screened for mutants that suppress the *osm-9*-dependent decrease in *odr-10*:: GFP expression. This screen was predicted to uncover genes capable of interacting with TRP pathways to regulate *odr-10* expression. I screened for suppressors of the *osm-9(n2743)* loss-of-function allele, which encodes a missense mutation that results in a G->E substitution in the second ankyrin motif of the channel. The behavioral phenotypes of *n2743* are comparable to the *osm-9(ky10)* null (Colbert et al., 1997). Interestingly, a second mutant, *osm-9(n1516)*, has a similar missense mutation in the first ankyrin motif, highlighting the importance of these putative protein-protein interaction domains for the function of TRP sensory channels. The *n2743* mutation disrupts the subcellular localization of OSM-9: Instead of localizing to the sensory cilia, OSM-9(n2743)::GFP remains in the neuronal cell body (Figure 3-9). Thus, the *n2743* gene product is present in AWA, but likely to be less active than the native, cilia-targeted channel. Suppressors of the *osm-9(n2743)* mutant could function by (i) boosting signal transduction through the mislocalized channel, by (ii) relocalizing the channel to the sensory cilia, or by

(iii) circumventing the need for *osm-9* function. Class (i) and (ii) suppressors can be distinguished by their effects on OSM-9*(n2743)*::GFP localization. Additionally, mutants in classes (i) and (ii) should fail to suppress the *osm-9(ky10)* null mutant, which has an early stop codon. By genetic analysis of the screen products, mutants could be sorted into classes, and then prioritized for further study.

I performed an F1 screen, looking for dominant mutations, rather than a F2 screen, which would yield both dominant and recessive mutations. My rationale was that a class (i) or (ii) phenotype could result from a novel protein function, but might be less likely to come from loss of protein function – unless the target was a dose-dependent negative regulator of *osm-9* pathways. As such, the screen was biased towards producing gain-of-function dominant mutants, but could also reveal dominant mutants due to haploinsufficiency or dominant negative activities[3]. The distinction among these modes of activity would be made after cloning and characterization of the genes. As a final way of biasing the screen, I opted to perform a behavioral enrichment. To optimize the screen for AWA-specific, TRP signaling-related mutants, I looked specifically for animals with restored AWA neuronal function. This was achieved by having animals perform a binary choice chemotaxis assay with diacetyl (1:500 dilution in ethanol) and benzaldehyde (1:1000). With such concentrations, most animals with normal AWA function prefer diacetyl, whereas *osm-9* mutants prefer

[3] Haploinsufficient means that protein dosage from only one wild-type copy of a gene is inadequate for normal cellular function. Gain-of-function means that the mutant protein has a novel activity which interferes with cellular function – for instance, it is constitutively active or produces a different molecule. Dominant negative mutant proteins interfere with the normal function of wild-type proteins, thereby eliminating cellular function.

benzaldehyde. Specific suppressors of *osm-9* would be predicted to chemotax to diacetyl, while animals with locomotion or generic neuronal defects would fail to chemotax to either odorant. In summary, the screen was designed to generate dominant mutants with enhanced AWA *odr-10*::GFP expression due to a genetic interaction with TRP signaling pathways.

Screening, backcrossing, and mutant selection

Approximately 69,000 F1 embryos were recovered from the mutagenized parental worms, representing ~138,000 haploid genomes. Four days after the mutagenesis, F1 adult animals were assayed for chemotaxis in the diacetyl/benzaldehyde choice paradigm. Animals capable of diacetyl chemotaxis were removed into S-basal solution, recovered to food for at least 3 hours, and visually screened for AWA *odr-10*::GFP expression under 10X and 40X fluorescence objectives.

After visually screening approximately 1300 animals, I recovered 61 GFP-expressing mutants. Three days later, I re-examined the GFP expression of at least 10 F2 progeny per F1, and eliminated lines that lacked AWA *odr-10*::GFP expression. Promising lines were passaged until at least the F4 generation to homozygose mutations, and frozen pending further study.

A handful of lines with bright AWA *odr-10*::GFP expression were selected for backcrossing[4]. AWA GFP expression data for selected lines is shown in Figure 3-10. Two backcrossed, relatively healthy lines with bright AWA *odr-10*::GFP expression were chosen for mapping and detailed analysis: *ky456* and

[4] Should anyone wish to examine these animals again, isolate and allele names are as follows: 14b-h/ky457, 46a-1/ky461, 49/ky422, 19-2/ky442, 5j/ky456, 2b-f/ky459, 6-4j/ky440, 48/ky541, 47/ky539, 60/ky538, and 37/ky427.

ky440. A third line, *ky541*, had promising AWA *odr-10*::GFP expression (as well as bright expression in the CEP and URX neurons) but grew slowly and was not analyzed in detail.

_ky456_ analysis and mapping

ky456 grows well and has bright AWA *odr-10*::GFP expression in *osm-9(n2743)*, *osm-9(ky10)*, and *osm-9(+)* backgrounds (Figure 3-11). *osm-9(n2743); ky456* was not suppressed for ASH high osmolarity avoidance, and was also defective for AWA diacetyl or 2-methylpyrazine chemotaxis. *osm-9(n2743); ky456* animals were proficient in chemotaxis to benzaldehyde or isoamyl alcohol, showing that AWC chemosensation and general neuronal function are unaffected by either mutation. Similarly, *osm-9(+); ky456* worms chemotax to AWA- and AWC-sensed odorants. By DiI analysis, amphid and phasmid sensory neuron structure were normal (data not shown).

Linkage was determined using strains carrying *odr-10*::GFP II and *osm-9(n2743)* IV chromosomes together with visible markers for the other chromosomes. *ky456* maps to the X chromosome: 1/165 animals bearing the *lon-2* marker for chromosome X also had *ky456*, placing the gene within one map unit of *lon-2(e678)*. The *odr-10*::GFP II ; *ky456 lon-2(e678)* X strain could be a useful reagent for further crosses with *ky456*.

To determine if *ky456* was to the left or right of *lon-2*, mapping strains were constructed with *dpy-23 lon-2* X and *lon-2 unc-6* X, and crossed to *ky456* males. *ky456* appears to map the right of *lon-2*: in one representative experiment, 30/48 Unc nonLon animals had the *ky456* phenotype, while 3/12 Lon nonUnc

animals had the *ky456* phenotype. These data suggest that *ky456* could lie between *unc-6* and *lon-2*.

For detailed mapping, I used a SNP-mapping strategy (Wicks et al., 2001) with the Hawaiian natural isolate, strain CB4856. *odr-10*::GFP II and *osm-9(n2743) dpy-13* IV chromosomes were crossed into the Hawaiian background, and backcrossed to CB4856 for 10 generations. In theory, this yielded a strain with mostly Hawaiian SNPs, except in close proximity to the markers retained from *N2*. Candidate SNP markers with high probability scores were identified on the Washington University Genome Sequencing Center *C. elegans* website[5], amplified, and digested with the appropriate enzyme. I identified valid SNPs at cosmid locations F46H6, R160, F55D10, and C52B9, but pursued an interesting candidate mutant before completing a detailed SNP mapping analysis.

One obvious candidate in the *ky456* region was the DAG kinase F46H6.2/*dgk-2*. DAG kinases metabolize the PUFA-containing signaling molecule DAG and are, thus, candidate regulators of TRP signaling pathways. Sequencing of F46H6.2 in *N2* and *ky456* backgrounds, including selected non-coding regions and predicted exons, did not reveal any mutations in *ky456*. In an experiment with small numbers of animals, PCR-amplification of the *dgk-2* genomic region from wild-type or *ky456* followed by injection into *odr-10*::GFP; *osm-9(n2743)* worms, failed to phenocopy *ky456* (as assayed by *odr-10*::GFP expression). Analysis of a *dgk-2(gk124)* deletion mutant from the *C. elegans* gene knockout consortium yielded no obvious AWA GFP phenotype, nor did this allele suppress *osm-9(n2743)* or *osm-9(ky10)* chemotaxis defects. Collectively, these data suggest that *ky456* is unlikely to be an allele of *dgk-2*.

[5] http://genome.wustl.edu/projects/celegans/index.php?snp=1

To clone *ky456*, it will be necessary to refine the map position using SNP markers and identify a minimal genetic interval. From there, one could use a PCR-based phenocopy approach as described below, or directly sequence candidate genes.

***ky440* analysis, mapping, cloning attempts, and early candidates**

ky440 animals showed very bright AWA *odr-10*::GFP expression, and occasionally suffered dendrite detachment from the tip of the nose. They grew slightly slowly relative to *N2*, and exhibited a reverse kinker uncoordinated phenotype, meaning that when tapped on the nose, they ratcheted and looped backwards rather than moving in a reverse sinusoidal wave of constant amplitude. *osm-9(n2743) ky440* animals were moderately suppressed for the ASH high osmolarity avoidance defect (Figure 3-11). Their locomotion phenotype precluded any detailed analysis of chemotaxis in *ky440*. *ky440* suppressed the *odr-10*::GFP expression defect of either *osm-9(n2743)* (Figure 3-10) or *osm-9(ky10)* (14/17 animals had bright *odr-10*::GFP), but the *ky440* phenotypes have not been analyzed in an *osm-9(+)* background. *ky440* appears to be a TRPV-dependent suppressor, in that it failed to suppress the *odr-10*::GFP expression defect of either *osm-9 ocr-2* or *osm-9; ocr-1* double mutant animals (Figure 3-12). This apparent sensitivity to the spectrum of TRPV genes in the background suggests that *ky440* may function in close proximity to TRPV channels.

Initial mapping of *ky440* with visible mutants placed it on either IV or V; relatively small numbers of F2 recombinants could be recovered from mapping crosses. In the course of generating an *osm-9(ky10) dpy-13; ky440* double, I

observed that very few Dpy animals were *ky440*, suggesting either a deleterious interaction among the two alleles, or that *ky440* was on IV.

Recombinants for SNP mapping were generated by crossing *ky440* males into the backcrossed *osm-9(n2743) dpy-13* Hawaiian strain (see *ky456* section above), and picking AWA GFP-ON and GFP-OFF animals. All GFP-OFF animals came from nonDpy or semiDpy parents, suggesting again that *ky440* was segregating away from the *osm-9 dpy-13* genomic region. I mapped against an initial panel of confirmed SNPs spanning IV, and two markers on V. There was no evidence of linkage to V. On IV, I discovered that the backcrossed Hawaiian strain retained a large chunk of N2 genomic DNA between –11.32 and +8.21, and again from +8.95 to +17.47. Outside of those regions, GFP-ON animals showed an overrepresentation of N2 SNPs around +8 on IV. Clearly, the backcrossed Hawaiian strain would be of no further use for this IV-linked mutant. One recombinant, ON17, had the potentially useful genotype *osm-9 dpy-13 ky440* or *osm-9 ky440 dpy-13*. By crossing Hawaiian strain CB4856 males into this potential flanked triple and isolating nonDpy progeny, I could generate recombinants within a ~3 cM genetic region and potentially split *osm-9* away from *ky440*.

Two panels of recombinants were generated in independent repeats of the CB4856 X ON17 cross. In brief, F2 progeny of each cross were assayed for avoidance of a high osmolarity 4M fructose ring. Animals with defective osmotic avoidance were cloned to individual plates. The F3 and F4 progeny were assayed for osmotic avoidance, nonDpy body shape, and AWA *odr-10*::GFP expression. Animals were thus classified as likely *osm-9 ky440 dpy-13(+)* recombinants, or *osm-9* non*ky440 dpy-13(+)* recombinants. Eleven recombinant lines had a likely *osm-9 ky440 dpy-13(+)* phenotype, and four were likely *osm-9*

non*ky440 dpy-13(+)* isolates. Any recombinant lines with partially penetrant GFP phenotypes were eliminated. For some lines, multiple siblings were picked, and their progeny were genotyped in parallel. Snip-SNPs were generated in the region between *osm-9* and *dpy-13*, at Y37E11B, W07G9, M02B7, F56D6, F47C12, and W03D2. Subsequently, sequencing SNPs were verified on cosmid ZC416 and along the YAC Y37E11. My mapping data with snip-SNPs and sequencing SNPs is summarized in Figure 3-12. The data are consistent with *ky440* residing between *osm-9* and *dpy-13*, as independent genetic experiments suggest. Analysis of AWA GFP-OFF animals suggests that *ky440* lies to the right of ZC416, and perhaps in the region of Y37E11AR(28189). Two of the AWA GFP-ON recombinant lines, A1 and 11A/B/C, map *ky440* to the far left of the interval. The remaining lines place it left of M02B7. Without a consistent result from all recombinants, the map position of *ky440* remains ambiguous.

To identify the genomic region required for the dominant *ky440* phenotype, I attempted to phenocopy the mutation in an *osm-9* background, focusing on the 70 KB region between ZC416 and Y37E11AL. Standard rescue approaches, where *N2* cosmid DNA is injected into a mutant animal to generate a wild-type phenotype, are unlikely to work for gain-of-function dominant mutants, rendering it necessary to perform the converse experiment of injecting mutant DNA into the wild-type background and looking for phenocopy of the dominant mutant. In brief, I amplified 9 overlapping PCR fragments from *ky440* genomic DNA spanning this region. The 9 PCR products amplified from *ky440* were combined in roughly equimolar amounts, mixed with the myo-3::RFP coinjection marker, and injected into *osm-9(n2743)* animals. If successful, this experiment would yield *osm-9* animals with bright AWA *odr-10*::GFP expression

due to the introduction of a *ky440* PCR fragment. In case the *ky440* phenotype was due to haploinsufficiency rather than gain-of-function effects, I also amplified the 9 PCR fragments from *osm-9* animals, combined them in roughly equimolar amounts, and injected into *osm-9 ky440* animals with the *myo-3*::RFP coinjection marker. Injections of *ky440* PCR products into *osm-9* animals yielded 8/31 lines with AWA *odr-10*::GFP expression, particularly after the F3 generation. To determine which PCR product contained the *ky440* mutation, the *ky440* PCR products were divided into two pools, then injected separately into *osm-9* with *myo-3*::RFP as coinjection marker. By the F3 generation, animals transformed with the left pool PCR products yielded some AWA *odr-10*::GFP expressing animals. Single PCR product injections, each representing one gene or intergenic region, were then injected into *osm-9* along with *myo-3*::RFP. Only pool F, containing an intergenic region, yielded lines with the AWA *odr-10*::GFP expression. Sequencing of this fragment revealed no mutations, however, and injection of this fragment into *osm-9* with *ofm-1*::GFP as the co-injection marker failed to yield AWA *odr-10*::GFP expressing progeny. Thus, the apparent "phenocopy" seen was likely an artifact due to an unfortunate mix of genomic DNA and *myo*-3::RFP co-injection marker.

Several candidate genes in the *ky440* genomic region were sequenced, including the calmodulin-like protein M02B7.6 and the *sina* family member Y37E11AR.2. Neither of these genes appeared to be mutated in *ky440*.

A new *ky440* candidate: NAPE-specific phospholipase D

Very recently, a duplicated metabolic protein at Y37E11AR.4 and Y37E11AR.3 was identified as an orthologue of N-acyl

phosphatidylethanolamine (NAPE) hydrolyzing phospholipase D, an enzyme that could produce anandamide and other endocannabinoid lipids. Given the role of PUFAs in TRPV-dependent signaling pathways, a mutation in a gene responsible for generating PUFA-derived signaling molecules is an excellent candidate for the gene mutated by *ky440*. Increased production of a TRPV pathway activator, or decreased production of a pathway inhibitor, would both result in enhanced neuronal activity and gene expression. Moreover, the location of these genes is consistent with SNP mapping data for recombinants 7-FA and 7-FE, which place the mutation at the right end of Y37E11AR.

To determine if *ky440* is an allele of Y37E11AR.4 or Y37E11AR.3, I employed a sequencing strategy. Long-range PCR products spanning Y37E11AR.4 were amplified with some difficulty, with a slight band size difference between *N2* and *ky440* products. Amplification of Y37E11AR.3 yielded multiple bands, rather than a single product suitable for sequencing. Within Y37E11AR.4 amplified from *ky440*, there is a possible G->A transition which results in a E->K charge substitution mutation in a region of the protein conserved from *Pseudomonas aeruginosa* to man. These data support a possible identification of *ky440* as an allele of Y37E11AR.4, a NAPE-specific phospholipase D.

Future directions: Is *ky440* a mutation in anandamide-generating phospholipase D?

As a TRPV-dependent suppressor of *osm-9*, *ky440* is likely to be an informative signal transduction mutant. The recent identification of candidate genes in a plausible genetic interval has brought renewed interest to this project.

An immediate goal is the confirmation of a mutation in Y37E11AR.4 by restriction digest; the *ky440* mutation would result in loss of a BanII restriction site in Y37E11AR.4. To exclude any rearrangements or mutations in flanking genes, further sequencing or Southern analysis should be performed.

If *ky440* is an allele of Y37E11AR.4, what is the effect of this dominant mutation on protein function, expression, and neuronal function? Dominant mutations can arise from haploinsufficient, gain-of-function, or dominant negative molecular functions; analysis of *ky440* gene expression and biochemical activity could distinguish among these three possibilities. The lesion might result in an unstable transcript and reduced message. This possibility could be assessed by quantitative RT-PCR, and might suggest a haploinsufficiency phenotype. Alternately, the protein's enzymatic activity could be different, consistent with a haploinsufficiency or gain-of-function phenotype. Heterologous expression of wild-type and mutant enzymes, followed by biochemical analysis of phospholipase activity, could reveal if the mutant protein has diminished or enhanced function. GC analysis might be useful in revealing whether *ky440* animals have an altered 20-carbon lipid profile.

Further experiments would include analysis of the Y37E11AR.4 cDNA and making transcriptional GFP fusions to determine cellular expression patterns. It would be important to make *N2* and *ky440* translational GFP fusions to determine subcellular localization and establish that Y37E11AR.4 expression in *osm-9* phenocopies the *ky440* mutation. RNAi or gene knockout attempts may aid in identifying the loss-of-function phenotype for this gene. Expression analysis and generation of a loss-of-function phenotype could further clarify the mechanism of dominance for the *ky440* mutation.

A more specific goal would be to understand how the lipid product of wild-type and mutant Y37E11AR.4 activity affects TRPV signaling pathways. Is the product of enzyme activity a TRPV activator or inhibitor? How does the *ky440* mutation affect levels of that molecule *in vivo*? How do different TRPV channel subunits interact with that molecule, and is there a specific domain of the protein responsible for that interaction? What stimulates NAPE-specific phospholipase D activity in the AWA neuron? Is endocannabinoid signaling involved in other sensory signaling pathways, such as ASH signal transduction? Do worms have retrograde endocannabinoid signaling between cells and tissues?

To date, most studies of phospholipase-TRP channel interactions have focused on members of the phospholipase C class. The importance of phospholipase D-TRP channel interactions has not been explored; indeed, the identity of the mammalian NAPE-specific phospholipase D activity was only appreciated within the last several months (Okamoto et al., 2004). AWA could be a useful model neuron for the detailed genetic and biochemical dissection of novel lipid-TRPV channel interactions downstream of GPCR activation.

Materials and Methods

Strain construction and genetic methods

C. elegans cultivation followed standard methods (Brenner, 1974). Worms were grown on HB101-seeded plates at 20 °C, except for PUFA synthesis mutant experiments in which OP50-seeded plates were used and for dauer formation experiments in which higher and lower cultivation temperatures were used. *odr-10*::GFP expression is not sensitive to *E. coli* diet in most genetic backgrounds, although it is extremely sensitive to starvation and contamination by non-*E. coli* bacteria. Mild temperature sensitivity of the AWA GFP expression phenotype was overcome by growing positive and negative control strains in parallel with temperature-shifted mutant strains. For all mutant strains, the presence of mutant alleles was confirmed by behavioral analyses and/or PCR analysis. Protocols for PCR genotyping of mutant strains are archived on the Bargmann laboratory server . The presence of the *odr-10*::GFP transgene was confirmed by visual inspection of tail fluorescence, which is *osm-9* independent.

Strains generated in the context of these studies included:
osm-9 suppressors: CX5058 *kyIs37* II; *osm-9(n2743) ky440* IV, CX5325 *kyIs37* II; *osm-9(n2743) ky440 dpy-13(e184)* IV, CX5535 *kyIs37* II; *osm-9(n2743) ky440 dpy-13(e184) ocr-2(ak47)* IV, CX5842 *kyIs37* II; *osm-9(n2743) ky440 dpy-13(e184)* IV; *ocr-1(ok132)* V, CX5844 *kyIs37* II; *osm-9(n2743) ky440 dpy-13(e184) ocr-2(ak47)* IV; *ocr-1(ok132)* V, CX4648 *kyIs37* II; *osm-9(n2743)* IV; *ky456* X, CX5032 *lin-15(n765ts)* X; *kyIs208*.

G-protein strains: CX5947 *kyIs37* II; *odr-3(n1605)* V, CX5944 *kyIs37* II; *odr-3(n2150)* V, CX5914 *kyIs37* II; *odr-3 gpa-3(pk35)* V, CX6319 *kyIs37* II; *odr-3 gpa-3(pk35); gpa-5(pk376) gpa-6(pk480)* V, CX6314 *egl-30(n686sd)* I; *kyIs37* II, CX6316 *egl-30(n686sd)* I; *kyIs37* II; *osm-9(n2743)* IV, CX6466 *kyIs37* II; *egl-8(md1971)* V, CX6463 *kyIs37* II; *osm-9(n2743)* IV; *egl-8(md1971)* V, CX5910 *kyIs37* II; *osm-9(n2743)* IV; *kyIs92* V, CX6886 *kyIs37* II; *osm-9(ky10) ocr-2(ak47)* IV; *kyIs92* V, CX6884 *kyIs37* II; *osm-9(ky10)* IV; *kyIs92* V, CX5038 *kyIs37* II; *dgk-1(nu199)* X, CX6311 *kyIs37* II; *dgk-2(gk124)* X.

Ca2+ signaling strains: CX5326 *kyIs37* II; *osm-9(n2743) unc-43(n498sd)* IV, CX5327 *kyIs37* II; *osm-9(ky10) unc-43(n498sd)* IV, CX5328 *kyIs37* II; *unc-43(n498sd)* IV, CX5453 *kyIs37* II; *osm-9(ky10) unc-43(n1186)* IV, CX5452 *kyIs37* II; *osm-9(n2743) unc-43(n1186)* IV, CX6018 *kyIs37* II; *egl-4(n479)* IV, CX6118 *kyIs37* II; *egl-4(n479) osm-9(n2743)* IV, CX6475 *kyIs37* II; *tax-6(p675)* IV, CX6462 *kyIs37* II; *osm-9(n2743) tax-6(p675)* IV, CX6889 *kyIs37* II; *unc-2(e55)* X.

PUFA synthesis strains:

BX74 *kyIs37* II; *fat-1(wa9)* IV, BX77 *kyIs37* II; *fat-4(wa14)* IV, BX78 *kyIs37* II; *elo-1(wa7)* IV, BX82 *kyIs37* II; *fat-4(wa14) fat-1(wa9)* IV, BX83 *kyIs37* II; *fat-3(wa22)* IV, BX86 *kyIs37* II; *fat-3(wa22) fat-1(wa9)* IV.

Dauer signaling strains:

CX6458 *kyIs37* II; *daf-2(e1370)* III, CX6309 *kyIs37* II; *daf-2(e1370)* III; *osm-9(n2743)* IV, CX6310 *kyIs37* II; *daf-7(e1372)* III, CX6453 *kyIs37* II; *daf-7(e1372)* III; *osm-*

9(n2743) IV, CX6461 *kyIs37* II; *lon-2(e678) daf-12(m20)* X, CX6456 *kyIs37* II; *daf-11(m47)* V, CX6450 *kyIs37* II; *osm-9(n2743)* IV; *daf-11(m47)* V, CX 6891 *kyIs37* II; *daf-18(nr2037)* IV, CX6892 *kyIs37* II; *daf-18(nr2037) osm-9(ky10) ocr-2(ak47)* IV.

Analysis of *odr-10*::GFP expression

Animals were mounted on a 2% agarose pad under sodium azide anesthesia under a glass coverslip and viewed under the 40X objective of a Zeiss axioplan compound microscope with a FITC filter set. GFP expression was scored as follows: +++, cilia, dendrite, axon, and soma visible; ++, axon, dendrite, and soma visible; +, dendrite and soma visible; dim, soma faintly visible; off, cell not visible. CEP and tail fluorescence were always visible, confirming that the *kyIs37* transgene was present. Images were captured with a CCD SpotCam (Diagnostic Instruments, Sterling Heights, MI) and associated software. Confocal images were obtained on a Bio-Rad MRC-600 confocal microscope, using a Nikon 40X or 63X objective, and analyzed using NIH Image software.

Analysis of bacterial lipid composition

Gas chromatography and thin layer chromatography experiments were performed in collaboration with Jenny Watts, Eric Phillips, and John Browse at Washington State University, Pullman. Gas chromatography preparation and parameters were similar to those published in Watts and Browse (Watts and Browse, 2002). Lipid extraction was similar to the method used by Bligh and Dyer (Bligh and Dyer, 1959), and TLC analysis methods were similar to those in Christi (Christi, 2003).

For thin layer chromatography (TLC) separation of phospholipids, lipids

were extracted at -20°C for at least 24 hours with occasional vortexing in 10mL lipid extraction solvent (10:10:1 chloroform:methanol:formic acid). Subsequently, 4.4 mL Hajra's solution was subsequently added, and the samples were vigorously shaken for 1 minute (Hajra, 1974). After centrifugation, the lower, chloroform phase was removed to a new tube with 2μL 1% BHT. Samples were extracted twice with 1mL chloroform, and solvent was removed under argon. *C. elegans* lipid extract was made up to 200μL in chloroform, while bacterial extract was made up to 1mL. TLC plates were activated at 110°C for 75 minutes, then cooled under argon for 15 minutes. Polar lipids were separated on 250um silica gel HL (Analtech Newark, DE) plates using a 65:43:3:2.6 chloroform:methanol:water:acetic acid solvent system. Neutral lipids were separated on 250um silica gel GHL (Analtech, Newark, DE) plates with an 80:20:3 hexane:diethyl ether:acetic acid solvent mixture. Lipid extracts were applied to TLC plates in triplicate under argon. Separated lipids were visualized using I_2 vapor, and marked with soft pencil. Each spot was collected immediately, and internal standard added prior to esterification and subsequent GC analysis.

Statistical analysis

The proportion of animals in the +++, ++, + categories was summed in Excel. Primer of Biostatistics 3.01 software (McGraw-Hill) was used to calculate standard error of proportion, and to compare proportions.

References:

Bligh, E. G., and Dyer, W. J. (1959). A rapid method of total lipid extraction and purification. Can J Med Sci *37*, 911-917.

Brenner, S. (1974). The genetics of *Caenorhabditis elegans*. Genetics *77*, 71-94.

Brundage, L., Avery, L., Katz, A., Kim, U.-J., Mendel, J. E., Sternberg, P. W., and Simon, M. I. (1996). Mutations in a *C. elegans* Gqα gene disrupt movement, egg laying, and viability. Neuron *16*, 999-1009.

Chang, S., Johnston, R. J., Jr., Frokjaer-Jensen, C., Lockery, S., and Hobert, O. (2004). MicroRNAs act sequentially and asymmetrically to control chemosensory laterality in the nematode. Nature *430*, 785-789.

Christi, W. W. (2003). Lipid Analysis, 3 edn (Bridgwater, England, The Oily Press (PJ Barnes and Associates)).

Chuang, H. H., Prescott, E. D., Kong, H., Shields, S., Jordt, S. E., Basbaum, A. I., Chao, M. V., and Julius, D. (2001). Bradykinin and nerve growth factor release the capsaicin receptor from PtdIns(4,5)P2-mediated inhibition. Nature *411*, 957-962.

Clapham, D. E. (2003). TRP channels as cellular sensors. Nature *426*, 517-524.

Colbert, H. A., Smith, T. L., and Bargmann, C. I. (1997). OSM-9, A novel protein with structural similarity to channels, is required for olfaction, mechanosensation, and olfactory adaptation in *Caenorhabditis elegans*. Journal of Neuroscience *17*, 8259-8269.

Colbran, R. J., and Brown, A. M. (2004). Calcium/calmodulin-dependent protein kinase II and synaptic plasticity. Curr Opin Neurobiol *14*, 318-327.

Gray, J. M., Karow, D. S., Lu, H., Chang, A. J., Chang, J. S., Ellis, R. E., Marletta, M. A., and Bargmann, C. I. (2004). Oxygen sensation and social feeding mediated by a *C. elegans* guanylate cyclase homologue. Nature *430*, 317-322.

Hajra, A. K. (1974). On extraction of acyl and alkyl dihydroxyacetone phosphate from incubation mixtures. Lipids *9*, 502-505.

Hardie, R. C. (2003). Regulation of TRP channels via lipid second messengers. Annu Rev Physiol *65*, 735-759.

Jansen, G., Thijssen, K. L., Werner, P., Horst, M. v. d., Hazendonk, E., and Plasterk, R. H. A. (1999). The complete family of genes encoding G proteins of *Caenorhabditis elegans*. Nature Genetics *21*, 414-419.

Johnston, R. J., and Hobert, O. (2003). A microRNA controlling left/right neuronal asymmetry in *Caenorhabditis elegans*. Nature *426*, 845-849.

Kennedy, S., Wang, D., and Ruvkun, G. (2004). A conserved siRNA-degrading RNase negatively regulates RNA interference in *C. elegans*. Nature *427*, 645-649.

Kuhara, A., Inada, H., Katsura, I., and Mori, I. (2002). Negative regulation and gain control of sensory neurons by the *C. elegans* calcineurin TAX-6. Neuron *33*, 751-763.

L'Etoile, N. D., Coburn, C. M., Eastham, J., Kistler, A., Gallegos, G., and Bargmann, C. I. (2002). The cyclic GMP-dependent protein kinase EGL-4 regulates olfactory adaptation in *C. elegans*. Neuron *36*, 1079-1089.

Lackner, M. R., Nurrish, S. J., and Kaplan, J. M. (1999). Facilitation of synaptic transmission by EGL-30 Gqalpha and EGL-8 PLCbeta: DAG binding to UNC-13 is required to stimulate acetylcholine release. Neuron *24*, 335-346.

Lans, H., Rademakers, S., and Jansen, G. (2004). A network of stimulatory and inhibitory Galpha-subunits regulates olfaction in *Caenorhabditis elegans*. Genetics *167*, 1677-1687.

Li, W., Kennedy, S. G., and Ruvkun, G. (2003). *daf-28* encodes a *C. elegans* insulin superfamily member that is regulated by environmental cues and acts in the DAF-2 signaling pathway. Genes Dev *17*, 844-858.

Matyash, V., Entchev, E. V., Mende, F., Wilsch-Brauninger, M., Thiele, C., Schmidt, A. W., Knolker, H. J., Ward, S., and Kurzchalia, T. V. (2004). Sterol-Derived Hormone(s) Controls Entry into Diapause in *Caenorhabditis elegans* by Consecutive Activation of DAF-12 and DAF-16. PLoS Biol *2*, e280.

Miller, K. G., Emerson, M. D., and Rand, J. B. (1999). Goalpha and diacylglycerol kinase negatively regulate the Gqalpha pathway in *C. elegans*. Neuron *24*, 323-333.

Nolan, K. M., Sarafi-Reinach, T. R., Horne, J. G., Saffer, A. M., and Sengupta, P. (2002). The DAF-7 TGF-beta signaling pathway regulates chemosensory receptor gene expression in *C. elegans*. Genes Dev *16*, 3061-3073.

Nurrish, S., Segalat, L., and Kaplan, J. M. (1999). Serotonin inhibition of synaptic transmission: Galpha(0) decreases the abundance of UNC-13 at release sites. Neuron *24*, 231-242.

Ogg, S., Paradis, S., Gottlieb, S., Patterson, G. I., Lee, L., Tissenbaum, H. A., and Ruvkun, G. (1997). The Fork head transcription factor DAF-16 transduces insulin-like metabolic and longevity signals in *C. elegans*. Nature *389*, 994-999.

Okamoto, Y., Morishita, J., Tsuboi, K., Tonai, T., and Ueda, N. (2004). Molecular characterization of a phospholipase D generating anandamide and its congeners. J Biol Chem *279*, 5298-5305.

Peckol, E. L., Troemel, E. R., and Bargmann, C. I. (2001). Sensory experience and sensory activity regulate chemosensory receptor gene expression in *Caenorhabditis elegans*. Proc Natl Acad Sci U S A *98*, 11032-11038.

Pierce-Shimomura, J. T., Faumont, S., Gaston, M. R., Pearson, B. J., and Lockery, S. R. (2001). The homeobox gene lim-6 is required for distinct chemosensory representations in *C. elegans*. Nature *410*, 694-698.

Prescott, E. D., and Julius, D. (2003). A modular PIP2 binding site as a determinant of capsaicin receptor sensitivity. Science *300*, 1284-1288.

Reiner, D. J., Newton, E. M., Tian, H., and Thomas, J. H. (1999). Regulation of a behavioral clock, muscle excitation, and two genetically defined targets by the *C. elegans unc-43* CaM Kinase II. Nature *402*, 199-203.

Riddle, D. L., and Albert, P. S. (1997). Genetic and Environmental Regulation of Dauer Larva Development. In *C. elegans* II, D. L. Riddle, T. Blumenthal, B. J. Meyer, and j. R. Priess, eds. (Cold Spring Harbor, Cold Spring Harbor Press), pp. 739-768.

Roayaie, K., Crump, J. G., Sagasti, A., and Bargmann, C. I. (1998). The Gα protein ODR-3 mediates olfactory and nociceptive function and controls cilium morphogenesis in *C. elegans* olfactory neurons. Neuron *20*, 55-67.

Sagasti, A., Hisamoto, N., Hyodo, J., Tanaka-Hino, M., Matsumoto, K., and Bargmann, C. I. (2001). The CaMKII UNC-43 activates the MAPKKK NSY-1 to execute a lateral signaling decision required for asymmetric olfactory neuron fates. Cell *105*, 221-232.

Sengupta, P., Chou, J. H., and Bargmann, C. I. (1996). *odr-10* encodes a seven transmembrane domain olfactory receptor required for responses to the odorant diacetyl. Cell *84*, 899-909.

Simmer, F., Tijsterman, M., Parrish, S., Koushika, S. P., Nonet, M. L., Fire, A., Ahringer, J., and Plasterk, R. H. (2002). Loss of the putative RNA-directed RNA polymerase RRF-3 makes *C. elegans* hypersensitive to RNAi. Curr Biol *12*, 1317-1319.

Tobin, D., Madsen, D., Kahn-Kirby, A., Peckol, E., Moulder, G., Barstead, R., Maricq, A., and Bargmann, C. (2002). Combinatorial expression of TRPV channel proteins defines their sensory functions and subcellular localization in *C. elegans* neurons. Neuron *35*, 307-318.

Troemel, E. R., Sagasti, A., and Bargmann, C. I. (1999). Lateral signaling mediated by axon contact and calcium entry regulates asymmetric odorant receptor expression in *C. elegans*. Cell *99*, 387-398.

Watts, J. L., and Browse, J. (2002). Genetic dissection of polyunsaturated fatty acid synthesis in *Caenorhabditis elegans*. Proc Natl Acad Sci U S A *99*, 5854-5859.

Wes, P. D., and Bargmann, C. I. (2001). *C. elegans* odour discrimination requires asymmetric diversity in olfactory neurons. Nature *410*, 698-701.

Wicks, S. R., Yeh, R. T., Gish, W. R., Waterston, R. H., and Plasterk, R. H. (2001). Rapid gene mapping in *Caenorhabditis elegans* using a high density polymorphism map. Nat Genet *28*, 160-164.

Yu, S., Avery, L., Baude, E., and Garbers, D. L. (1997). Guanylyl cyclase expression in specific sensory neurons: a new family of chemosensory receptors. Proc Natl Acad Sci U S A *94*, 3384-3387.

Zhang, S., Sokolchik, I., Blanco, G., and Sze, J. Y. (2004). *Caenorhabditis elegans* TRPV ion channel regulates 5HT biosynthesis in chemosensory neurons. Development *131*, 1629-1638.

Figure 3-1: Model for AWA signal transduction

The bacterial metabolite diacetyl is sensed by the ODR-10 G-protein coupled receptor, which then activates the ODR-3 G-protein (as well as other G-proteins, as discussed elsewhere in this chapter). ODR-3 activity indirectly activates an ion channel formed by OSM-9, OCR-2, and OCR-1 subunits. Channel opening depolarizes AWA, leading to behavioral and transcriptional responses.

Figure 3-1

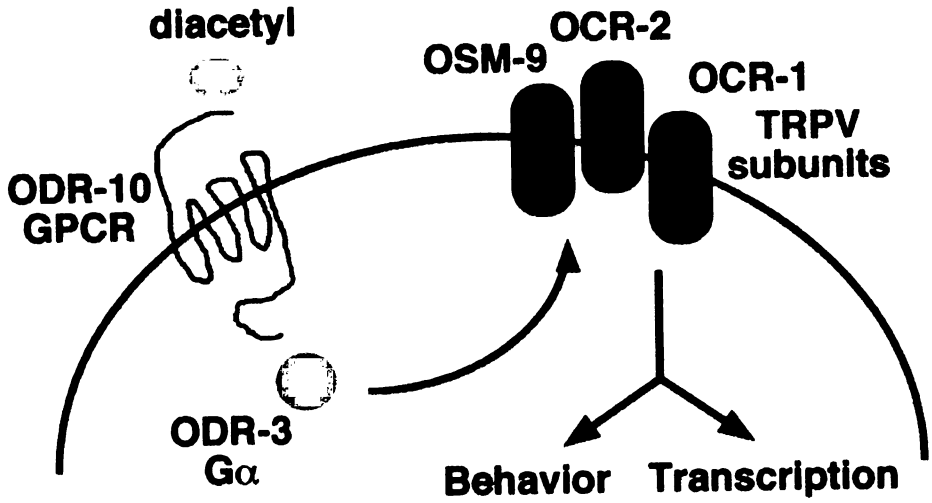
diacetyl
OCR-2
OSM-9
OCR-1
TRPV
subunits
ODR-10
GPCR
ODR-3
Gα
Behavior
Transcription

Figure 3-2: Activity-dependent regulation of *odr-10*::GFP expression

A. Representative confocal image of the left AWA neuron expressing *odr-10*::GFP in a wild-type animal. Cilia, dendrite, soma, and axon are all visible. Anterior is to the left, posterior to the right, ventral is down in all images. B. Representative confocal image of the anterior part of an *odr-10::GFP; osm-9(n2743)* animal. *odr-10*::GFP fluorescence is not visible. Both images were taken with a 63X objective. C. *odr-10*::GFP expression in AWA at various times after egg laying in *N2*, *osm-9*, *ocr-2*, and *osm-9 ocr-2* strains. In wild-type and mutant animals, *odr-10*::GFP expression is seen throughout L1 and L3 larval stages in AWA and other, unidentified head neurons. By adulthood, *osm-9* and *ocr-2* mutant animals have lost AWA *odr-10*::GFP expression, as shown in Figures 3-2b, 3-3, and 3-4.

Figure 3-2

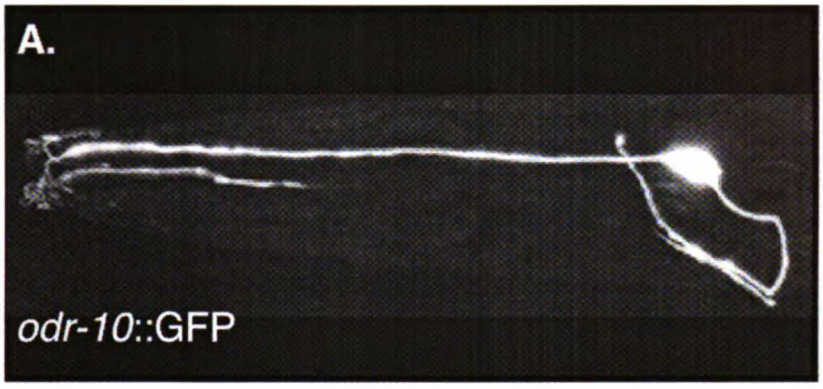

C.

Time since egg laying	*genotype*	**% with AWA *odr-10*::GFP**	**N**
unhatched embryos	*N2*	43	7
	osm-9	40	10
	ocr-2	40	10
	osm-9 ocr-2	14	7
<30 min (L1)	*N2*	100	29
	osm-9	100	26
	ocr-2	96	27
	osm-9 ocr-2	84	19
24 h (L1)	*N2*	96	49
	osm-9	100	53
	ocr-2	100	47
	osm-9 ocr-2	99	71
44 h (L3)	*N2*	96	28
	osm-9	97	34
	ocr-2	100	36
	osm-9 ocr-2	100	47

Figure 3-3: G-proteins and Ca^{2+} signaling regulate *odr-10*::GFP expression

Percent of animals expressing bright AWA GFP in the soma and at least one process, scored under a 40X fluorescence objective. Error is standard error of proportion. *odr-3* G-protein mutants, but not *egl-30* Gq mutants, have defects in AWA GFP expression. Overexpression of *odr-3* suppresses *osm-9(n2743)*. A constitutively-active *unc-43* CaMKII allele suppresses *osm-9*.

Figure 3-3

	% AWA GFP-ON	error	N	
N2	88	3.7	76	
osm-9(n2743)	3	2.1	68	
odr-3(n1605)	48	2.7	335	G-protein
odr-3(n2150)	36	3.2	227	
gpa-3(pk35)	100	0	168	G-protein
odr-3(n2150) gpa-3(pk35)	21	2.4	295	
odr-3 gpa-3; gpa-5 gpa-6	100	0	92	G-proteins
odr-3(XS)	100	0	50	
osm-9(n2743); odr-3(XS) CX5910	74	4.2	110	
egl-30(n686sd)	100	0	156	Gq
egl-30(n686sd); osm-9(n2743)	29	3.6	157	
egl-8(md1971) cross 1	71	2.8	258	PLCβ
egl-8(md1971) cross 2	44	2.8	308	
dgk-2(gk124)	95	2.6	71	diacylclycerol kinase
unc-43(n1186)	98	2.2	41	CaMKII lf
unc-43(n498sd)	100	0	40	CaMKII gf
osm-9(n2743) unc-43(n498sd)	99	1.2	74	
osm-9(ky10) unc-43(n498sd)	100	0	27	
unc-2(e55)	81	3.8	107	P/Q-type Ca2+ channel
ocr-2(yz5)	88	5.6	34	TRPV channel
egl-4(n479)	89	3.3	92	PKG
tax-6(p675)	100	0	123	calcineurin

Figure 3-4: *odr-3*(XS) is an *osm-9* suppressor in AWA and ASH

A. Percent of animals expressing bright AWA GFP in the soma and at least one process, scored under a 40X fluorescence objective. Error is standard error of proportion. *odr-3*(XS) strongly suppresses *osm-9(ky10)*, and weakly suppresses *osm-9(ky10) ocr-2(ak47)* double mutants. B. ASH avoidance of high osmolarity glycerol. *odr-3*(XS) suppresses the 1M glycerol avoidance defect of *osm-9* animals. Data are shown in graphic form, and in a table. Statistical analysis by ANOVA and Student's t-test with Bonferroni correction for multiple comparisons, *$P<0.05$.

Figure 3-4

A.

	% AWA GFP-ON	error	N
N2	92	1.7	267
osm-9(n2743)	5.8	1.6	207
osm-9(ky10) ocr-2(ak47)	2.1	1.2	140
osm-9(ky10); odr-3(XS)	59	2.2	499
osm-9(ky10) ocr-2(ak47); odr-3(XS)	36	2.2	487
osm-9(n2743); odr-3(XS) new isolates	46	2.4	418

B.

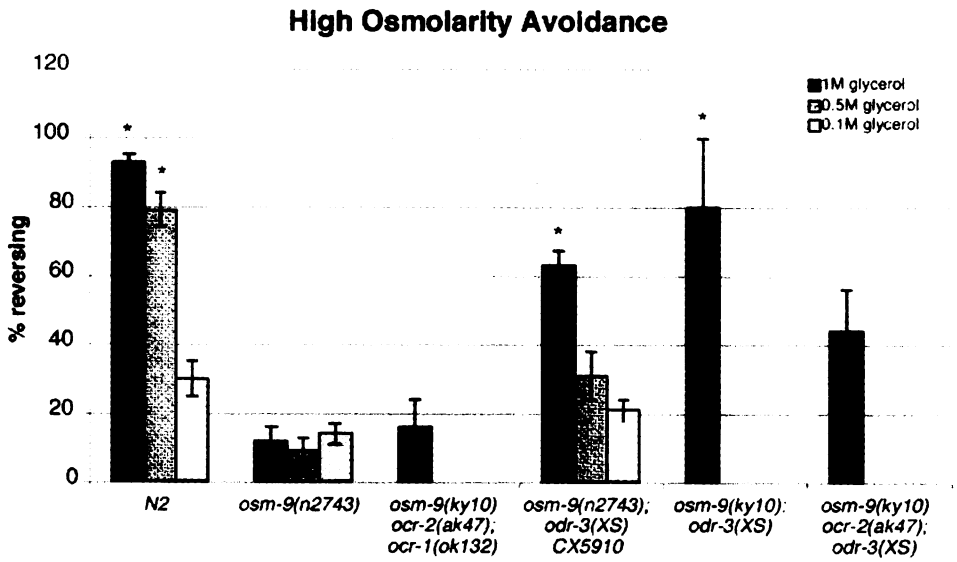

	1M glycerol	0.5M glycerol	0.1M glycerol
N2	93 ± 2	79 ± 5	30 ± 5
osm-9(n2743)	12 ± 4	9 ± 4	14 ± 3
osm-9(ky10) ocr-2(ak47); ocr-1(ok132)	16 ± 8		
osm-9(n2743); odr-3(XS) CX5910	63 ± 4	31 ± 7	21 ± 3
osm-9(ky10); odr-3(XS)	80 ± 20		
osm-9(ky10) ocr-2(ak47); odr-3(XS)	44 ± 12		

Figure 3-5: PUFA synthesis mutants have diet-dependent *odr-10*::GFP expression defects

A. Percent of animals expressing bright AWA GFP in the soma and at least one process, scored under a 40X fluorescence objective. Error is standard error of proportion. Animals mutant for *fat-1*, *fat-4*, or *fat-3* have strong AWA *odr-10*::GFP expression defects only when maintained on an OP50 *E. coli* diet. B. Thin layer chromatography and GC analysis of lipid content for HB101 and OP50 strains of *E. coli*. The two bacteria differ in their proportions of phosphatidylglycerol and cardiolipin (labeled as "upper") head groups, and in the proportions of certain acyl groups.

Figure 3-5

A.

		% AWA GFP-ON	error	N	
HB101	*N2(WT)*	91.7	1.7	267	
	osm-9(n2743)	5.8	1.6	207	
	elo-1(wa7)	100	0	37	elongase
	fat-1(wa9)	80	3.5	132	n-3 desaturase
	fat-4(wa14)	98	1	204	Δ5 desaturase
	fat-3(wa22)	81	3.5	128	Δ6 desaturase
	fat-4 fat-1	92	1.8	236	
	fat-3 fat-1	81	4.2	86	
OP50	*N2(WT)*	97	2	74	
	osm-9(n2743)	1.2	1.2	83	
	elo-1(wa7)	89	3	111	
	fat-1(wa9)	30	3.2	201	
	fat-4(wa14)	47	4.4	129	
	fat-3(wa22)	49	5.6	79	
	fat-4 fat-1	38	4.6	110	
	fat-3 fat-1	57	9.7	26	

B.

	phosphatidyl ethanolamine		phosphatidyl glycerol		non-polar lipids		"upper"	
	HB101	OP50	HB101	OP50	HB101	OP50	HB101	OP50
% of lipid	71.0%	71.6%	6.8%	12.0%	17.0%	14.4%	5.2%	0.0%
14:0	4.1%	2.1%	6.6%	2.8%	5.9%	3.8%	6.4%	0.0%
15:0	7.8%	1.5%	7.2%	1.7%	8.5%	2.9%	8.0%	0.0%
16:0	34.2%	37.8%	45.6%	42.8%	28.1%	30.9%	45.1%	0.0%
C17:iso	0.6%	0.2%	2.5%	0.9%	1.0%	0.7%	3.1%	0.0%
16:1	25.0%	2.0%	3.7%	1.1%	20.0%	1.3%	8.4%	0.0%
17:delta	7.2%	17.5%	3.9%	11.9%	4.1%	6.3%	5.8%	0.0%
18:0	1.1%	2.9%	9.3%	5.0%	4.6%	8.2%	6.9%	0.0%
18:1n7	17.9%	18.8%	12.8%	11.5%	25.9%	25.8%	9.3%	0.0%
?	1.5%	3.7%	0.0%	3.0%	1.3%	3.2%	2.6%	0.0%
19:delta	0.5%	11.1%	8.5%	15.9%	0.6%	14.1%	4.3%	0.0%
?	0.0%	2.4%	0.0%	3.5%	0.0%	2.9%	0.0%	0.0%

Figure 3-6: Model for integrated regulation of dauer development

Cyclic GMP, TGFβ, insulin, and sterol signaling pathways cooperate to regulate a reproductive developmental switch. Emerging data from numerous labs, including the Riddle, Ruvkun, Thomas, and Antebi groups, suggests a model where TGFβ signaling and an insulin cassette regulate production of a steroid ligand for the *daf-12* nuclear hormone receptor. *daf-12* and the FOXO transcription factor *daf-16* are both required for dauer formation. The insulin signal for the *daf-2* receptor is still not known, although transcription and behavioral studies are identifying potential candidates. Blue, dauer formation-defective strains. Yellow, dauer formation-constitutive strains.

Figure 3-6

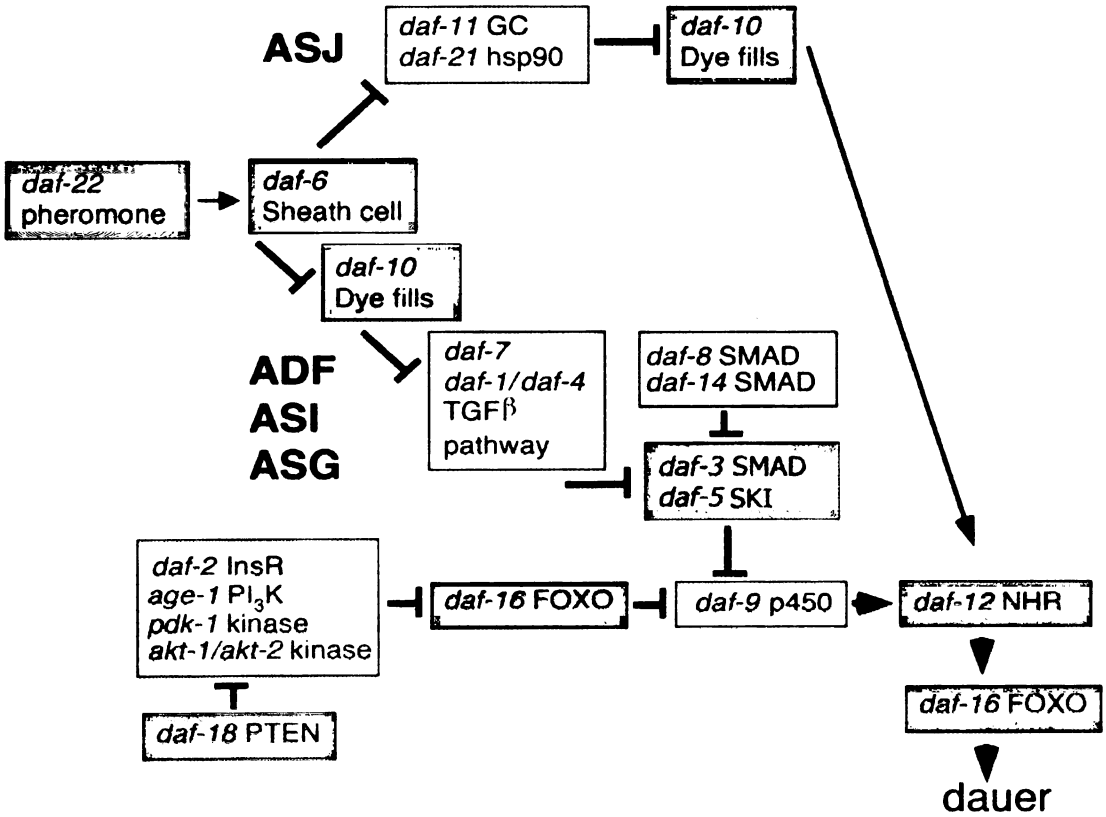
ASJ
daf-11 GC
daf-21 hsp90
daf-10
Dye fills
daf-22
pheromone
daf-6
Sheath cell
daf-10
Dye fills
ADF
ASI
ASG
daf-7
daf-1/daf-4
TGFβ
pathway
daf-8 SMAD
daf-14 SMAD
daf-3 SMAD
daf-5 SKI
daf-2 InsR
age-1 PI3K
pdk-1 kinase
akt-1/akt-2 kinase
daf-16 FOXO
daf-9 p450
daf-12 NHR
daf-18 PTEN
daf-16 FOXO
dauer

Figure 3-7: Insulin signaling can regulate *odr-10*::GFP expression

Percent of animals expressing bright AWA GFP in the soma and at least one process, scored under a 40X fluorescence objective. Error is standard error of proportion. The guanylyl cyclase and TGFβ branches of the dauer regulatory pathway have little impact on AWA *odr-10*::GFP expression. Dauer formation and *daf-2* mutants suppress the AWA GFP expression defect of *osm-9(n2743)*, upstream of *daf-16* activity.

Figure 3-7

	% AWA GFP-ON	error	N	
N2 (WT)	91.7	1.7	267	
osm-9(n2743)	5.8	1.6	207	
osm-9(n2743) dauers	100	0	60	
daf-11(m47ts)	99	1.1	78	guanylyl cyclase
osm-9(n2743); daf-11(m47ts)	6.9	2.5	101	
daf-7(e1372ts)	100	0	295	TGFβ
daf-7(e1372ts); osm-9(n2743)	27	3.6	151	
daf-4(m63ts)	96	3.8	26	TGFβ receptor
daf-2(e1370)	100	0	94	insulin receptor
daf-2(e1370); osm-9(n2743)	61	2.4	408	
daf-16(mu86)	88	2	277	FOXO
daf-16(m26)	98	1.9	56	
daf-16(m26); osm-9(n2743)	14	2.7	170	
daf-16(mu86); daf-2(e1370)	95	1.3	310	
daf-16(mu86); daf-2(e1370); osm-9(n2743)	1.9	1.4	101	
daf-18(nr2037)	79	2.4	287	PTEN
osm-9(n2743) daf-18(nr2037)	47	7	51	
osm-9(ky10) ocr-2(ak47) daf-18(nr2037)	11	2.6	150	
lon-2(e678) daf-12(m20)	66	5.2	83	NHR

Figure 3-8: Candidate genes for a neuronal RNAi screen

Potential targets that should be tested in a small-scale neuronal RNAi screen in *eri-1; lin-15b* or *rrf-3* backgrounds, scoring both AWA *odr-10*::GFP expression and ASH high osmolarity avoidance phenotypes. By analogy to *Drosophila* phototransduction, phospholipase C genes are candidate AWA regulators. The importance of PUFA signaling in AWA behavior and gene expression regulation suggests that other lipid-processing enzymes, including endocannabinoid system components, may also be important targets. A variety of triacyl- and diacylglycerol lipases can also be prioritized for further study. Annotations are from multiple releases of WormBase (http://www.wormbase.org), including release WS132.

Figure 3-8

	locus	gene name	notes
	b0212.5	*osm-9*	control for AWA, ASH RNAi
	c30a5.7	*unc-86*	control for neuronal RNAi
phospholipases	t01e8.3	*plc-3*	PLC gamma, deletion now available
	y75b12b.6	*plc-2*	norpA orthologue?
	f31b12.1	*plc-1*	Ras-associated, PLC epsilon
	k10f12.3	*pll-1*	PI-PLC
	f15b9.6		PLA2
	f35c11.5		PLA2
	c07e3.9		PLA2, human and fly homologues
	c03h5.4		PLA2, human and fly homologues
	y37e11ar.4		*ky440?* NAPE-PLD
	y37e11ar.3		NAPE-PLD
lipid second messenger systems	b0218.1		fatty acid amide hydrolase
	f58h7.2		fatty acid amide hydrolase
	y56a3a.12		fatty acid amide hydrolase
	y56a3a.5		fatty acid amide hydrolase
Other lipid signaling	f53h8.4	*sms-2*	Sphingomyelin synthase
	h21p03.3	*sms-1*	Sphingomyelin synthase
	y22d7al.8	*sms-3*	Sphingomyelin synthase
	f53b1.2		SM synthase-related hits
DAG/triacylglycerol lipases	f58b6.1		cytoplasmic, arabidopsis hit
	y49e10.18		cytoplasmic, fungal hits
	k03h6.2		cytoplasmic, fly and yeast hits
	y110a7a.7		secreted, arabidopsis hit
	t21h3.1		secreted, fungal hit
	t10b5.7		secreted, human (neuronal) and arabidopsis hits
	k08b12.1		secreted, yeast hit
	f28h7.3		secreted, fungal hits
	y49e10.16		secreted, fungal hits
	b0035.13		secreted, human and fungal hits
	t08b1.4		secreted, only nematode hits
	f58b6.5		secreted, only nematode hits, no cDNA
	f46g10.4		membrane, yeast and plant hits
	c39b5.5		ER membrane, plant hits
	zk262.3		plant and yeast hits
	zk262.2		in neuronal sheath cells; non-worm hits
	y51a2b.4		plant hits
	y46h3a.4		plant and fly hits
	c14e2.6		human and fungal hits
	h41c03.2		cytoplasmic, human and fungal hits
	f25a2.1		non-worm hits
	c40h1.7		non-worm hits
	y51h4a.5		non-worm hits

Figure 3-9: OSM-9(*n2743*) channels are mislocalized

A. False-colored confocal image of the OLQ mechanosensory neurons labeled with the OSM-9::GFP3 translational fusion. The OLQ sensory cilia are clearly visible. B. False-colored confocal image of the OLQ mechanosensory neurons labeled with the OSM-9(n2743)::GFP3 translational fusion. The ankyrin repeat mutation eliminates cilia expression of the channel, although staining is still seen in the soma. Both images were taken with a 63X objective.

Figure 3-9

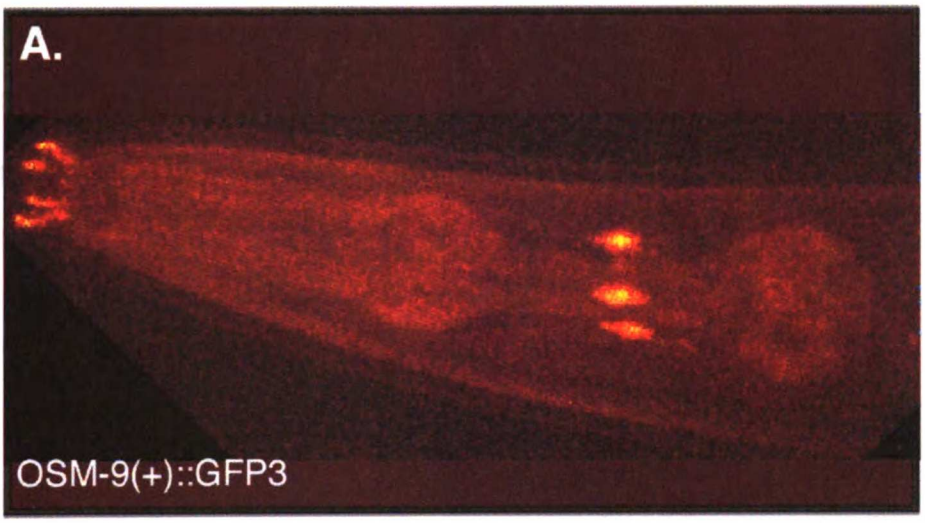

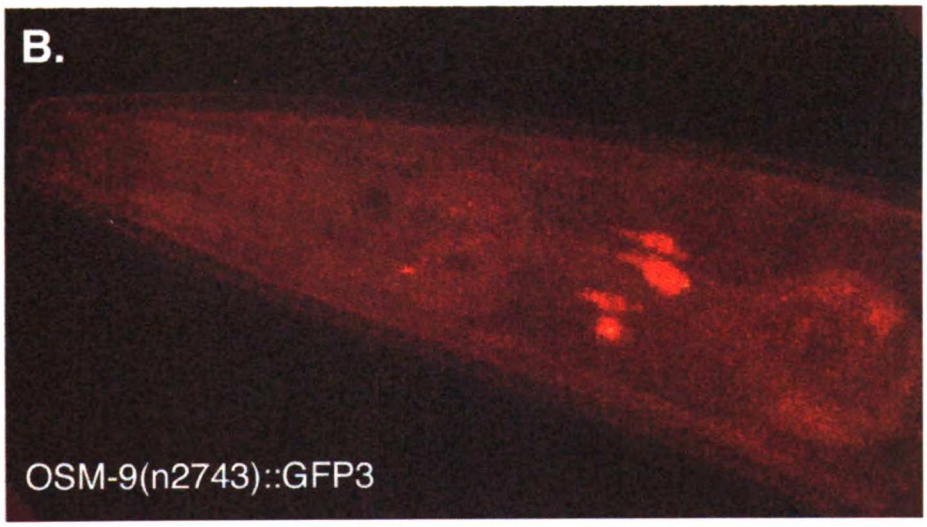

Figure 3-10: Identification of *osm-9(n2743)* suppressors

A. Percent of animals of a given genotype expressing bright AWA GFP in the soma and at least one process, scored under a 40X fluorescence objective. Error is standard error of proportion. B. Representative fluorescence images of wild-type, *osm-9*, and suppressor strains at 40X.

Figure 3-10

A.

	% AWA GFP-ON	error	N
N2 (WT)	96	1.9	108
osm-9(n2743)	6	1.7	195
osm-9(n2743); ky439	64	3.5	186
osm-9(n2743); ky456	94	1.5	245
osm-9(n2743) ky440	93	2.5	107
osm-9(n2743); ky459	57	3.7	175
osm-9(n2743); ky541	99	0.9	119
osm-9(n2743); ky461	42	4.5	118

B.

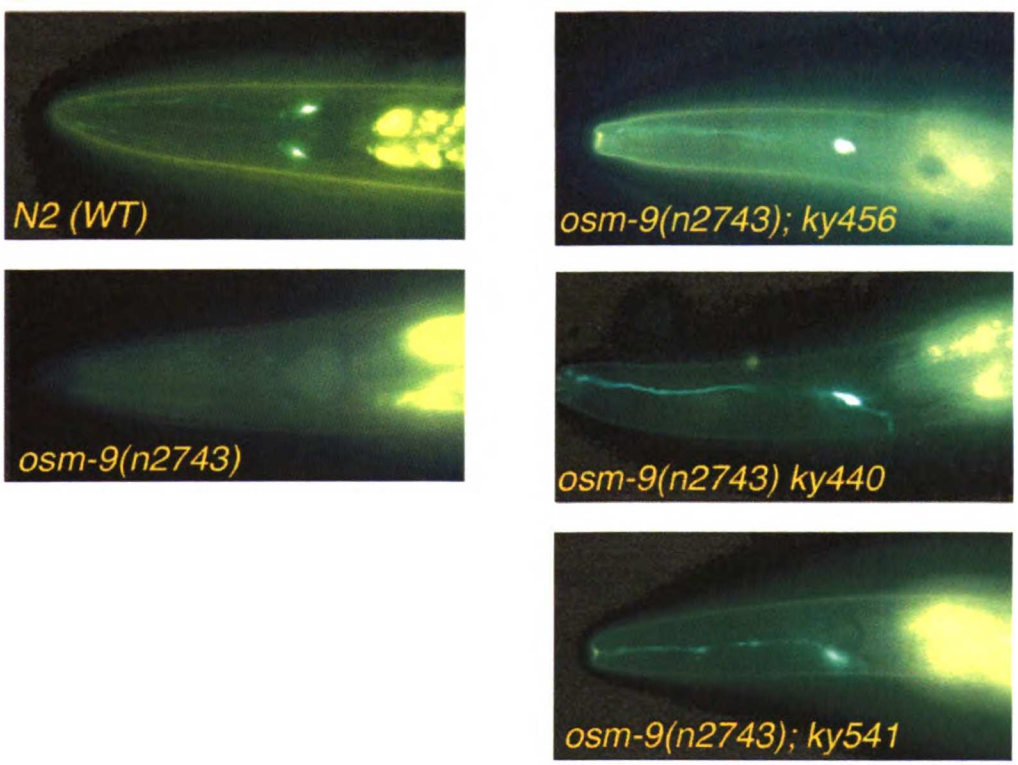

Figure 3-11: AWA, AWC, and ASH phenotypes of *ky456* and *ky440*

A. Bright AWA *odr-10*::GFP expression in *osm-9; ky456* and *osm-9(+); ky456* animals. B. ASH-mediated avoidance of a high osmolarity 4M fructose ring. *ky456* fails to suppress the *osm-9* defect in high osmolarity avoidance, while *ky440* partially suppresses the *osm-9* high osmolarity avoidance defect. At least 6 independent assays and 57 animals examined per genotype. Error is standard error of the mean. Statistical analysis by ANOVA and Student's t-test with Bonferroni correction, *$p<0.05$. C. *ky456* chemotaxis to standard concentrations of AWA and AWC-sensed odorants. *osm-9; ky456* animals are defective for chemotaxis to AWA-sensed odorants but proficient for chemotaxis to AWC-sensed odorants (preliminary data). *osm-9(+); ky456* animals chemotax to AWA and AWC-sensed odorants; at least 4 independent assays per genotype. Error is standard error of the mean.

Figure 3-11

A.

	% expressing *odr-10*::GFP	N
N2	100 ± 0	14
osm-9(n2743)	0 ± 0	24
osm-9(n2743); ky456 lon-2 L	93.6 ± 0.022	125
osm-9(+); ky456 lon-2 J	87.5 ± 0.052	40
osm-9(+); ky456 lon-2 I	86.7 ± 0.047	53
osm-9(ky10) dpy-13; ky456	78.4 ± 0.035	139

B.

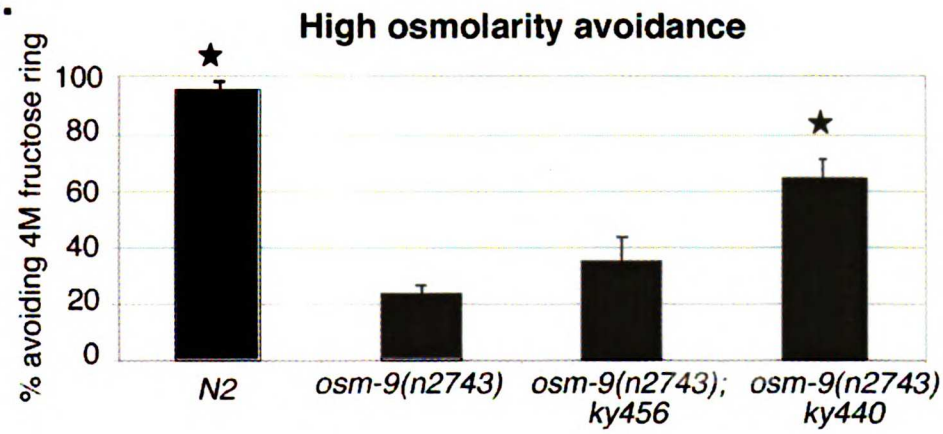

C.

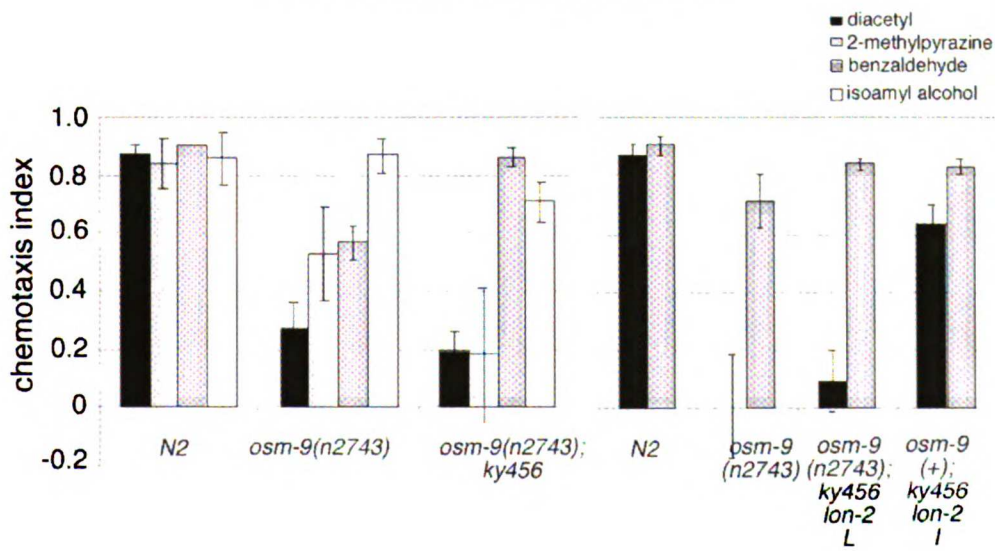

Figure 3-12: *ky440* suppression of *osm-9(n2743)* is TRPV-dependent

Percent of animals expressing bright AWA GFP in the soma and at least one process, scored under a 40X fluorescence objective. Data are shown graphically and as proportion of suppressed animals. Error is standard error of proportion. *ky440* suppresses *osm-9(n2743)* if an *ocr-1* or *ocr-2* TRPV channel subunit is also present.

Figure 3-12

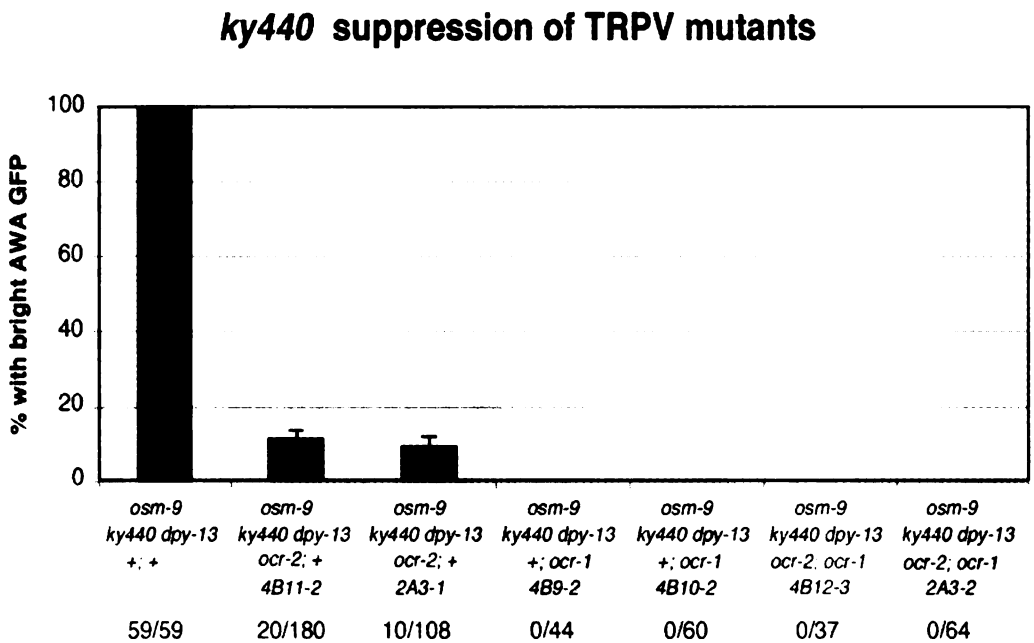
ky440 suppression of TRPV mutants
% with bright AWA GFP
100
80
60
40
20
0
osm-9 ky440 dpy-13 +; +
osm-9 ky440 dpy-13 ocr-2; + 4B11-2
osm-9 ky440 dpy-13 ocr-2; + 2A3-1
osm-9 ky440 dpy-13 +; ocr-1 4B9-2
osm-9 ky440 dpy-13 +; ocr-1 4B10-2
osm-9 ky440 dpy-13 ocr-2, ocr-1 4B12-3
osm-9 ky440 dpy-13 ocr-2; ocr-1 2A3-2
59/59
20/180
10/108
0/44
0/60
0/37
0/64

Figure 3-13: *ky440* maps between *osm-9* and *dpy-13*

SNP mapping of *ky440* with *N2*/Hawaiian recombinant lines. Horizontal axis, individual SNP markers or genetic markers and approximate genetic locations on chromosome IV. Vertical axis, individual recombinant lines with bright AWA *odr-10*::GFPexpression (top) or absent AWA *odr-10*::GFPexpression (bottom). Pink boxes, *N2* polymorphism, yellow boxes, CB4856 polymorphism. Data do not yield an unambiguous result for the location of *ky440*. 11a/b/c are sibling recombinants, as are 28b/d, k1/3, and 7f-a/7f-e. Recombinants from 7 and 11 are inconsistent with a single map position.

Figure 3-13

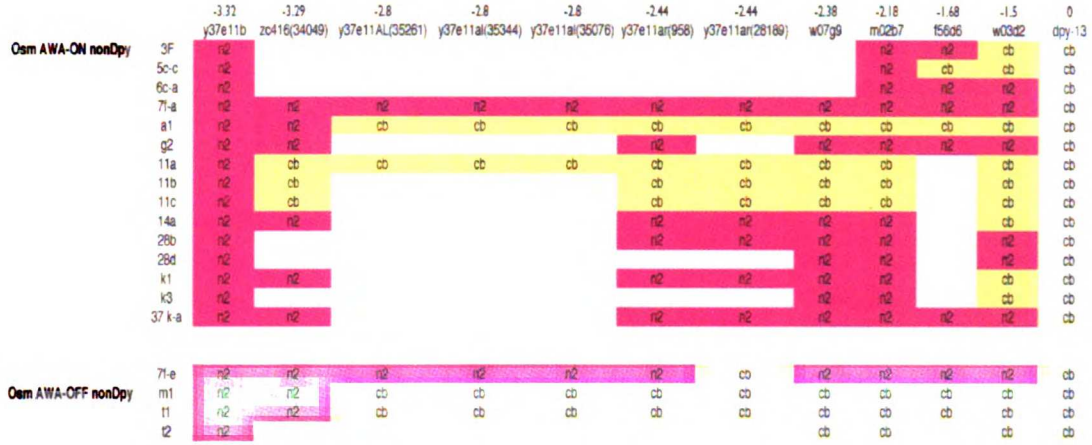
-3.32 y37e11b
-3.29 zc416(34049)
-2.8 y37e11AL(35261)
-2.8 y37e11al(35344)
-2.8 y37e11al(35076)
-2.44 y37e11ar(958)
-2.44 y37e11ar(28189)
-2.38 w07g9
-2.18 m02b7
-1.68 f56d6
-1.5 w03d2
0 dpy-13
Osm AWA-ON nonDpy
3F
5c-c
6c-a
7f-a
a1
g2
11a
11b
11c
14a
26b
26d
k1
k3
37 k-a
Osm AWA-OFF nonDpy
7f-e
m1
t1
t2

Chapter four:

Future directions

This thesis describes molecular pathways essential for TRPV-dependent chemosensation and nociception in *C. elegans*. Animals mutant in polyunsaturated fatty acid synthesis have cell-specific chemosensory, mechanosensory, and osmosensory defects. Application of certain exogenous PUFAs is sufficient to restore and elicit sensory behavior, and induces rapid, robust, TRPV-dependent Ca^{2+} transients in sensory neurons. These observations suggest that PUFAs act in close proximity to TRPV ion channels *in vivo* as lipid second messengers in sensory neurons. Additional modulation of TRPV signaling is provided by G-proteins, CaM kinase II, and insulin pathways.

Future directions: PUFA signaling and TRPV channels

Do PUFAs gate TRPV channels *in vivo*? Our results support this tantalizing possibility, but are also consistent with PUFA metabolites acting indirectly to activate *C. elegans* TRPV channels in sensory neurons.

To address this question directly, structure-function studies would seem most appropriate. The most direct approach would be to introduce mutant OSM-9 or OCR-2 channels (or worm-mammalian chimeric channels) into the ASH neurons of TRPV-deficient worms, and assay behavioral or Ca2+ responses to discrete PUFAs (or select metabolites). Attention could be focused on residues and motifs involved in ligand gating of mammalian TRPV1 and TRPV4 channels. An alternate approach would be to express *C. elegans* OSM-9 and OCR-2 channels in mammalian cells or *Xenopus* oocytes, and record responses to applied PUFAs. After recording initial responses, channel mutants could then be screened to identify residues important for PUFA responsiveness. Either experiment would be a significant step forward in verifying that PUFAs interact

with TRPV channels at discrete sites. Follow-up studies could focus on identifying PUFA-interacting channel sequences through domain swapping or mutagenesis approaches. Such experiments would be tedious in *C. elegans* due to the effort involved in characterizing large numbers of transgenic strains; heterologous expression in cultured cells might be wisest as an initial step, followed by *in vivo* analysis of the most promising candidate channel mutants.

If PUFAs or related molecules directly gate TRPV channels *in vivo*, what is the endogenous source of these lipid messengers? *C. elegans* is well-suited to the identification of novel signal transduction components. A behavioral or visual forward genetic screen for ASH or AWA mutants could identify new PUFA signaling genes, although alleles of many known sensory signaling genes would also be found. A gas chromatography-based secondary screen could be a quick and useful way of separating lipid-specific behavioral/visual mutants from other mutants. As an alternate approach, RNAi screens against candidate lipid signaling genes have the advantage of being rapid and directed, but subject to the limitations of RNAi in neurons. Given the speed of RNAi screening, it would seem to be the wiser first-pass approach, followed by a traditional screen if necessary.

The *ky440* TRPV suppressor may be a key component of AWA and ASH PUFA sensory signaling pathways, and I eagerly anticipate its further characterization. If *ky440* is a mutation in a novel N-acylethanolamine-specific phospholipase D, *C. elegans* will emerge as a promising system for exploring endocannabinoid lipid signal transduction. It is not yet possible to genetically manipulate both PUFA synthesis and metabolism in other metazoan model

organisms, making worms uniquely suited for the exploration of lipid effects on ion channels and other sensory transduction molecules.

Identification of novel PUFA signaling components may shed light not just on worm sensory signaling, but also on other worm and mammalian signaling contexts. PUFAs may modulate the activity of worm TRP channels in mechanosensory and fertility pathways. It would be interesting and straightforward to look at male *fat-3* or *fat-4 fat-1* PUFA synthesis mutants for subtle defects in TRPP-dependent male mating behavior (Barr and Sternberg, 1999), or to ask if TRP-3 sperm Ca^{2+} currents (Xu and Sternberg, 2003) are compromised in PUFA mutants. For study of mammalian TRP pathways, manipulating PUFA levels *in vivo* is a challenge. The standard approach is to starve rodents of dietary lipids for several generations, then assay the animal for a given phenotype. With recent advances in mammalian RNAi, including gene silencing by systemic administration (Soutschek et al., 2004), it may soon be possible to remove *fat-1* or *fat-4* activity and see an effect on mammalian TRP channel function. In contexts where TRP channels are involved in mechanosensation, the acyl group composition of membrane phospholipids may be of critical importance for channel function.

PUFA levels may also modulate TRP channels expressed in cardiovascular tissue-associated neurons or in the central nervous system. TRP channels could contribute to documented (but mechanistically unclear) effects of dietary PUFAs on mental development and prevention of cardiovascular disease. Such speculation could be borne out by identifying TRP channels in neurons associated with specific, measurable functions, and determining if neuronal properties change with physiological manipulation of omega-3 fatty acid content.

Future directions: lipids as environmental signals?

Our finding that exogenous PUFAs stimulate ASH avoidance responses raises the intriguing possibility that *C. elegans* may be able to detect and respond to lipid cues in the soil environment. Worms are already known to respond to lipid-like cues from conspecifics: the constitutively-secreted *C. elegans* dauer pheromone induces population density-dependent developmental changes. Might there be additional salient lipid cues in worms' native environment, originating from other species?

Fungi, bacteria, and plants synthesize and modify a diverse array of lipids and related molecules, some of which have been implicated as inter-organism communication molecules. Soil fungi can produce a diverse array of PUFAs, including AA and EPA (Sakuradani et al., 2004). *Pseudomonas aeruginosa*, a bacterium which can be toxic and repulsive to *C. elegans*, is capable of modifying soil PUFAs into potential signaling molecules (Kuo and Nakamura, 2004). A wide variety of bacteria, including pathogenic species, secrete acyl-homoserine lactones to facilitate quorum sensing; there is evidence that plants and *C. elegans* may sense and respond to these bacterial cues (Bauer and Mathesius, 2004). Similarly, plants synthesize the LNA derivative jasmonate and related compounds, and respond to fatty acid derivatives from other species, including predators (Lait et al., 2003; Weber, 2002). There are isolated examples of lipid-related compounds acting as signifiers of social role within an ant colony (Greene and Gordon, 2003) and promoting marine algal biofilm formation (Joint et al., 2002). Thus, potential interspecies communication lipids are synthesized and may be present in nematode environments.

Providing that there are locally-secreted, stable lipid-related compounds are in soil, *C. elegans* could employ those substances as short-range, ASH-detected signals to avoid predatory fungi, pathogenic bacteria, or noxious plants. Alternately, low concentrations of environmental PUFAs could act to sensitize sensory transduction pathways in AWA and other neurons that detect long-range, volatile attractants, so that worms are better able to chemotax towards a delimited region of food. *osm-9*, *ocr-2*, and related TRPV channels are found in many amphid sensory neurons, raising the possibility that environmental lipids could modulate the activity of multiple sensory modalities. Since AWA chemoreceptor expression is sensitive to a worm's bacterial diet, environmental lipids could have both short- and long-term consequences for chemosensory integration. By developing behavioral assays which simultaneously test the interaction among two genetic species, such as worms and soil bacteria, we may uncover salient interspecies communication pathways critical for feeding and defense in a complex environment.

Conclusion

My studies have elucidated the contributions of PUFA synthesis pathways to TRPV channel function in *C. elegans* chemosensory and nociceptive neurons. In addition, they have identified candidate modulators of TRPV pathways, including well-studied insulin signaling pathways and possibly novel lipid second messenger systems. Future progress in understanding *C. elegans* sensory signaling will involve integration of lipid signaling with other transduction mechanisms. PUFAs may also turn out to be important regulators of mammalian TRP channels in their diverse sensory and non-sensory contexts.

References:

Barr, M. M., and Sternberg, P. W. (1999). A polycystic kidney-disease gene homologue required for male mating behaviour in *C. elegans*. Nature *401*, 386-389.

Bauer, W. D., and Mathesius, U. (2004). Plant responses to bacterial quorum sensing signals. Curr Opin Plant Biol *7*, 429-433.

Greene, M. J., and Gordon, D. M. (2003). Social insects: Cuticular hydrocarbons inform task decisions. Nature *423*, 32.

Joint, I., Tait, K., Callow, M. E., Callow, J. A., Milton, D., Williams, P., and Camara, M. (2002). Cell-to-cell communication across the prokaryote-eukaryote boundary. Science *298*, 1207.

Kuo, T. M., and Nakamura, L. K. (2004). Diversity of oleic acid, ricinoleic acid and linoleic acid conversions among *Pseudomonas aeruginosa* strains. Curr Microbiol *49*, 261-266.

Lait, C. G., Alborn, H. T., Teal, P. E., and Tumlinson, J. H., 3rd (2003). Rapid biosynthesis of N-linolenoyl-L-glutamine, an elicitor of plant volatiles, by membrane-associated enzyme(s) in *Manduca sexta*. Proc Natl Acad Sci U S A *100*, 7027-7032.

Sakuradani, E., Abe, T., Iguchi, K., and Shimizu, S. (2004). A novel fungal omega3-desaturase with wide substrate specificity from arachidonic acid-producing *Mortierella alpina* 1S-4. Appl Microbiol Biotechnol.

Soutschek, J., Akinc, A., Bramlage, B., Charisse, K., Constien, R., Donoghue, M., Elbashir, S., Geick, A., Hadwiger, P., Harborth, J., *et al.* (2004). Therapeutic silencing of an endogenous gene by systemic administration of modified siRNAs. Nature *432*, 173-178.

Weber, H. (2002). Fatty acid-derived signals in plants. Trends Plant Sci *7*, 217-224.

Xu, X. Z., and Sternberg, P. W. (2003). A *C. elegans* sperm TRP protein required for sperm-egg interactions during fertilization. Cell *114*, 285-297.

Appendix A:

Mammalian TRPV ion channels

respond to applied PUFAs

Our behavioral and Ca^{2+} imaging studies with *C. elegans* TRPV channels suggested that their mammalian relatives might also respond to exogenous PUFAs. To address this question directly, we performed PUFA avoidance assays on *C. elegans* strains expressing the mammalian TRPV channels TRPV1 and TRPV4 in the ASH sensory neurons. The results are preliminary, but suggest that different TRPV channels are sensitive to distinct PUFAs.

To determine if mammalian TRPV channels respond to PUFAs *in vivo*, we exposed ASH::TRPV1 animals to various concentrations of EPA and LA. TRPV1 transgenics responded robustly to EPA (data not shown, n=10 assays, 250 animals), but also showed strong avoidance of LA (Figure A-1). Wild-type *C. elegans* had no avoidance response to LA at identical concentrations. Surprisingly, the TRPV1 response to PUFAs required *C. elegans* TRPV channels: LA avoidance was absent in *osm-9 ocr-2*; ASH::TRPV1 transgenic animals. These results suggest that LA has a functional interaction with TRPV1 that can convey a behavioral output in this expression system.

By contrast, transgenic expression of TRPV4 in ASH did not yield heightened avoidance responses to LA (data not shown, n=5 assays, 125 animals. Thus, unlike TRPV1-mediated capsaicin avoidance behavior (Tobin et al., 2002), LA avoidance depends on the presence of endogenous *C. elegans* TRPV channels. In other words, the combination of TRPV channels in ASH confers sensitivity to LA. Transgenic (over)expression of TRPV1 may amplify a weak ASH response to LA; alternately, TRPV1 may coassemble with OSM-9 or OCR-2 subunits to create a LA-sensitive channel in ASH. Further structural analysis and lipid studies could distinguish among these two interesting possibilities. In addition,

Ca^{2+} imaging of ASH responses to LA exposure in wild-type and ASH::TRPV1 animals may reveal differences in Ca^{2+} transients, providing insight into the coding of behavioral responses to aversive stimuli.

Reference:

Tobin, D., Madsen, D., Kahn-Kirby, A., Peckol, E., Moulder, G., Barstead, R., Maricq, A., and Bargmann, C. (2002). Combinatorial expression of TRPV channel proteins defines their sensory functions and subcellular localization in *C. elegans* neurons. Neuron *35*, 307-318.

Figure A-1: TRPV channels specify ASH-mediated lipid avoidance

A. Wild-type, *osm-9*, and *fat-3* fail to avoid the PUFA LA. Direct exposure to 100 μM-4 mM LA in a drop test assay did not elicit significant avoidance responses. N2 and *osm-9* data are re-plotted from Figure 2-7. B. TRPV1 transgenic animals show TRPV-dependent LA avoidance. ASH::TRPV1 transgenics robustly avoid LA at a range of concentrations, but only if *osm-9* and *ocr-2* are present. n, number of animals assayed, (exp), number of independent behavioral experiments (25 animals per assay). Shaded box, responses significantly different from wild-type by ANOVA and Student's t-test with Bonferroni correction for multiple comparisons, $P<0.05$.

Figure A-1

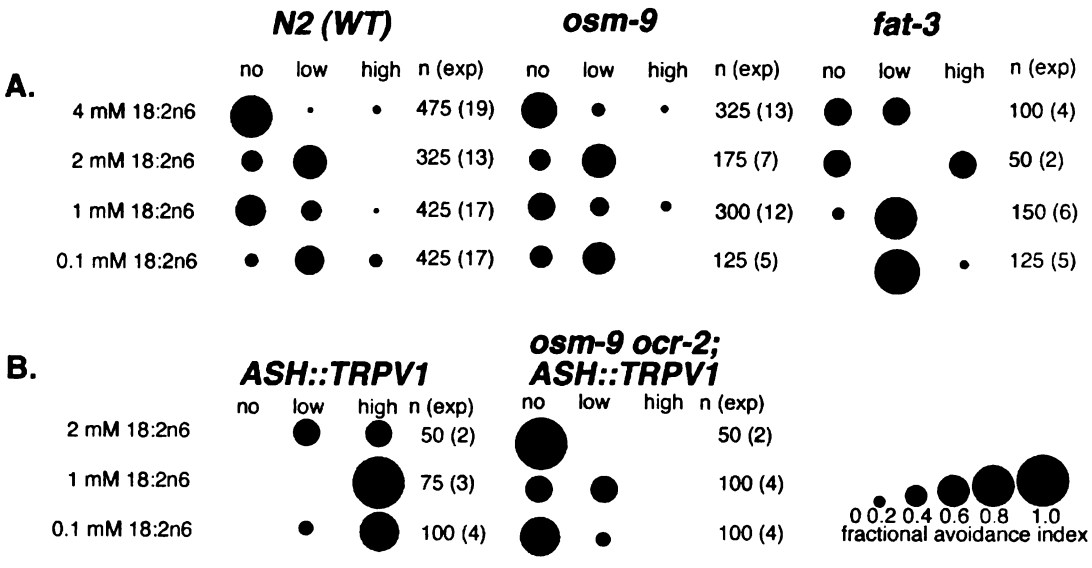
A.
N2 (WT)
osm-9
fat-3
no low high n (exp)
4 mM 18:2n6 475 (19) 325 (13) 100 (4)
2 mM 18:2n6 325 (13) 175 (7) 50 (2)
1 mM 18:2n6 425 (17) 300 (12) 150 (6)
0.1 mM 18:2n6 425 (17) 125 (5) 125 (5)
B.
ASH::TRPV1
osm-9 ocr-2; ASH::TRPV1
no low high n (exp)
2 mM 18:2n6 50 (2) 50 (2)
1 mM 18:2n6 75 (3) 100 (4)
0.1 mM 18:2n6 100 (4) 100 (4)
0 0.2 0.4 0.6 0.8 1.0
fractional avoidance index

The San Francisco Library

7374906
3 1378 00737 4906